University of São Paulo
"Luiz de Queiroz" College of Agriculture

Geophysics techniques on the evaluation of natural processes in the pedosphere, at different pedoenvironment and its contribution for digital soil mapping

Danilo César de Mello

Dissertation presented to obtain the degree of Master in Science. Area: Soil and Plant Nutrition

Piracicaba
2020

Danilo César de Mello
Agronomist

Geophysics techniques on the evaluation of natural processes in the pedosphere, at different pedoenvironment and its contribution for digital soil mapping

Advisor:
Prof. Dr. **JOSÉ ALEXANDRE MELO DEMATTÊ**

Dissertation presented to obtain the degree of Master in Science. Area: Soil and Plant Nutrition

Piracicaba
2020

Dados Internacionais de Catalogação na Publicação
DIVISÃO DE BIBLIOTECA – DIBD/ESALQ/USP

Mello, Danilo César de

Geophysics techniques on the evaluation of natural processes in the pedosphere, at different pedoenvironment and its contribution for digital soil mapping / Danilo César de Mello. - - Piracicaba, 2020.

124 p.

Dissertação (Mestrado) - - USP / Escola Superior de Agricultura "Luiz de Queiroz".

1. Gammaespectrometria 2. Susceptibilidade magnética do solo 3. Pedologia 4. Pedometria 5. Geofísica I. Título

A minha familia e amigos que me apoiaram em momentos dificeis

DEDICO

AGRADECIMENTOS

A todos os sagrados Orixás, em especial Ogum por abrir as portas da pós graduação nessa excelente Instituição, a Oxossi e Obá pelos conhecimentos adquiridos e a Oxalá pela força e luz que me iluminou durante essa importante etapa em minha vida profissional.

Ao todo o Centro Espirita de Umbanda Mãe Iemanjá pelo apoio e alinhamento da vida espiritual com profissional e pessoal, me permitindo ter uma base religiosa fundamental para enfrentar problemas de todos os tipos durante a pós graduação.

A toda minha familia, da qual fazem parte minha mãe Divina Rosalina Santana que sempre me apoiou, meu irmão Cristiano Aparecido de Mello no suporte familiar em minha ausência, devido aos estudos e, meu pai Afonso Ribeiro de Mello.

A meus demais familiares José Roberto Oquendo Cabrero, Izabel Ribeiro de Mello, Diego Oquendo Cabrero, Roseli Ferre Mello, Claudio Ribeiro de Mello, Guilherme Ferri Mello, Maria Aparecidade Mello e Esmeralda Mello pelo apoio secundário.

Ao meu ex-orientador de graduação Jão Luiz Lani por ter me encaminhado para ESALQ e ter contribuido com a aplicabilidade do conhecimento em minha atual linha de pesquisa e maravilhosas liçoes de reflexão sobre o conhecimento

Ao professor Oswaldo Pinto Ribeiro Filho pelo apoio geral em minha vida acadêmica e profissional.

Ao meu atual orientador professor José alexandre Melo Demattê que foi um excelente orientador e amigo e, ter me concedido a oportunidade de fazer parte de um dos maiores grupos de estudos em pedometria do mundo, mesmo sabendo de minhas limitações com processamento, permitindo-me conhecer e começar do zero o entendimento e o desenvolvimento de um trabalho dentro dessa linha de pesquisa. Aproveito para agradecer também a paciência para com minha pessoa durante minha permanência no grupo perante dificuldades pessoais inclusive pelo apoio quando perdi completamente a audição esquerda.

Ao professor Tiago Osório Ferreira que foi praticamente um pai aqui na ESALQ, mesmo não sendo meu orientador, contribuiu de forma marcante para meu crescimento pessoal e profissional como um exemplo de pessoa, professor, pesquisador e um amigo que levarei para a vida.

A Sara Ramos dos Santos que foi meu anjo da guarda aqui na ESALQ.

Ao professor Pablo Vidal Torrado pelas críticas sarcásticas, porém construtivas profissionalmente, pelos conhecimentos em processos de pedogênese e demais terminologias em peedologia. Também pelos maravilhosos cafés da salinha.

Ao professor Miguel Cooper pela oportunidade de atuar como monitor na disciplina Recuperação de Áreas Degradadas e assistir a disciplina de física do solo como ouvinte contribuindo significativamente para meu conhecimento em ciência do solo. Também agradeço por não ter me colocado fogo por assistir aula no primeiro dia com uma camisa da UFV (mas que Viçosa é melhor é...rsrsrs).

Ao professor Carlos Ernesto Schaefer da Universidade Federal de Viçosa, pessoa mais inteligente que tive o prazer de conhecer, onde muitas das idéias e assuntos nas discussões desse trabalho são fruto das aulas e palestras ministradas por ele durante minha graduação, inclusive ideia de projeto de doutorado.

A TODO o grupo GEOSCIS pelo apoio geral durante o desenvolvimento de minhas atividades, cujo o qual não seria possível o desenvolvimento desse trabalho. Grupo altamente profissional e o melhor grupo de trabalho/pesquisa que já tive o prazer de conhecer e fazer parte.

Raul Poppiel, que me auxiliou desde antes de eu vir para ESALQ, baixar imagens que não existia de gamma do estado de são Paulo (kkkk)...obrigado pela paciência (mas que as vezes se estressava kkkk) com minha lerdeza e desorganização e por toda a ajuda e apoio.

Fellipe Alcantara Oliveira Mello que foi o meu co-orientador, pegando na minha mão e me ensinando a planejar e organizar um paper (inclusive na cobrança heheh) e tambem a executar parte do processamento em cursos particulares e gratuitos de SAGAGIS (kkkk).

José Lucas Safanelli pelo curso gratis de QGIS no inicio (kkkk) e também pela paciência com minha lerdeza e burrice em geoprocessamento...obrigado pelo seu apoio na parte estatística e processamento, que também foi fundamental para execução desse trabalho.

Nélida Elizabet Quiñonez Silvero pela paciênc...essa não tem muita paciência não (hahahah)....brincadeiras a parte, me deu um aporte crucial para execução desse trabalho em estatística, processamento no R e imagens, onde sem o apoio dela, com certeza esse trabalho na teria saído.

Arnaldo Barros e Souza pelos dicas de como tingir o cabelo e não deixar orelha manchada (hahah)....agradeço apoio desde minha chegada em Piracicaba, parte de manuseio de sensores e processamento e dicas profissionais.

Rodnei Rizzo, orientador substituto sempre atolado de afazeres, mas que sempre tinha tempo para me orientar e ensinar sobre pesquisa científica, organização de ideias e e auxilio com processamento.

Luis Augusto Di Loreto Di Raimo verdadeiro parceiro no trabalho e amigo (único defeito que é de Mato Grosso...o povinho...hahahah) agradeço apoio essencial com figuras e processamento, sem você também o trabalho não teria sido finalizado.

Aos ICS queridos Maria Eduarda Bispo Resende (best friend dos ICs), Lucas Rabelo Campos (o acanhado), Andres Mauricio Rico Gomez (esse tive dificuldade pois esse fala um idioma singular, o Portunhol), Merlym Taynara Accorsi Amorin (docinho de pessoa), Gabriel Pimenta Barbosa de Sousa (esse rapazinho se eu for contar...melhor deixar quieto...kkkk), Fabio Chaddad (me arranhou com arame farpado que usa no braço), Claúdia Maria (Cráudia que bagunçava o café)....agradeço pela bagunça e momentos de descontração como alivio de estresse e, é claro agradeço pela coleta em campo e organização do banco de dados e os almoços no Rucas.

Também agradeço:

Ao Conselho Nacional de Desenvolvimento Científico e Tecnológico (CNPQ – processo 131715/2018-6) pela concessão de bolsa de estudos.

A Divisão de Atendimento à Comunidade (ESALQ) pela concessão de moradia estudantil que permitiu minha permanência na ESALQ e cidade de Piracicaba.

A população brasileira em geral que é quem indiretamente financiou meus estudos na referida Instituição.

"O que vale na vida não é o ponto de partida e sim a caminhada. Caminhando e semeando, no fim terás o que colher".

Cora Coralina

CONTENTS

RESUMO

Técnicas geofísicas na avaliação de processos naturais que ocorrem na pedosfera, em diferentes pedoambientes e sua contribuição para o mapeamento digital de solos

O uso de técnicas geofísicas aplicadas em geologia recentemente vem sendo utilizadoas para estudos em ciências do solo. Entretanto, a maioria dos estudos concentram-se em modelagem e mapeamento de atributos do solo, com pouca ou nenhuma ênfase na compreensão dos processos que ocorrem na pedosfera, bem como na inter-relação entre processos e fatores pedoambientais (geologia, relevo, pedogeoquímica e hidrologia). A pesquisa foi realizada com o objetivo de utilizar sensores geofísicos proximais (gamma e susceptibilímetro) para a compreensão dos processos naturais que ocorrem na pedosfera (pedogênese, pedogeomorfológicos, pedogeoquímicos), bem como a relação desses processos com os atributos do solo e a contribuição para o mapeamento digital pedológico, destacando o potencial e a limitação da técnica. A área de estudo está localizada no estado de São Paulo - Brasil. Os dados geofísicos foram coletados com sensores de campo, usando gamaespectrômetro e susceptibilímetro, em 89 pontos. Além disso, foram realizadas tradagens (0-20 cm) nesses mesmos pontos, para análises físico-químicas tradicionais. Esses dados foram combinados com a descrição morfológica e classificação do solo em vários perfis, geoprocessados e analisados estatísticamente utilisando-se os softwares *ArcGIS, SAGAGIS* e *R.* A litologia contribuiu fortemente para os teores de urânio, tório, potássio (radionuclídeos) e suscetibilidade magnética (SM) em classes de solo menos evoluídas. Por outro lado, nas classes de solo mais evoluídas, a pedogênese teve maior influência no teor de radionuclídeos e na SM. Os processos pedogeomorfológicos afetam a distribuição de radionuclídeos e MS devido ao transporte e deposição de materiais e efeito erosivo, aproximando a superfície do solo com material de origem. O comportamento geoquímico dos radionuclídeos e as vias pedogeoquímicas de formação de minerais ferrimagnéticos são controlados pelo intemperismo e condições ambientais da pedosfera, cuja drenagem é uma das mais importantes. Os radionuclídeos apresentaram boa correlação principalmente com a textura do solo, enquanto a SM apresentaram com a textura do solo, CEC e Fe2O3. A SM identificaram as áreas de transição entre as classes de solos e litologia, bem como variações nos teores de radionuclídeos, fornecendo uma ferramenta potencial para estratificação de classes de solos e mapeamento digital pedológico. Para cada pedoambiente específico, é necessário estabelecer um modelo conceitual para interpretar o conteúdo de MS e radionuclídeos do solo e sua relação com os processos da pedosfera, uma vez que muitas variáveis com características diferentes afetam o conteúdo e a distribuição de radionuclídeos, bem como os valores de MS.

Palavras-chave: Gammaespectrometria, Susceptibilidade magnética do solo, Pedologia, Pedometria, Geofísica

ABSTRACT

Geophysics techniques on the evaluation of natural processes in the pedosphere, at different pedoenvironment and its contribution for digital soil mapping

The use of geophysical techniques applied in geology has recently been used for soil science studies. However, most studies focus on attribute modeling and mapping, with little or no emphasis on understanding the processes that occur in the pedosphere, as well as on the interrelationship between the processes and environmental factors (geology, relief, pedogeochemistry and hydrology). The research was carried out aiming the use of proximal geophysical sensors (gamma and susceptibilimeter) for the understanding of naturally occurring processes in the pedosphere (pedogenetic, pedogeomorphological, pedogeochemical), the relationship of these processes with soil attributes and the contribution to digital soil mapping, highlighting the potential and limitation of the technique. The study area is located in São Paulo State – Brazil. The geophysical data were collected using field sensors using gammaspectrometer and susceptibilimeter, at 89 points. Also, augers were performed (0-20cm) in these same points to traditional physical-chemical analyses. These data were combined soil morphological description and classification in various profiles, geoprocessed and statistical analyses was undertaken using the softwares *ArcGIS*, *SAGAGIS* and *R*. The lithology strong contribute uranium, torium, potassium (radionuclides) content in and magnetic susceptibility (MS) in less evolved soil classes. On the other hand, in more evolved soil classes the pedogenesis had more influence in radionuclides content and MS. Pedogeomorphological processes affect distribution of radionuclides and MS by transport and deposition of materials and erosional effect, oncoming soil surface of parent material. The geochemical comportment of radionuclides and pedogeochemical pathways of ferrimagnetic minerals formation are controled by weathering and pedosphere conditions, wich drainage is one of the most important. Radionuclides had good correlation mainly with soil texture, while MS had with soil texture, CEC and Fe2O3. MS identified the transition areas between soil classes, lithology as well as radionuclides variation content, providing a potential tool for soil classes stratification and digital pedological mapping. For each particular pedoenvironment a conceptual model to interpret soil MS and radionuclides contentits and their relation with pedosphere processes, need to be stablish, once many variables, with different characteristics affect radionuclides content and distribution, as well as MS values.

Keywords: Gammaspectrometry, Soil magnetic susceptibility, Pedology, Pedometry, Geophysic

1. THEORETICAL BACKGROUND

1.1. Geophysics

Geophysics comprehend the science that study the Earth surface and internal proprieties throughout physical principles (Parasnis, 1986). It is a non-destructive and non-invasive means of remotely investigating surface and subsurface of the Earth, using physical phenomenon related to its constitution (Ruffell and McKinley, 2008), inferring the distribution of Earth´s physical proprieties (Johansson and Åkerman, 2008).

Geophysical surveys are the acquisition of a physical data set on land surface in a specific area. The main physical proprieties are thermal conductivity, electrical conductivity, propagation velocity of elastic waves, density, temperature, natural radiation emission and magnetic susceptibility (Domra Kana et al., 2015). These proprieties are determinate mainly by variation of physical-chemical attributes of structure of subsurface Earth and rocks which, at least in one place present discontinuities, being possible to identify throughout technique (Domra Kana et al., 2015).

According to Parker et al., (2010) geophysics techniques can be used in soil science to study attributes and sediments. This technique allows studies and data acquisition of Earth surface and subsurface, physical and hydrological processes at high resolution (Binley et al., 2015), as well as, the analyses of interaction between surface and subsurface compartments in pedosphere system (Falco et al., 2019). Besides, recently researchers have been made effort to improve geophysical methods to mapping soil attributes (Romero-Ruiz et al., 2018).

There are many geophysics techniques used in geological prospection with potential to be used in soil science studies, such as seismic, gravimetric, thermometric, electromagnetic, magnetic and radiometric (Rutherford and Soddy, 1902).

1.2. Historical background of radiation and gamma-ray usage

Gamma spectrometry can be understood as measuring the natural emission of gamma radiation (passive remote sensing) produced by the earth's surface, including soil, rocks and sediments (Wilford et al., 1997). This methodology began after the discovery of the three components of α, β and γ radiation by Rutherford in 1902 and the later discovery and formulation of the theory of radioactive decay in 1919 (principle of gamma-spectrometric measurement) by this same scientist, along with work developed by Rutherford and Soddy, (1902).

After the discovery of radioactivity and radioactive decay, it was not long before methods for measuring this energy were developed. The first detectors were built in the mid-twentieth century, where the sensitivity of detectors made the greatest advances between the 1940s and 1950s. During this period the need for uranium exploration for war use in the Second World War required research to be carried out. in order to identify new mines of this mineral. Thus, the first countries to use aerogamaespectometry for 12 geological purposes were Canada, the United States, and Russia in 1947 and later Australia in 1951 in search of uranium (Pickup and Marks, 2000; Wilford et al., 1997).

After 1960, the development of laboratory gamma spectrometry began and major applications in aerial gamma spectrometry for the purpose of mineral exploration and environmental monitoring. The main applications of gamma spectrometry are: identification of outcrop points and/or igneous intrusions, characterization of undifferentiated intrusions, mineral prospecting, fertilizer influence analysis, oil exploration and environmental control areas for exploration or leakage of radioactive elements (Ribeiro et al., 2013; Ulbrich et al., 2009; Carrino et al., 2007; Conceição and Bonotto, 2003; Lüning and Kolonic, 2003).

Recently, researchers were carried out using gamma ray spectrometry to study soil attributes and pedology, as works developed by Herrmann et al., (2010) and Schuler et al., (2011). These researchers conducted soil mapping in Thailand from radiometric and lithological data. The work of these researchers showed the efficiency of gamma-spectrometry in predicting various soil attributes and weathering stage. According to Stenberg et al., (2010), some of the attributes of soils that can be determined and quantified with gamma-spectrometry are: clay content, total organic carbon, mineralogy and water content.

1.3. Radiometric technique: Radiation, radioactivity, radionuclides and gamma spectrometry

Radiation refers to type of energy transmission in small particles moving at high speed, or by light-like electromagnetic waves and can be classified in several types according to electromagnetic spectrum. On the other hand, radioactivity is directly related to the nucleus of atom and nuclear reactions that causes nucleus changes and transformation in other elements (Rutherford and Soddy, 1902).

According to Minty, (1997) there are some physically unstable elements of natural occurrence in the nature. These elements tend to reach a stable form throughout radioactive decay and nuclei disintegration. Radioactive decay is a statistical variable that demonstrates the probability of an atom's disintegration within a given time frame (Mernagh and Miezitis, 2008).The change to unstable form to stable form and nuclei change, emit a natural energetic ionizing radiation that, according to penetration power can be classified in alpha, beta and gamma.

Given this, alpha particles have lesser penetration energy and can be barred by thin sheet of paper. Beta particle has an intermediate penetrative energy, ionizing the air for a few centimeters and can pass through a metal blade with some millimeters thick. With respect to gamma, it has highest penetrative energy and can penetrate up to 30 centimeters in rock and tens of meters in the air. It is important to realize that, these radiations have no charge. As a consequence, they cannot be diverted by electric or magnetic fields, exhibiting the characteristics of an electromagnetic wave (Minty, 1997).

The Uranium (U), Thorium (Th) and Potassium (K) are the single unstable elements naturally occurring in the earth's crust that emit gamma rays, during radioactive decay, with sufficient energy intensity for detection in gammaspectrometric surveys and are considered radionuclides (Minty, 1997).

Radionuclides are natural radioactive elements that emit radiation and are governed by the law of radioactive decay, a process that generates gamma rays and are of short wavelength electromagnetic spectrum. The most commonly used electromagnetic spectra in geological studies (gammaspectrometric surveys) are energy spectra between 0.2 and 3 MeV, encompassing the energy spectra of U, Th and K (**Fig. 1**) (Minty, 1997).

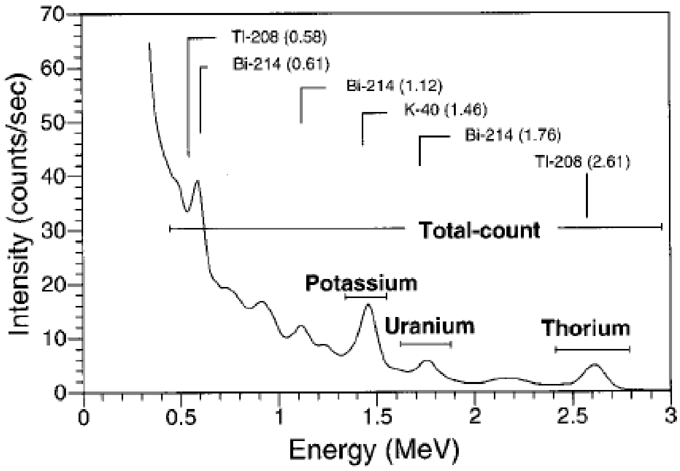

Figure 1: Natural gamma ray Spectrum highlight the potassium, uranium and thorium channels (Wilford et al., 1997).

Spectrometry can be understanding as the science concerned with the measurement of spectra, which in turn, comprises a large spectral line (**Fig. 2**). Spectrometry is based on the interaction of the radiation emitted by some sample with the detector, and the qualitative and quantitative discrimination of radioisotopes present in the sample, result of these interaction (Lindon et al., 2016). Gamma spectrometry, is the spectrometry and geophysical technique (radiological) that generates data from gamma radiation emitted by naturally occurring radionuclides in rocks, minerals, soils and sediments, mainly U, Th and K (Minty, 1988).

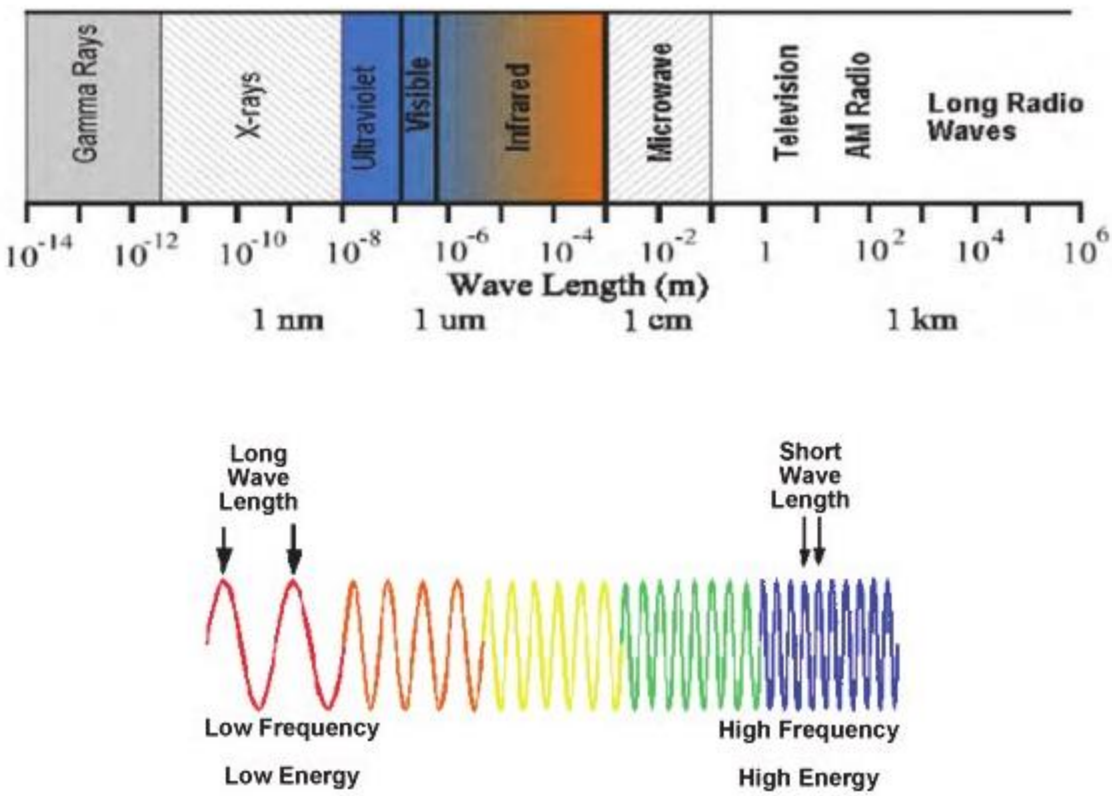

Figure 2: different electromagnetic spectrum and type of waves, frequency and penetration (Ashraf et al., 2011).

In gamma spectrometry, the thorium (Th) and uranium (U) elements are indirectly quantified via absorption energy, (approximately 2.62 MeV and 1.76 MeV, respectively), through the thallium (Tl_{208}) and bismuth (Bi_{214}) child elements (**Fig. 3**), respectively. The K_{40} is quantified in its entirety, including K in the rock and mineral structure, as well as K adsorbed to soil minerals, and is directly measured by the absorption energy of 1.46 MeV, resulting from decay from K^{40} to Ar^{40} (Fig. **X**). Since the Th and U elements are indirectly quantified, they are called eTh and eU, respectively (Minty, 1997).

a)

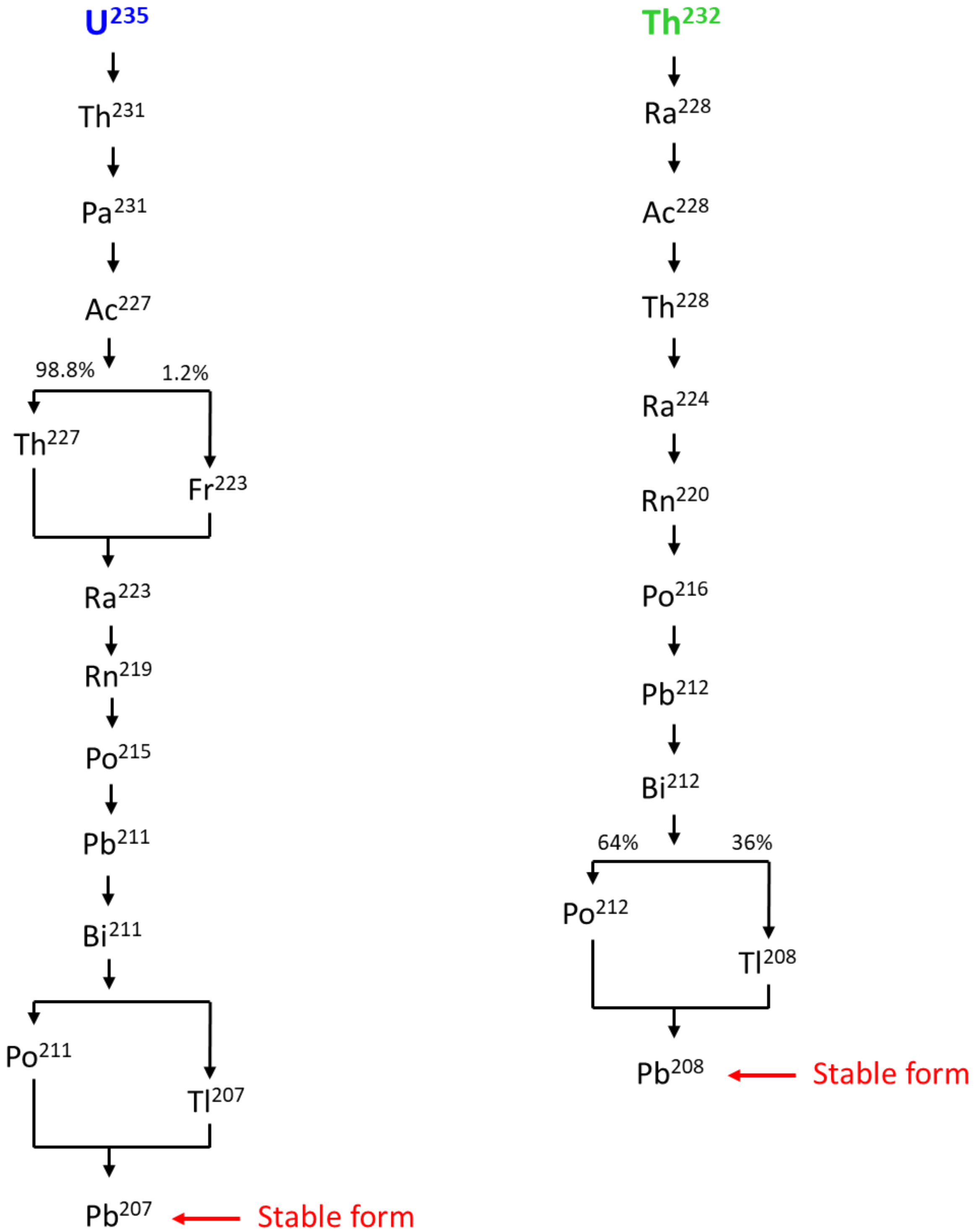
U235
Th231
Pa231
Ac227
98.8%
1.2%
Th227
Fr223
Ra223
Rn219
Po215
Pb211
Bi211
Po211
Tl207
Pb207
Stable form
Th232
Ra228
Ac228
Th228
Ra224
Rn220
Po216
Pb212
Bi212
64%
36%
Po212
Tl208
Pb208
Stable form

b)

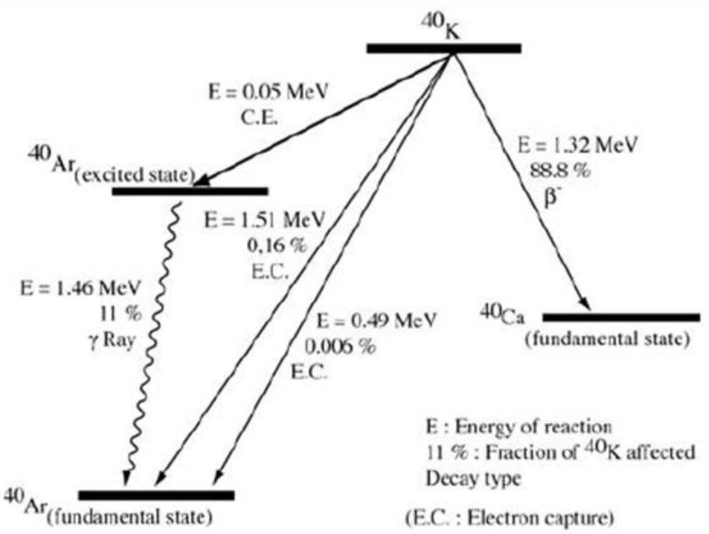

Figure 3: a) U^{235} and Th^{232} decay series adapted from Minty, (1997), simplified after Radiological Health Handbook (1970), and Ivanovich and Harmon (1982). b) K^{40} decay series, adapted from (Gillot et al., 2006).

1.4. Radionuclides physico-chemical attributes in mineralogical, geological and geochemical aspects in the pedosphere

Uranium exist in tetravalent and hexavalent forms in nature (**Fig. 4**). It is positively correlated concentration with the silica content of igneous rocks, being more abundant in intrusive felsic rocks and less common in ultramafic rocks. U occurs in rock minerals such as quartz, biotite, horblende and feldspar or trace minerals such as zirconium, epidote, apatite, titanite, monazite, among others, in the form of traces. Its most common mineral form is Uranite UO_2, U_3O_8. The mobility of this element is extremely dependent on pH and redox potential conditions. The U may be leached with soluble minerals under oxidizing conditions or precipitated under reducing conditions (Lancmuir and Herman, 2002). U^{4+} and Th^{4+} released by weathering can be adsorbed on the surface of clay minerals, iron and aluminum oxides and organic matter in the form of impurities and traces. Concentrations vary depending on the content and types of clay minerals. Unlike Th, the oxidized form of U (uranil) is soluble, which gives U greater instability under weathering conditions than Th. In intense weathering and favorable conditions, the uranium is preferably removed, with the U/Th ratio being a measure of the degree of material change (Dickson & Scott, 1997).

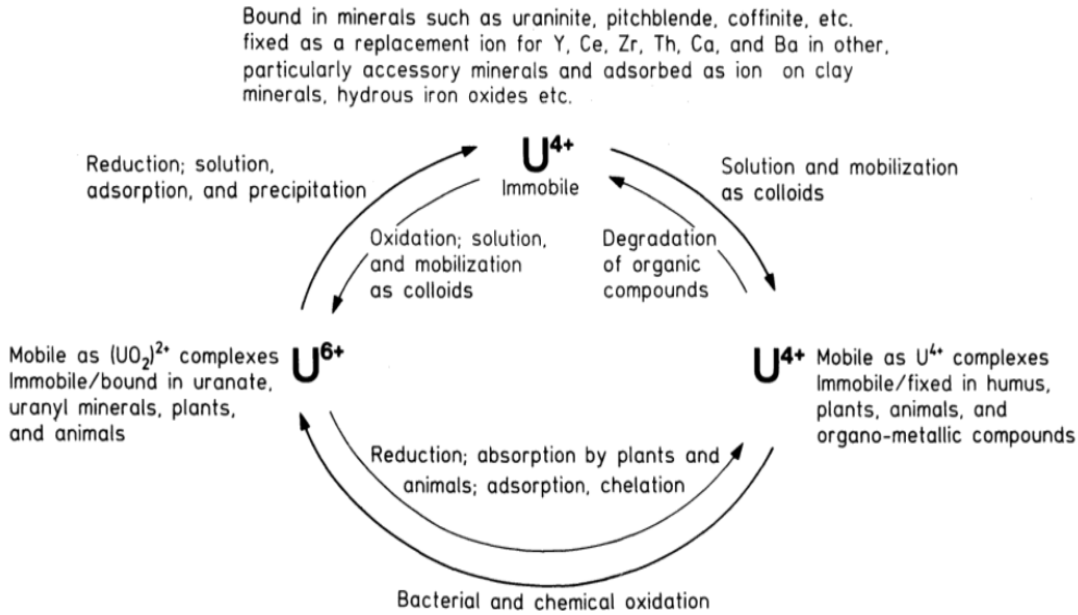

Figure 4: Interconversion cycle of U^{4+} and U^{6+} in nature (after Boyle, 1982) adapted by Dahlkamp, (1993).

The thorium (Th) only exists in the tetravalent forms in nature and reduction processes have no important in its geochemistry cycle (**Fig 5**). Th found in quartz and feldspar minerals in rocks, or forming other minerals such as thorianite, monazite, cheralite, huttonite and thorita. This element has a large ionic radius and has little affinity for the solid phase. Its precipitation following magma crystallization is associated with other incompatible elements (HFSE or LREE group) such as zirconium, niobium, hafnium, tantalum, uranium, K and rare earth elements. Th is most abundant in felsic igneous rocks such as granites, rhyolites and gneisses. The Th present in the minerals occurs as a tetravalent Th^{4+} ion. In solution, the Th^{4+} ion forms complexes with chlorides, fluorides, nitrates, sulfates, carbonates, phosphates, silicates, acetates, organic matter and others (Mernagh and Miezitis, 2008). Associated with organic complexes Th is very dynamic, with great mobility in solution with pH below 8.0 (Lancmuir and Herman, 2002). In the sand fraction of soils, Th and U are associated to a greater degree with minerals of Zr (zircon) and Ti (anatase and rutilium), whose affinity is due to the great stability and resistance of these minerals to weathering. Generally, the higher expression of these minerals is associated with their relative residual concentration due to the advanced weathering state with clay destruction. They may also be associated with ferruginous nodules and concretions, also residual in conditions of intense weathering.

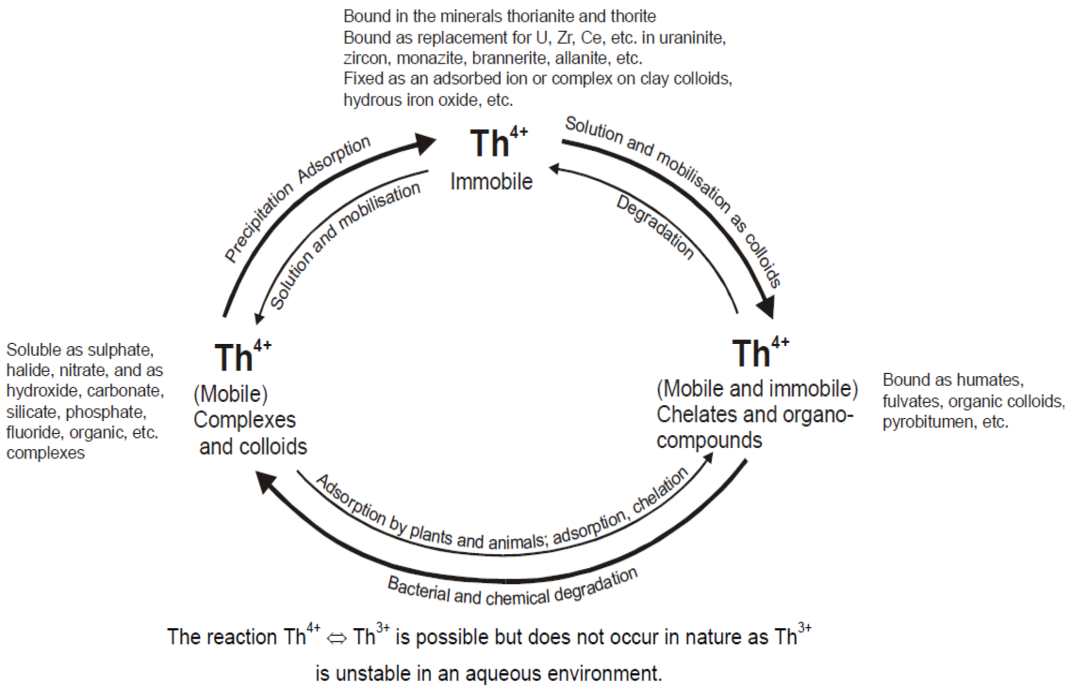

Figure 5: Cycle of Th^{4+} interconversions in nature (modified from Boyle, 1982) and adapted by Mernagh and Miezitis, (2008).

In relation to K, the main source on the earth's surface comes from the decomposition of igneous rocks. K is a highly incompatible element with melting magma (HFSE group), being more abundant in acid plutonic rocks, proportionally to the silica increment. Compared to these rocks, in mafic minerals, olivines and pyroxenes the K contents are lower. Potassium minerals include orthoclase and microline; feldspar, muscovite, biotite and amphibole. In soil K contents are associated with the intensity of weathering. Due to the solubility and mobility of these minerals there is marked depletion of K content during the advancement of pedogenesis. In conditions of intense weathering and free drainage K soil is easily removed by leaching the profile. The K + ion released in solution can be adsorbed on the clay surface replacing Si^{4+}, Al^{3+}, Fe^{2+} and Mg^{2+}, mainly as a function of pH. K detected in gamma spectrometric surveys in soils is generally related to minerals in which it is part of the structure, such as micas, potassium feldspars and illites, as well as soils where there is a possibility of formation of expansive clay minerals such as montmorillonite (Dickson & Scott, 1997).

1.5. Distribution of radionuclides in rocks and soils

Previous research undertaken by Wilford et al., (1997) in Australia, demonstrated a positive correlation between silica content and radionuclides in igneous rock, which felsic rocks present the highest radionuclide content (Fig. 6). All radionuclides tend to increase with increasing silica contents in the rock, however, the thorium contents increase overmuch (Dickson & Scott, 1997; Mernagh and Miezitis, 2008). On the other hand, in metamorphic rocks, there are decreases in radionuclides content, with increases in metamorphic degrees (Mernagh and Miezitis, 2008).

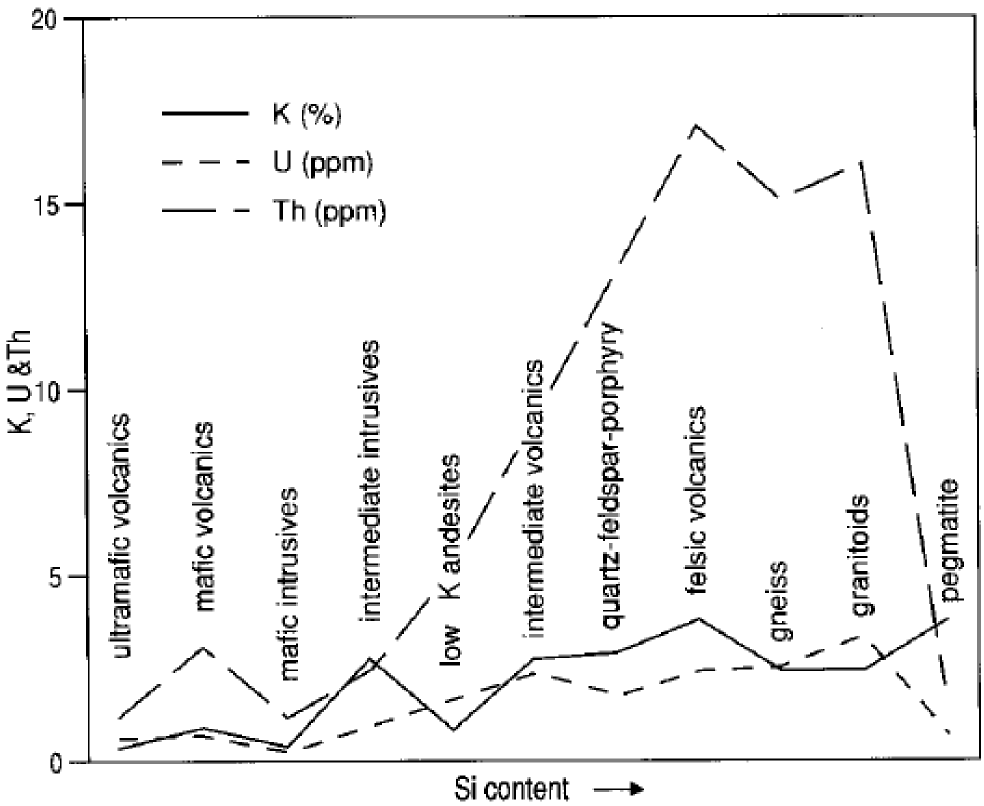

Figure 6: variation in average of Uranium, thorium and Potassium in igneous rock with increasing in acidity (silica content) (Dickson & Scott, 1997).

In sedimentary rocks, there is certain variability of radionuclides content (**Tab. 1**), due to the nature of formation of this type of rock, throughout sedimentary cycle (Boyle, 1982). Therefore, sedimentary rocks reflect the parent material pre-weathered and minor radionuclides content compared to immature sediments (Dickson & Scott, 1997).

Table 1: Uranium and thorium content according to rock type. Adapted from Boyle, (1982).

Rock type	***Radionuclides***	
	U (ppm)	***Th (ppm)***
Igneous		
Ultrabasics (peridotite, dunite, etc.)	0.02	0.1
Basic intrusives and extrusives (gabbro, basalt, etc.)	0.6	3
Intermediate intrusives and extrusives (diorite, andesite, etc.)	2	5
Acid intrusives and extrusives (granite, rhyolite, etc.)	4.5	15
Alkali-rich (sienites, alkali granites)	up to 100	up to 100
Metamorphic		
Quartizites, meta-greywacke, meta-conglomerate	1.5	5
Marbe and crystaline dolomite	0.5	1
Phyllite, meta-argillite, slate	2.5	10
Schists (igneous parentage)	2	6
Gneisses and granulites	3	10
Sedimentary		
Arenites and rudites (sandstone, arkose, greywacke, conglomerate)	1.5	5
Lutites (shales, argillites)	3.5	12
Precipitates (limestone, dolomite, siderite)	1.5	1
Evaporite (halite, silvite)	0.1	0.2

Due to the large variation of radionuclides in the same rock group, it is very difficult to predict a given concentration of radionuclides in each specific rock. Therefore, a petrographic classification based on radionuclides concentration cannot be performed (Dickson & Scott, 1997).

Second Boyle, (1982) the Th content in soil is relatively high, varying from 0.1 ppm to 50 ppm with an average of about 1 ppm (**Tab. 2**). In residual soils, the Th content depends of parent material, which the high values occur on acid igneous rock, schists and gneisses, whereas the lowest in basic igneous rock. The Th overly values (200 - 1000 ppm or higher) occur in soils, clays, laterite or bauxite developed from thorium-rich pegmatites or alkaline rocks.

The U in soil has a complex behavior, due to several chemical species form and various environmental factors that influence its behavior. As result, there is a great variability of U content in soil (**Tab. 2**). There are two main processes that affect U mobility on inorganic soils: sorption and complexation. The main soil attributes related to these processes are clay type and content, iron and aluminum oxides, organic matter and biological activity (transformation and fixation). So, the system of U distribution and concentration in pedosphere is complex, due to all of these environmental factors act simultaneously (Vandenhove et al., 2007). Other important soil attribute related to U content is pH and its relationship with sorption process. Increases in pH results in more available negatively charged binding sites on clay surface. As a consequence, more U is adsorbed on mineral particle surface. The opposite it is also true. Above pH 6, the fraction of U that is complexed by carbonates increases. As a result, it tends to enhance the U mobility in soil (Koch-Steindl and Pröhl, 2001).

Potassium has high solubility and mobility in pedosphere, under strong weathering conditions like tropical environments, resulting in loss in soil solutions or sorption in clay minerals (Ulbrich et al., 2009; Wilford et al., 1997). Due to this, the K content in soil is generally low compared to other radionuclides (**Table 2**).

Table 2: Radionuclides content in Australian rock and soil. Adapted from (Dickson & Scott, 1997)

Rock type	***Rock***			***Soil***		
	K *(%)*	***U*** *(ppm)*	***Th*** *(ppm)*	***K*** *(%)*	***U*** *(ppm)*	***Th*** *(ppm)*
Intrusives						
Granitoids	0.3 – 4.5	0.4 – 7.8	2.3 – 4.5	0.4 – 3.9	0.5 – 7.8	2.0 - 37
Gneissic	2.4 – 3.8	2.1 – 3.6	18 - 55	0.7 – 1.9	1.6 – 3.8	6.0 - 19
Pegmatite	2.6 – 5.5	0.3 - 1	0.3 – 9.6	-	-	-
Aplites	0.6 - 4	1.8	3 - 20	-	-	-
Quartz-feldspar porphyry	1.5	1.3 – 2.9	6 - 14	-	-	-
Intermediate intrusives	0.7 – 5.6	0.1 – 1.2	0.8 – 6.1	0.7 – 3.4	1.5 – 2.3	2.9 – 8.4
Mafic intrusive	0.1 – 0.8	0.0 – 1.1	0.0 – 3.1	-	-	-
Extrusives						
Felsic volcanics	2 – 4.4	1.4 - 13	13 - 28	1.8 – 3.2	1.3 – 2.4	10 - 18
Intermediate volcanics	1.8 – 4.1	0.9 – 5.6	1.5 - 15	1.0 – 2.7	1.2 – 3.6	4.0 - 17
Low-K andesites	0.7 – 0.9	1.0 – 2.5	3.8	0.8 – 1.5	1.2 – 1.5	4.0 – 6.0
Mafic volcanics	0.3 – 1.3	0.3 – 1.3	2.0 – 5.0	0.2 – 1.4	0.6 – 2.5	3.3 - 13
Ultramafic volcanics	0.2 - 0.9	0.3 – 0.9	0.0 – 4.0	0.6	2	6.0
Sedimentary						
Archaean shales	0.4 – 1.6	0.3 – 1.3	1.5	0.8	1.2	3.0
Other shales	0.1 - 4	1.6 – 3.8	10 - 55	0.7 – 3.0	1.2 - 5	6.0 - 19
Arenites	0.0 – 5.5	0.7 – 5.1	4.0 - 22	0.1 – 2.4	1.2 – 4.4	7.0 - 18
Carbonates	0.0 – 0.5	0.4 – 2.9	0.0 – 2.9	-	-	-

1.6. Perspectives of gamma spectrometry in soil science

Many works, in addition to geology studies, demonstrate several applicability of gamma spectrometry in pedosphere studies such as soil texture prediction (Priori et al., 2014; Heggemann et al., 2017; Coulouma et al., 2016; Egmond et al., 2018), weathering index (Wilford, 2012), soil survey and digital soil mapping (Moonjun et al., 2017), organic carbon mapping (Dierke and Werban, 2013), geochemical studies (Guagliardi et al., 2013; Paisani et al., 2013), pedogenesis processes (Schuler et al., 2011), pedogeomorphology and landscape evolution (Triantafilis et al., 2013). With advances in remote sensing and arise of new geotechnologies, it will be possible to combine these technologies with geophysical gamma survey to be used in soil science, in order to understand natural processes in pedosphere, soil attributes modelling and mapping, as well as the usage of these information establish farming planning and environmental management.

1.7. Magnetic proprieties and methods

The magnetic susceptibility *K*, is defined by M = [*K*] x H, which M is the induced magnetization of the material and H is the inductive magnetic field, it is the degree to which a substance can be magnetized (Rochette et al. 1992), having applicability in geophysical surveys of magnetic susceptibility throughout magnetic methods. The magnetic methods are well established in applied geophysics as an investigative methods used to understand the magnetic elements in petrophysics and optimize field data acquisition and interpretation (Clarck & Emerson, 1991).

The tree chemical element which are magnetizable are iron (Fe), cobalt (Co) and nickel (Ni). However, the magnetic attributes of rocks, soil and minerals are iron dependent, once Fe is 40 times more abundant than the sum of all other magnetic elements in the earth's crust (Coey, 1987).

The MS is determined by magnetic particle concentrations, grain sizes, grain shapes and mineralogy (Thompson and Oldfield, 1986). There are two main methods to measure of MS: field measures, which is reported as dimensionless volume units (e.g., X 10^{-5} (SI units)) and, laboratory measurements, reported in mass-based units (e.g., X 10^{-8} m^3 x Kg^{-1} (SI units)) (Mullins, 1977).

1.8. Magnetic susceptibility in minerals and soils

The magnetic behavior of minerals is result of magnetic moment produced by electron orbiting their nucleus and spinning around their axis (Mullins, 1977). According to magnetic moment and strength of each mineral, they can be classified as ferrimagnetic, ferromagnetic, diamagnetic, paramagnetic and anti-ferromagnetic (**Tab. 3**) (Dearing, 1994; Mullins, 1977).

In ferromagnetic minerals, mainly in iron crystalline, occur an interaction between adjacent atomic spin magnetic moments, which millions of atoms behave collectively as a tiny magnet. Ferrimagnetic minerals, which in turn, the same phenomenon occurs but, in this particular case, two out of three of the magnetic moment up in one direction, whereas the other one is oppositely aligned. In antiferromagnetic minerals, adjacent atomic magnetic moments naturally align themselves in opposite direction resulting in zero magnetic moment. Diamagnetic minerals have zero magnetic moment and, when it is applying a magnetic field, the electrons motions tend to organize in the direction opposite to the applied field. On the other hand, in paramagnetic minerals, with small magnetic moment, when subjected to a magnetic field, the electrons tend to line up in the direction of the magnetic field (**Figure 7**) (Mullins, 1977).

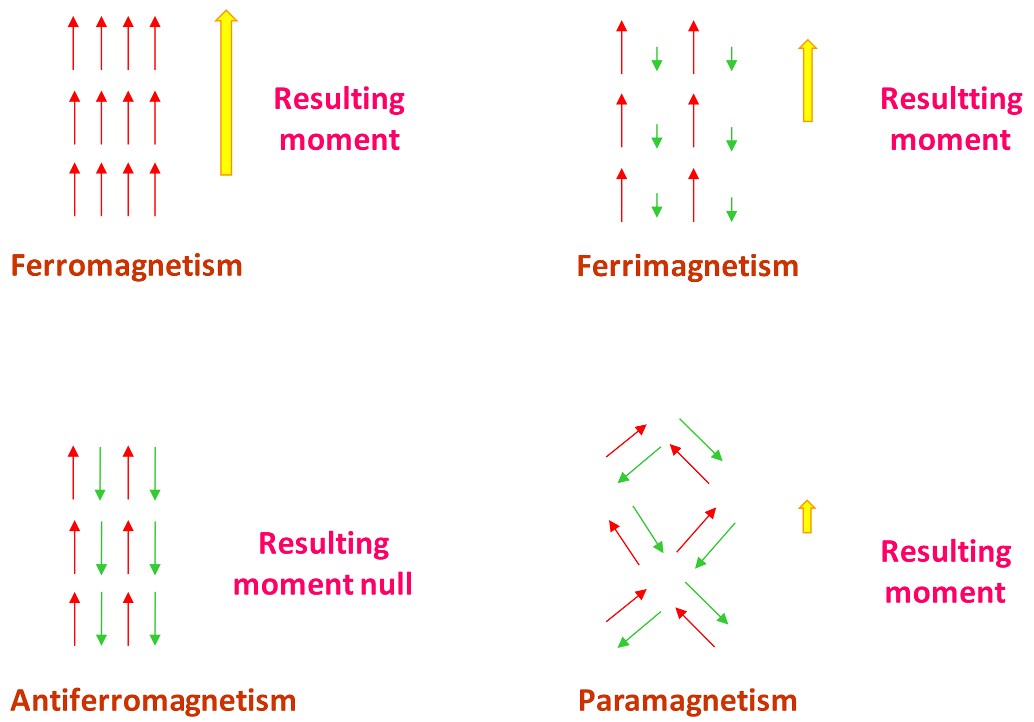

Figure 7: different kind of magnetic comportament (adapted from Luque, 2008).

According to Mullins, (1977), the two most important magnetic minerals in soils are magnetite and maghemite. Despite of that, there other minerals in soil with great variability of MS (**Tab. 3**).

Table 3: Magnetic susceptibilities for several iron oxides and soil constituents adapted from (Van Dam et al., 2004) (data Maher, 1998; Thompson, R., Oldfield, 1986).

Material	Chemical form	Magnetic status	Magnetic susceptibility (10-8 m3 kg-1)
Water	H_2O	Diamagnetic	-0.9
Quartz	SiO_2	Diamagnetic	-0.6
Pyrite	Fe_2O_3	Paramagnetic	30
Ferrihydrite	$5Fe_2O_3.9H_2O$	Paramagnetic	40
Lepdocrocite	g-FeO.OH	Paramagnetic	70
Ilmentite	$FeTiO_3$	Superparamagneitic	200
Hematite	a-Fe_2O_3	Antiferromagnetic	60
Goethite	a-FeO.OH	Antiferromagnetic	70
Pyrrhotite	Fe_7S_8 / Fe_8S_9 / Fe_9S_{10}	Ferrimagnetic	~5,000
Maghemite	g-Fe_2O_3	Ferrimagnetic	40,000
Magnetite	Fe_3O_4	Ferrimagnetic	50,000

Ferromagnetic and ferrimagnetic minerals are strongly magnetic susceptibility, with large positive MS values, such as magnetite and maghemite. Diamagnetic minerals with negative and low MS such as quartz and orthoclase. On the other hand, paramagnetic minerals have positive and low MS, such as ferrihydrite, biotite, pyroxenes, olivines. Anti-ferromagnetic minerals have positive and negative magnetic moment resulting in magnetic moment null, but the spin results in positive moderate magnetic susceptibility, such as goethite and hematite (Deng, 2015; Van Dam et al., 2004).

The pedogeochemical pathways of iron-mineral released from parent material and neoformation of magnetic minerals, are showed in **Figure 8**. The various pathways depend of pedoenvironmental conditions, as pH, drainage, micro-organisms activities, temperature, organic matter content. Ferrihydrite is mineral precursor to hematite and goethite formation, as well as magnetite and maghemite. To pedogenesis of main magnetic minerals in pedosphere (magnetite and maghemite), it is required presence of Fe III in parent material and the liberation of Fe to soil system throughout weathering.

Once the Fe is in soil system, it is subject to pedoenvironmental conditions. If the organic matter content is high (in pH 3 – 8), the Fe can complex with it, decreasing Fe availability in soil system. As a result, ferrihydrite formation will be reduced and goethite formation will be favorable. On the other hand, in low organic matter content, ferrihydrite is formed and can follow the pathway of hematite. If the temperature is high (favorable to complete dehydration) and drainage efficient (no redox conditions) hematite is formed. Also, ferrihydrite is precursor of magnetite and maghemite. If dehydration is partial in efficient oxidizing conditions, magnetite will be formed. However, once magnetite is formed and, if oxidizing is slowly on magnetite occur, it will be convert to maghemite (Dearing et al., 1996; Schwertmann, 1988).

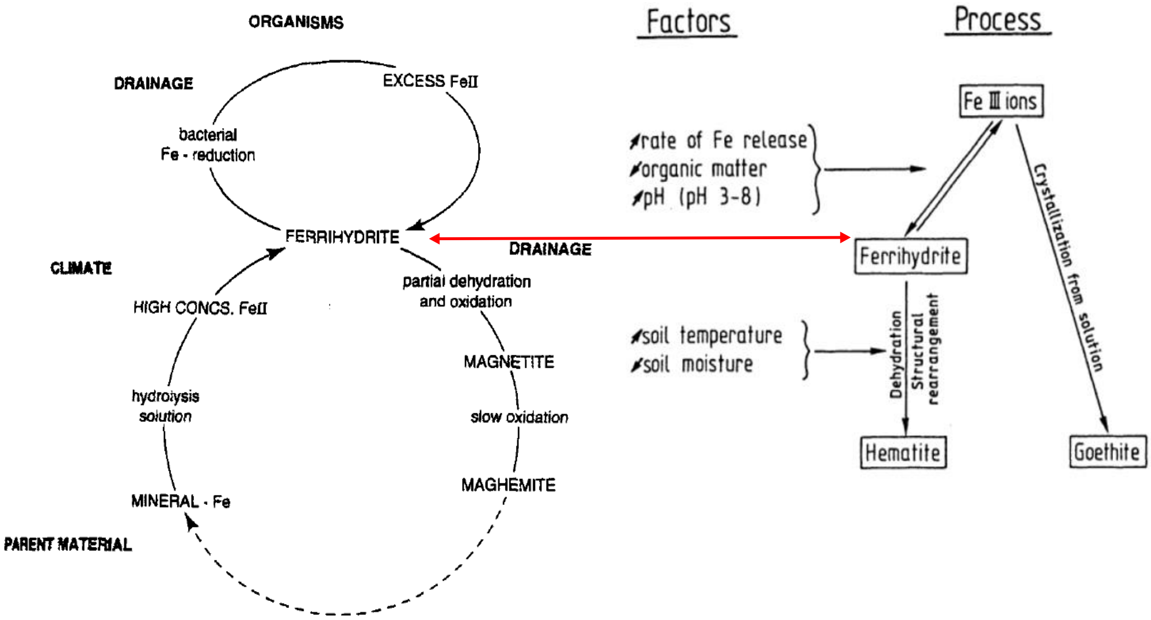

Figure 8: Schematic representation of pedogeochemical pathways of formation of magnetic minerals in pedosphere system (adapted from Dearing et al., 1996; Schwertmann, 1988).

1.9. Perspectives magnetic susceptibility in soil science

Recently, many researchers were in order to evaluate soil processes throughout MS (Blundell et al. 2009; Sarmast et al. 2017; Ayoubi et al. 2018; Cervi et al. 2019; Gholamzadeh et al. 2019). The knowledge of these processes and combination of the MS with other sensors and technologies can be used as a tool in soil classification and digital mapping (Sarmast et al. 2017; Cervi et al. 2019). As a result, it will be possible to undertake farming and environmental planning and monitoring, in order to reach a sustainable land use and management.

REFERENCES

A. R. Fisher, 1925. No Title Statistical Methods for Research Workers. Oliver Boyd.

Ab’Sáber, 1957. Geomorfologia do Sítio Urbano de São Paulo.

Abbaszadeh Afshar, F., Ayoubi, S., Besalatpour, A.A., Khademi, H., Castrignano, A., 2016. Integrating auxiliary data and geophysical techniques for the estimation of soil clay content using CHAID algorithm. J. Appl. Geophys. 126, 87–97. https://doi.org/10.1016/j.jappgeo.2016.01.015

Alastair Ruffell, J.M., 2008. Geoforensics, in: Geoforensics. p. 288.

Alomari, A.H., Saleh, M.A., Hashim, S., Alsayaheen, A., 2019. Investigation of natural gamma radiation dose rate (GDR) levels and its relationship with soil type and underlying geological formations in Jordan. J. African Earth Sci. 155, 32–42. https://doi.org/10.1016/j.jafrearsci.2019.04.006

Alvares, C.A., Stape, J.L., Sentelhas, P.C., De Moraes Gonçalves, J.L., Sparovek, G., 2013. Köppen’s climate classification map for Brazil. Meteorol. Zeitschrift 22, 711–728. https://doi.org/10.1127/0941-2948/2013/0507

Arnedo, M.A., Rubiano, J.G., Alonso, H., Tejera, A., González, A., González, J., Gil, J.M., Rodríguez, R., Martel, P., Bolivar, J.P., 2017. Mapping natural radioactivity of soils in the eastern Canary Islands. J. Environ. Radioact. 166, 242–258. https://doi.org/10.1016/j.jenvrad.2016.07.010

Arrouays, D., Grundy, M.G., Hartemink, A.E., Hempel, J.W., Heuvelink, G.B.M., Hong, S.Y., Lagacherie, P., Lelyk, G., McBratney, A.B., McKenzie, N.J., Mendonca-Santos, M. d. L., Minasny, B., Montanarella, L., Odeh, I.O.A., Sanchez, P.A., Thompson, J.A., Zhang, G.-L., 2014. GlobalSoilMap: Toward a Fine-Resolution Global Grid of Soil Properties, in: Advances in Agronomy 125. pp. 93–134. https://doi.org/10.1016/B978-0-12-800137-0.00003-0

Asgari, N., Ayoubi, S., Demattê, J.A.M., 2018. Soil drainage assessment by magnetic susceptibility measures in western Iran. Geoderma Reg. 13, 35–42. https://doi.org/10.1016/j.geodrs.2018.03.003

Atalay, İ.C.S.S.K.M.E., 2018. Pedogeomorphology, in: The Soils of Turkey. Springer, Cham, pp. 75–103.

Aydin, A., Ferré, E.C., Aslan, Z., 2007. The magnetic susceptibility of granitic rocks as a proxy for geochemical composition: Example from the Saruhan granitoids, NE Turkey. Tectonophysics 441, 85–95. https://doi.org/10.1016/j.tecto.2007.04.009

Ayoubi, S., Abazari, P., Zeraatpisheh, M., 2018. Soil great groups discrimination using magnetic susceptibility technique in a semi-arid region, central Iran. Arab. J. Geosci. 11. https://doi.org/10.1007/s12517-018-3941-4

Ayoubi, S., Adman, V., 2019. Iron Mineralogy and Magnetic Susceptibility of Soils Developed on Various Rocks in Western Iran. Clays Clay Miner. 67, 217–227. https://doi.org/10.1007/s42860-019-00020-5

Ayoubi, S., Adman, V., Yousefifard, M., 2019. Use of magnetic susceptibility to assess metals concentration in soils developed on a range of parent materials. Ecotoxicol. Environ. Saf. 168, 138–145. https://doi.org/10.1016/j.ecoenv.2018.10.024

Ayoubi, S., Mirsaidi, A., 2019. Magnetic susceptibility of Entisols and Aridisols great groups in southeastern Iran. Geoderma Reg. 16, e00202. https://doi.org/10.1016/j.geodrs.2018.e00202

Barlow, J., Lennox, G.D., Ferreira, J., Berenguer, E., Lees, A.C., Nally, R. Mac, Thomson, J.R., Ferraz, S.F.D.B., Louzada, J., Oliveira, V.H.F., Parry, L., Ribeiro De Castro Solar, R., Vieira, I.C.G., Aragaõ, L.E.O.C., Begotti, R.A., Braga, R.F., Cardoso, T.M., Jr, R.C.D.O., Souza, C.M., Moura, N.G., Nunes, S.S., Siqueira, J.V., Pardini, R., Silveira, J.M., Vaz-De-Mello, F.Z., Veiga, R.C.S., Venturieri, A., Gardner, T.A., 2016. Anthropogenic disturbance in tropical forests can double biodiversity loss from deforestation. Nature 535, 144–147. https://doi.org/10.1038/nature18326

Baumann, M., Gasparri, I., Piquer-Rodríguez, M., Gavier Pizarro, G., Griffiths, P., Hostert, P., Kuemmerle, T., 2017. Carbon emissions from agricultural expansion and intensification in the Chaco. Glob. Chang. Biol. 23, 1902–1916. https://doi.org/10.1111/gcb.13521

Bazaglia Filho, O., Rizzo, R., Lepsch, I.F., Prado, H. do, Gomes, F.H., Mazza, J.A., Demattê, J.A.M., 2013. Comparison between detailed digital and conventional soil maps of an area with complex geology. Rev. Bras. Ciência do Solo 37, 1136–1148. https://doi.org/10.1590/s0100-06832013000500003

Beamish, D., 2015. Relationships between gamma-ray attenuation and soils in SW England. Geoderma 259–260, 174–186. https://doi.org/10.1016/j.geoderma.2015.05.018

Beamish, D., 2013. Gamma ray attenuation in the soils of Northern Ireland, with special reference to peat. J. Environ. Radioact. 115, 13–27. https://doi.org/10.1016/j.jenvrad.2012.05.031

Becegato, V.A., Becegato, V.R., Baum, C.A., Lavnitcki, L., Paulino, A.T., 2019. Multivariate statistical analysis correlating 238 U, 232 Th, and 40 K equivalent activities in soil to geochemical data from an agricultural area. J. Soils Sediments 19, 1901–1910. https://doi.org/10.1007/s11368-018-2161-6

Berkowitz, B., Dror, I., Yaron, B., 2008. Contaminant Geochemistry, Contaminant Geochemistry. https://doi.org/10.1007/978-3-540-74382-8

Binley, A., Hubbard, S.S., Huisman, J.A., Revil, A., Robinson, D.A., Singha, K., Slater, L.D., 2015. The emergence of hydrogeophysics for improved understanding of subsurface processes over multiple scales. Water Resour. Res. 1–30. https://doi.org/10.1002/2015WR017016.Received

Blundell, A., Dearing, J.A., Boyle, J.F., Hannam, J.A., 2009. Controlling factors for the spatial variability of soil magnetic susceptibility across England and Wales. Earth-Science Rev. 95, 158–188. https://doi.org/10.1016/j.earscirev.2009.05.001

Brevik, E.C., Calzolari, C., Miller, B.A., Pereira, P., Kabala, C., Baumgarten, A., Jordán, A., 2016. Soil mapping, classification, and pedologic modeling: History and future directions. Geoderma 264, 256–274. https://doi.org/10.1016/j.geoderma.2015.05.017

Broschat, T.K., 1995. Nitrate, phosphate, and potassium leaching from container-grown plants fertilized by several methods. HortScience 30, 74–77.

Camargo, O.A.; Moniz, A.C.; Jorge, J.A. & Valadares, J.M.A.S., 1986. Métodos de análise química, mineralógica e física de solos do Instituto Agronômico do estado de São Paulo. Bol. técnico 106, 94.

Camargo, L.A., Marques Júnior, J., Pereira, G.T., Bahia, A.S.R. de S., 2014. Clay mineralogy and magnetic susceptibility of Oxisols in geomorphic surfaces. Sci. Agric. 71, 244–256. https://doi.org/10.1590/S0103-90162014000300010

Cervi, E.C., Maher, B., Poliseli, P.C., de Souza Junior, I.G., da Costa, A.C.S., 2019. Magnetic susceptibility as a pedogenic proxy for grouping of geochemical transects in landscapes. J. Appl. Geophys. 169, 109–117. https://doi.org/10.1016/j.jappgeo.2019.06.017

Coey, J.M.D., 1987. Magnetic order in trioctahedral sheet silicates: A review, in: Proceedings of the International Clay Conference, Denver, 1985, The Clay Minerals Society, Bloomington,. pp. 261–266.

Cook, S.E., Corner, R.J., Groves, P.R., Grealish, G.J., 1996. Use of airborne gamma radiometric data for soil mapping. Aust. J. Soil Res. 34, 183–194. https://doi.org/10.1071/SR9960183

Cooper, M., Vidal-Torrado, P., Grimaldi, M., 2010. Soil structure transformations from ferralic to nitic horizons on a toposequence in southeastern Brazil. Rev. Bras. Ciência do Solo 34, 1685–1699. https://doi.org/10.1590/s0100-06832010000500021

Coulouma, G., Caner, L., Loonstra, E.H., Lagacherie, P., 2016. Analysing the proximal gamma radiometry in contrasting Mediterranean landscapes: Towards a regional prediction of clay content. Geoderma 266, 127–135. https://doi.org/10.1016/j.geoderma.2015.12.006

Curi, N., Franzmeier, D.P., 1984. Toposequence of Oxisols from the Central Plateau of Brazil. Soil Sci. Soc. Am. J. 48, 341–346. https://doi.org/10.2136/sssaj1984.03615995004800020024x

D. A. Clarck & D. W. Emerson, 1991. Notes on rock magnetization characteristics in applied geophysical studies. Explor. Geophys. 22, 547–555.

Da Costa, A.C.S., Bigham, J.M., Rhoton, F.E., Traina, S.J., 1999. Quantification and characterization of maghemite in soils derived from volcanic rocks in southern Brazil. Clays Clay Miner. 47, 466–473. https://doi.org/10.1346/CCMN.1999.0470408

Dahlkamp, F.J., 1993. Uranium Ore Deposits. Springer.

Damaceno, J.G., de Castro, D.L., Valcácio, S.N., Souza, Z.S., 2017. Magnetic and gravity modeling of a Paleogene diabase plug in Northeast Brazil. J. Appl. Geophys. 136, 219–230. https://doi.org/10.1016/j.jappgeo.2016.11.006

De Jong, E., Pennock, D.J., Nestor, P.A., 2000. Magnetic susceptibility of soils in different slope positions in Saskatchewan, Canada. Catena 40, 291–305. https://doi.org/10.1016/S0341-8162(00)00080-1

De Wispelaere, L., Marcelino, V., Regassa, A., De Grave, E., Dumon, M., Mees, F., Van Ranst, E., 2015. Revisiting nitic horizon properties of Nitisols in SW Ethiopia. Geoderma 243–244, 69–79. https://doi.org/10.1016/j.geoderma.2014.12.021

Dearing, J.A., 1999. Environmental Magnetic Susceptibility., 2 nd. ed, Using the Bartington MS2 system. Chi Publishing, Kenilworth, UK.

Dearing, J.A., 1994. Environmental magnetic susceptibility, using the Bartington MS2 system.

Dearing, J.A., Hay, K.L., Baban, S.M.J., Huddleston, A.S., Wellington, E.M.H., Loveland, P.J., 1996. Magnetic susceptibility of soil: An evaluation of conflicting theories using a national data set. Geophys. J. Int. 127, 728–734. https://doi.org/10.1111/j.1365-246X.1996.tb04051.x

Demattê, J.A.M., Araújo, S.R., Fiorio, P.R., Fongaro, C.T., Nanni, M.R., 2015. Espectroscopia VIS-NIR-SWIR na avaliação de solos ao longo de uma topossequência em Piracicaba (SP). Rev. Cienc. Agron. 46, 679–688. https://doi.org/10.5935/1806-6690.20150054

Deng, D.N., 2015. A comparative study of hand-held magnetic susceptibility instruments. M.Sc. Thesis 207.

Dennerley, C., Huang, J., Nielson, R., Sefton, M., Triantafilis, J., 2018. Identifying soil management zones in a sugarcane field using proximal sensed electromagnetic induction and gamma-ray spectrometry data. Soil Use Manag. 34, 219–235. https://doi.org/10.1111/sum.12410

Dickson, B.L.; Scott, K.M., 1997. Interpretation of aerial gamma-ray surveys – adding the geochemical factors. J. Aust. Geolology Geophys. 17, 187–200.

Dierke, C., Werban, U., 2013. Relationships between gamma-ray data and soil properties at an agricultural test site. Geoderma 199, 90–98. https://doi.org/10.1016/j.geoderma.2012.10.017

Domra Kana, J., Djongyang, N., Raïdandi, D., Njandjock Nouck, P., Dadjé, A., 2015. A review of geophysical methods for geothermal exploration. Renew. Sustain. Energy Rev. 44, 87–95. https://doi.org/10.1016/j.rser.2014.12.026

Egmond, F.M. Van, Veeke, S. Van Der, Knotters, M., Koomans, R.L., Limburg, J., 2018. Mapping soil texture with a gamma-ray spectrometer : comparison between UAV and proximal measurements and traditional sampling. WOt-technical Rep. 137, 58p.

EMBRAPA, 2017. Manual de metodos de analises, Manual de métodos de análise de solo.

EMBRAPA, 2011. Documentos 132 Manual de Métodos de. Embrapa 230.

Fabris, J.D., De Jesus Filho, M.F., Coey, J.M.D., Mussel, W.D.N., Goulart, A.T., 1997. Iron-rich spinels from Brazilian soils. Hyperfine Interact. 110, 23–32. https://doi.org/10.1023/A:1012619331408

Falco, N., Wainwright, H., Dafflon, B., Léger, E., Peterson, J., Steltzer, H., Wilmer, C., Rowland, J.C., Williams, K.H., Hubbard, S.S., 2019. Investigating Microtopographic and Soil Controls on a Mountainous Meadow Plant Community Using High-Resolution Remote Sensing and Surface Geophysical Data. J. Geophys. Res. Biogeosciences 124, 1618–1636. https://doi.org/10.1029/2018JG004394

FAOSTAT, 2003. Food and Agriculture Organization of the United Nations, Statistical Databases.

Ferreira, A., Daraktchieva, Z., Beamish, D., Kirkwood, C., Lister, T.R., Cave, M., Wragg, J., Lee, K., 2018. Indoor radon measurements in south west England explained by topsoil and stream sediment geochemistry, airborne gamma-ray spectroscopy and geology. J. Environ. Radioact. 181, 152–171. https://doi.org/10.1016/j.jenvrad.2016.05.007

Filho, B., 2012. Universidade de São Paulo Escola Superior de Agricultura " Luiz de Queiroz " Comparação entre mapas de solos obtidos pelos métodos convencional e digital numa área complexa Osmar Bazaglia Filho Piracicaba. Master Diss. Soils Plant Nutr. 190 p.

Filistovič, V., Maceika, E., Tarasiuk, N., Lukšiene, B., Konstantinova, M., Buivydas, Š., Koviazina, E., Puzas, A., 2015. Model of Non-equilibrium Multiphase Contaminant Transport in Lake Water-Sediment System. Water. Air. Soil Pollut. 226. https://doi.org/10.1007/s11270-015-2455-x

Fine, P., Singer, M.J., Verosub, K.L., 1992. Use of magnetic-susceptibility measurements in assessing soil uniformity in chronosequence studies. Soil Sci. Soc. Am. J. 56, 1195–1199. https://doi.org/10.2136/sssaj1992.03615995005600040032x

Foley, 2011. Sustain the Planet ? Sci. Am. 305, 60–65.

Fontes, M.P.F., De Oliveira, T.S., Da Costa, L.M., Campos, A.A.G., 2000. Magnetic separation and evaluation of magnetization of Brazilian soils from different parent materials. Geoderma 96, 81–99. https://doi.org/10.1016/S0016-7061(00)00005-7

Ghilardi, M., Kunesch, S., Styllas, M., Fouache, E., 2008. Reconstruction of Mid-Holocene sedimentary environments in the central part of the Thessaloniki Plain (Greece), based on microfaunal identification, magnetic susceptibility and grain-size analyses. Geomorphology 97, 617–630. https://doi.org/10.1016/j.geomorph.2007.09.007

Gholamzadeh, M., Ayoubi, S., Shahrivar, F.S., 2019. Using magnetic susceptibility measurements to differentiate soil drainage classes in central Iran. Stud. Geophys. Geod. 63, 465–484. https://doi.org/10.1007/s11200-018-0679-0

Gillot, P.Y., Hildenbrand, A., Lefèvre, J.C., Albore Livadie, C., 2006. The K/Ar dating method: principle, analytical techniques, and application to holocene volcanic eruptions in Southern Italy. Acta Vulcanol. 18, 55–66.

Godfray, H.C.J., Beddington, J.R., Crute, I.R., Haddad, L., Lawrence, D., Muir, J.F., Pretty, J., Robinson, S., Thomas, S.M., Toulmin, C., 2010. Food Security: The Challenge of Feeding 9 Billion People. Science (80-.). 327, 812 LP – 818. https://doi.org/10.1126/science.1185383

Govedarica, D.D., Gavrilov, M.B., Zeremski, T.M., Govedarica, O.M., Hambach, U., Tomić, N.A., Sentić, I., Marković, S.B., 2019. Relationships between heavy metal content and magnetic susceptibility in road side loess profiles: A possible way to detect pollution. Quat. Int. 502, 148–159. https://doi.org/10.1016/j.quaint.2018.01.020

GRANT, U.S., 1900. Contact metamorphism of a basic igneous rock. Geol. Soc. Am. Bull. 11, 503–510. https://doi.org/10.1130/gsab-11-503

Grimley, D.A., Arruda, N.K., Bramstedt, M.W., 2004. Using magnetic susceptibility to facilitate more rapid, reproducible and precise delineation of hydric soils in the midwestern USA. Catena 58, 183–213. https://doi.org/10.1016/j.catena.2004.03.001

Grimley, D.A., Vepraskas, M.J., 2000. Magnetic susceptibility for use in delineating hydric soils. Soil Sci. Soc. Am. J. 64, 2174–2180. https://doi.org/10.2136/sssaj2000.6462174x

Grison, H., Petrovsky, E., Kapicka, A., Stejskalova, S., 2016. Magnetic and chemical parameters of andic soils and their relation to selected pedogenesis factors. Catena 139, 179–190. https://doi.org/10.1016/j.catena.2015.12.005

Guagliardi, I., Buttafuoco, G., Apollaro, C., Bloise, A., De Rosa, R., Cicchella, D., 2013. Using gamma-ray spectrometry and Geostatistics for assessing geochemical behaviour of radioactive elements in the lese catchment (southern Italy). Int. J. Environ. Res. 7, 645–658.

Hanesch, M., Rantitsch, G., Hemetsberger, S., Scholger, R., 2007. Lithological and pedological influences on the magnetic susceptibility of soil: Their consideration in magnetic pollution mapping. Sci. Total Environ. 382, 351–363. https://doi.org/10.1016/j.scitotenv.2007.04.007

Hartemink, A.E., Krasilnikov, P., Bockheim, J.G., 2013. Soil maps of the world. Geoderma 207–208, 256–267. https://doi.org/10.1016/j.geoderma.2013.05.003

Heggemann, T., Welp, G., Amelung, W., Angst, G., Franz, S.O., Koszinski, S., Schmidt, K., Pätzold, S., 2017. Proximal gamma-ray spectrometry for site-independent in situ prediction of soil texture on ten heterogeneous fields in Germany using support vector machines. Soil Tillage Res. 168, 99–109. https://doi.org/10.1016/j.still.2016.10.008

Herrmann, L., Schuler, U., Rangubpit, W., Erbe, P., Surinkum, A., Zarei, M., Stahr, K., 2010. The potential of gamma-ray spectrometry for soil mapping. 19th World Congr. Soil Sci. 117–120.

Hooper, R.L., 1987. Factors affecting the magnetic susceptibility of baked rocks above a burned coal seam. Int. J. Coal Geol. 9, 157–169.

IUSS Working Group WRB, 2015. World reference base for soil resources 2014. International soil classification system for naming soils and creating legends for soil maps, World Soil Resources Reports No. 106. https://doi.org/10.1017/S0014479706394902

Ivanovich, M., Harmon, R.S., 1982. Uranium series disequilibrium: applications to environmental problems. Oxford University Press, USA.

J. A. Quaggio, Raij, B., 2001. Determination of pH in calcium chloride and total acidity. Chem. Anal. Fertil. Eval. Trop. Soils. Inst. Agronômico Campinas, Campinas 181–188.

Jiménez, C., Benavides, J., Ospina-Salazar, D.I., Zúñiga, O., Ochoa, O., Mosquera, C., 2017. Relationship between physical properties and the magnetic susceptibility in two soils of Valle del Cauca Relación entre propiedades físicas y la susceptibilidad magnética en dos suelos del Valle del Cauca. Cauca. Rev. Cienc. Agri 34, 33–45. https://doi.org/10.22267/rcia.173402.70

Johansson, M., Åkerman, H.J., 2008. Thawing Permafrost and Thicker Active Layers in Sub-arctic Sweden. Permafr. Periglac. Process. 19, 279–292. https://doi.org/10.1002/ppp

Jordanova, N., Jordanova, D., Mokreva, A., Ishlyamski, D., Georgieva, B., 2019. Temporal changes in magnetic signal of burnt soils – A compelling three years pilot study. Sci. Total Environ. 669, 729–738. https://doi.org/10.1016/j.scitotenv.2019.03.173

Jordanova, N., Jordanova, D., Petrov, P., 2016. Soil magnetic properties in Bulgaria at a national scale-Challenges and benefits. Glob. Planet. Change 137, 107–122. https://doi.org/10.1016/j.gloplacha.2015.12.015

Kelly, J.M., Resources, N., Lafayette, W., 1977. Acid precipitation effects on soil pH and base saturation of exchangeable sites 1, 401–408.

Kempen, B., Brus, D.J., Stoorvogel, J.J., Heuvelink, G.B.M., de Vries, F., 2012. Efficiency Comparison of Conventional and Digital Soil Mapping for Updating Soil Maps. Soil Sci. Soc. Am. J. 76, 2097. https://doi.org/10.2136/sssaj2011.0424

Khan, F.A., Fenton, T.E., 2010. Factors Affecting Potassium Status of Alluvial-Derived Soils of Western Iowa. Soil Sci. Soc. Am. J. 60, 836. https://doi.org/10.2136/sssaj1996.03615995006000030023x

Koch-Steindl, H., Pröhl, G., 2001. Considerations on the behaviour of long-lived radionuclides in the soil. Radiat. Environ. Biophys. 40, 93–104. https://doi.org/10.1007/s004110100098

Koons, R.D., Helmke, P.A., Jackson, M.L., 1980. Association of Trace Elements with Iron Oxides During Rock Weathering1. Soil Sci. Soc. Am. J. 44, 155. https://doi.org/10.2136/sssaj1980.03615995004400010032x

Lancmuir, D., Herman, J.S., 2002. 1-S2.0-0016703780902264-Main 44, 1–14.

Laubenstein, M., Plastino, W., Povinec, P.P., Fabbri, V., Aprili, P., Balata, M., Bella, F., Cardarelli, A., De Deo, M., Gallese, B., Ioannucci, L., Nisi, S., Antonecchia, D., Del Pinto, C., Giarrusso, G., 2013. Radionuclide mapping of the Molise region (Central Italy) via gamma-ray spectrometry of soil samples: Relationship with geological and pedological parameters. J. Radioanal. Nucl. Chem. 298, 317–323. https://doi.org/10.1007/s10967-012-2353-2

Li, J., Heap, A.D., 2008. A Review of Spatial Interpolation Methods for Environmental Scientists. Aust. Geol. Surv. Organ. GeoCat# 68, 154. https://doi.org/http://www.ga.gov.au/image_cache/GA12526.pdf

Lim, C.H., Jackson, M.L., 1986. Dissolution for total elemental analysis, in: Madison (Ed.), Methods of Soil Analysis. Part 2: Chemical and Microbiological Properties. American Society of Agronomy, pp. 1–12.

Lindon, J.C.G.E.T.D.W.K., 2016. Encyclopedia of Spectroscopy and Spectrometry, 3 edition. ed. Elsevir.

Lourenço, A.M., Sequeira, E., Sant'Ovaia, H., Gomes, C.R., 2014. Magnetic, geochemical and pedological characterisation of soil profiles from different environments and geological backgrounds near Coimbra, Portugal. Geoderma 213, 408–418. https://doi.org/10.1016/j.geoderma.2013.07.035

Lu, S., Wang, H., Bai, S., 2009. Heavy metal contents and magnetic susceptibility of soils along an urban - Rural gradient in rapidly growing city of eastern China. Environ. Monit. Assess. 155, 91–101. https://doi.org/10.1007/s10661-008-0420-5

Luque, E.C.L., 2008. Propiedades magnéticas de los óxidos de hierro en suelos mediterráneos. Universidad de Córdoba, Córdoba.

Maher, B.A., 1998. Magnetic properties of modern soils and quaternary loessic paleosols: Paleoclimatic implications. Palaeogeogr. Palaeoclimatol. Palaeoecol. 137, 25–54. https://doi.org/10.1016/S0031-0182(97)00103-X

Maher, B.A., Taylor, R.M., 1988. Formation of ultrafine-grained magnetite in soils. Nature 336, 368–370. https://doi.org/10.1038/336368a0

Marques, J., Siqueira, D.S., Camargo, L.A., Teixeira, D.D.B., Barrón, V., Torrent, J., 2014. Magnetic susceptibility and diffuse reflectance spectroscopy to characterize the spatial variability of soil properties in a brazilian haplustalf. Geoderma 219–220, 63–71. https://doi.org/10.1016/j.geoderma.2013.12.007

Mathé, V., Lévêque, F., 2003. High resolution magnetic survey for soil monitoring: Detection of drainage and soil tillage effects. Earth Planet. Sci. Lett. 212, 241–251. https://doi.org/10.1016/S0012-821X(03)00241-3

Maxbauer, D.P., Feinberg, J.M., Fox, D.L., 2016. Magnetic mineral assemblages in soils and paleosols as the basis for paleoprecipitation proxies: A review of magnetic methods and challenges. Earth-Science Rev. 155, 28–48. https://doi.org/10.1016/j.earscirev.2016.01.014

McBratney, A.B., Mendonça Santos, M.L., Minasny, B., 2003. On digital soil mapping, Geoderma. https://doi.org/10.1016/S0016-7061(03)00223-4

McFadden, M., Scott, W.R., 2013. Broadband soil susceptibility measurements for EMI applications. J. Appl. Geophys. 90, 119–125. https://doi.org/10.1016/j.jappgeo.2013.01.009

Mernagh, T.P., Miezitis, Y., 2008. A Review of the Geochemical Processes Controlling the Distribution of Thorium in the Earth ' s Crust and Australia ' s Thorium Resources 48.

Meyer, S. et al, 2019. Creating soil texture maps for precision liming using electrical resistivity and gamma ray mapping, 19th ed.

Michel, F.M., Barrón, V., Torrent, J., Morales, M.P., Serna, C.J., Boily, J.F., Liu, Q., Ambrosini, A., Cismasu, A.C., Brown, G.E., 2010. Ordered ferrimagnetic form of ferrihydrite reveals links among structure, composition, and magnetism. Proc. Natl. Acad. Sci. U. S. A. 107, 2787–2792. https://doi.org/10.1073/pnas.0910170107

Minty, B.R.S., 1997. GA1687.pdf.

Minty, B.R.S., 1988. A Review of Airborne Gamma-Ray Spectrometric Data-Processing Techniques. Aust. Gov. Publ. Serv.

Mokhtari Karchegani, P., Ayoubi, S., Lu, S.G., Honarju, N., 2011. Use of magnetic measures to assess soil redistribution following deforestation in hilly region. J. Appl. Geophys. 75, 227–236. https://doi.org/10.1016/j.jappgeo.2011.07.017

Moonjun, R., Shrestha, D.P., Jetten, V.G., van Ruitenbeek, F.J.A., 2017. Application of airborne gamma-ray imagery to assist soil survey: A case study from Thailand. Geoderma 289, 196–212. https://doi.org/10.1016/j.geoderma.2016.10.035

Morais, P.A. de O., Souza, D.M. de, Carvalho, M.T. de M., Madari, B.E., de Oliveira, A.E., 2019. Predicting soil texture using image analysis. Microchem. J. 146, 455–463. https://doi.org/10.1016/j.microc.2019.01.009

Muhammad Aqeel Ashraf;Mohd Jamil MaahMohd Jamil Maah; Ismail Bin YusoffIsmail Bin Yusoff, 2011. Introduction to Remote Sensing of Biomass. https://doi.org/10.5772/16462

Mullins, C.E., 1977. Magnetic Susceptibility of the Soil and Its Significance in Soil Science – a Review. J. Soil Sci. 28, 223–246. https://doi.org/10.1111/j.1365-2389.1977.tb02232.x

Nanni, M.R., Demattê, J.A.M., 2006. Spectral Reflectance Methodology in Comparison to Traditional Soil Analysis. Soil Sci. Soc. Am. J. 70, 393. https://doi.org/10.2136/sssaj2003.0285

Nico Van Breemen and Peter Buurman, 2003. Soil Formation, 2 nd. ed, KLUWER ACADEMIC PUBLISHERS. Laboratory of Soil Science and Geology, NEW YORK, BOSTON, DORDRECHT, LONDON, MOSCOW. https://doi.org/10.1017/CBO9781107415324.004

Oliveira, D. De, Santos, A.H.B. dos, 2008. Trajetórias do rio Capivari : implicações de um impacto meteorítico na drenagem no reverso. Geografias 04, 69–76.

P. Driessen, J. Deckers, O. Spaargaren, F.N., 2001. Lecture notes on the major soils of the world.

Paisani, J.C., Pontelli, M.E., de Barros Corrêa, A.Ô.C., Rech Rodrigues, R.A., 2013. Pedogeochemistry and micromorphology of oxisols - A basis for understanding etchplanation in the Araucárias Plateau (Southern Brazil) in the Late Quaternary. J. South Am. Earth Sci. 48, 1–12. https://doi.org/10.1016/j.jsames.2013.07.011

Pansu, M., Gautheyrou, J., 2006. Handbook of Soil Analysis – Mineralogical, Organic and Inorganic Methods. Springer, Netherlands.

Parasnis, D.S., 1986. Principles of Applied Geophysics, 4ª. ed.

Parker, R., Ruffell, A., Hughes, D., Pringle, J., 2010. Geophysics and the search of freshwater bodies: A review. Sci. Justice 50, 141–149. https://doi.org/10.1016/j.scijus.2009.09.001

Phil Bierwirth,Paul Gessler, McKane, and D., 1996. Proceedings of the 8th Australasian Remote Sensing Conference. Proc. 8th Australas. Remote Sens. Conf. 1–3.

Pinheiro, E.A.R., de Jong van Lier, Q., Inforsato, L., Šimůnek, J., 2019. Measuring full-range soil hydraulic properties for the prediction of crop water availability using gamma-ray attenuation and inverse modeling. Agric. Water Manag. 216, 294–305. https://doi.org/10.1016/j.agwat.2019.01.029

Priori, S., Bianconi, N., Costantini, E.A.C., 2014. Can γ-radiometrics predict soil textural data and stoniness in different parent materials? A comparison of two machine-learning methods. Geoderma 226–227, 354–364. https://doi.org/10.1016/j.geoderma.2014.03.012

R W Boyle, 1982. Geochemical prospecting for thorium and uranium deposits. Elsevier Scientific Publishing Company, Amsterdan.

Rahimi, M.R., Ayoubi, S., Abdi, M.R., 2013. Magnetic susceptibility and Cs-137 inventory variability as influenced by land use change and slope positions in a hilly, semiarid region of west-central Iran. J. Appl. Geophys. 89, 68–75. https://doi.org/10.1016/j.jappgeo.2012.11.009

Randall Schaetzel and Sharon Anderson, 2005. Soil Genesis and Geomorphology.

Rawlins, B.G., Lark, R.M., Webster, R., 2007. Understanding airborne radiometric survey signals across part of eastern England. Earth Surf. Process. Landforms 32, 1503–1515. https://doi.org/10.1002/esp.1468

Read, C.F., Duncan, D.H., Ho, C.Y.C., White, M., Vesk, P.A., 2018. Useful surrogates of soil texture for plant ecologists from airborne gamma-ray detection. Ecol. Evol. 8, 1974–1983. https://doi.org/10.1002/ece3.3417

Reinhardt, N., Herrmann, L., 2019. Gamma-ray spectrometry as versatile tool in soil science: A critical review. J. Plant Nutr. Soil Sci. 182, 9–27. https://doi.org/10.1002/jpln.201700447

Ribeiro, F.C.A., Silva, J.I.R., Lima, E.S.A., do Amaral Sobrinho, N.M.B., Perez, D. V., Lauria, D.C., 2018. Natural radioactivity in soils of the state of Rio de Janeiro (Brazil): Radiological characterization and relationships to geological formation, soil types and soil properties. J. Environ. Radioact. 182, 34–43. https://doi.org/10.1016/j.jenvrad.2017.11.017

Robinson, D.A., Panagos, P., Borrelli, P., Jones, A., Montanarella, L., Tye, A., Obst, C.G., 2017. Soil natural capital in Europe; A framework for state and change assessment. Sci. Rep. 7, 1–14. https://doi.org/10.1038/s41598-017-06819-3

Rochette, P., Jackson, M., Aubourg, C., 1992. Rock magnetism andn the interpretation of magnetic susceptibility. Rev. Geophys. 30, 209–226.

Rodríguez Martín, J.A., Arias, M.L., Grau Corbí, J.M., 2006. Heavy metals contents in agricultural topsoils in the Ebro basin (Spain). Application of the multivariate geoestatistical methods to study spatial variations. Environ. Pollut. 144, 1001–1012. https://doi.org/10.1016/j.envpol.2006.01.045

Roman, S.A., Johnson, W.C., Geiss, C.E., 2013. Grass fires-an unlikely process to explain the magnetic properties of prairie soils. Geophys. J. Int. 195, 1566–1575. https://doi.org/10.1093/gji/ggt349

Romero-Ruiz, A., Linde, N., Keller, T., Or, D., 2018. A Review of Geophysical Methods for Soil Structure Characterization. Rev. Geophys. 56, 672–697. https://doi.org/10.1029/2018RG000611

Rossel, R.A.V., Taylor, H.J., McBratney, A.B., 2007. Multivariate calibration of hyperspectral γ-ray energy spectra for proximal soil sensing. Eur. J. Soil Sci. 58, 343–353. https://doi.org/10.1111/j.1365-2389.2006.00859.x

Rutherford and Soddy, 1902. The cause and nature of radioactivity - Part I, Journal of African Earth Sciences. https://doi.org/10.1016/j.jafrearsci.2017.04.031

Rutherford, E., Soddy, F., 1902. XLI. The cause and nature of radioactivity .—Part I . London, Edinburgh, Dublin Philos. Mag. J. Sci. 4, 370–396. https://doi.org/10.1080/14786440209462856

S. R. Cattle, S. N. Meakin, P.R. and R.G.C., 2003. Using radiometric data to identify æolian dust additions to topsoil of the Hillston district, western NSW. Aust. J. Soil Res.

Santos-Francés, F., Gil Pacheco, E., Martínez-Graña, A., Alonso Rojo, P., Ávila Zarza, C., García Sánchez, A., 2018. Concentration of uranium in the soils of the west of Spain. Environ. Pollut. 236, 1–11. https://doi.org/10.1016/j.envpol.2018.01.038

Santos, H.L., Júnior, J.M., Matias, S.S.R., Siqueira, D.S., Pereira, G.T., 2011. Suscetibilidade magnética na identificação de compartimentos da paisagem em uma vertente. Rev. Bras. Ciencias Agrar. 6, 710–716. https://doi.org/10.5039/agraria.v6i4a1347

Sarmast, M., Farpoor, M.H., Esfandiarpour Boroujeni, I., 2017. Magnetic susceptibility of soils along a lithotoposequence in southeast Iran. Catena 156, 252–262. https://doi.org/10.1016/j.catena.2017.04.019

Sawyer, E.W., 1986. The influence of source rock type, chemical weathering and sorting on the geochemistry of clastic sediments from the Quetico Metasedimentary Belt, Superior Province, Canada. Chem. Geol. 55, 77–95. https://doi.org/10.1016/0009-2541(86)90129-4

Schuler, U., Erbe, P., Zarei, M., Rangubpit, W., Surinkum, A., Stahr, K., Herrmann, L., 2011. A gamma-ray spectrometry approach to field separation of illuviation-type WRB reference soil groups in northern Thailand. J. Plant Nutr. Soil Sci. 174, 536–544. https://doi.org/10.1002/jpln.200800323

Schwertmann, U., 1988. Occurrence and formation of iron oxides in various pedoenvironments. Iron soils clay Miner. 267–308. https://doi.org/10.1007/978-94-009-4007-9_11

Shenggao, L., 2000. Lithological factors affecting magnetic susceptibility of subtropical soils, Zhejiang Province, China. Catena 40, 359–373. https://doi.org/10.1016/S0341-8162(00)00092-8

Shenggao, L., 1998. Magnetic properties and iron oxide mineralogy of subtropical soils and environmental implications. Zhejiang University, China.

Silva, S.M.P. da, Crósta, A.P., Ferreira, F.J.F., Beurlen, H., Silva, A.M., Santos, L.F. dos, 2010. Espectrometria de raios gama de granitos pegmatíticos da Província Pegmatítica da Borborema (PPB), nordeste do Brasil. Rev. Bras. Geofísica 28, 673–690. https://doi.org/10.1590/s0102-261x2010000400011

Silvério, D. V., Bustamante, M., Brando, P.M., Macedo, M.N., Coe, M.T., Beck, P.S.A., 2015. Agricultural expansion dominates climate changes in southeastern Amazonia: The overlooked non-GHG forcing. Environ. Res. Lett. 10. https://doi.org/10.1088/1748-9326/10/10/104015

Singer, M.J., Fine, P., 1989. Pedogenic factors affecting magnetic susceptibility of northern California soils. Soil Sci. Soc. Am. J. 53, 1119–1127. https://doi.org/10.2136/sssaj1989.03615995005300040023x

Singer, M.J., Verosub, K.L., Fine, P., TenPas, J., 1996. A conceptual model for the enhancement of magnetic susceptibility in soils. Quat. Int. 34–36, 243–248. https://doi.org/10.1016/1040-6182(95)00089-5

Siqueira, D.S., Marques, J., Matias, S.S.R., Barrón, V., Torrent, J., Baffa, O., Oliveira, L.C., 2010. Correlation of properties of Brazilian Haplustalfs with magnetic susceptibility measurements. Soil Use Manag. 26, 425–431. https://doi.org/10.1111/j.1475-2743.2010.00294.x

Smith, R.C., Rose, A.W., 1975. Geology and Geochemistry of Triassic Diabase in Pennsylvania. Bull. Geol. Soc. Am. 86, 943–955. https://doi.org/10.1130/0016-7606(1975)86<943:GAGOTD>2.0.CO;2

Snnecker, J.P., 2000. Materiais Magnéticos Doces e Materiais Ferromagnéticos Amorfos. Rev. Bras. Ensino Física 22, 396–405.

Solutions, R., 2009. Spectrum stabilization and calibration for the RSI RS-125 and RS-230 handheld spectrometers.

Souza Junior, I.G. de, Costa, A.C.S. da, Vilar, C.C., Hoepers, A., 2010. Mineralogia e susceptibilidade magnética dos óxidos de ferro do horizonte B de solos do Estado do Paraná. Ciência Rural 40, 513–519. https://doi.org/10.1590/s0103-84782010000300003

Spassov, S., Egli, R., Heller, F., Nourgaliev, D.K., Hannam, J., 2004. Magnetic quantification of urban pollution sources in atmospheric particulate matter. Geophys. J. Int. 159, 555–564. https://doi.org/10.1111/j.1365-246X.2004.02438.x

Staff, S.S., 2017. Soil Survey Manual - Soil Taxonomy, Soil Survey Manual.

Sturchio, N.C., 2003. Uranium-series disequilibrium: Applications to Earth, Marine, and environmental sciences. Geochim. Cosmochim. Acta 57, 4327–4328. https://doi.org/10.1016/0016-7037(93)90331-p

Taylor, M J, Smettem, K., Pracilio, G., Verboom, W., 2002. Relationships between soil properties and high-resolution radiometrics, central eastern Wheatbelt, Western Australia. Explor. Geophys. 33, 95–102.

Taylor, Miranda J, Smettem, K., Smettem, K., Pracilio, G., Verboom, W., 2002. Relationships between soil properties and high-resolution radiometrics , central eastern Relationships between soil properties and high-resolution radiometrics , central eastern Wheatbelt , Western Australia 33, 95–102. https://doi.org/10.1071/EG02095

Thompson, R., Oldfield, F., 1986. Environmental Magnetism. Allen and, 227.

Triantafilis, J., Gibbs, I., Earl, N., 2013. Digital soil pattern recognition in the lower Namoi valley using numerical clustering of gamma-ray spectrometry data. Geoderma 192, 407–421. https://doi.org/10.1016/j.geoderma.2012.08.021

U. C. Sharma, 1998. Influence of soil texture and rainfall on leaching of potassium and its recovery by potato (Solonum tuberosum). Indian J. Agric. Sci. 59, 713–717.

Ulbrich, H.H.G.J., Ulbrich, M.N.C., Ferreira, F.J.F., Alves, L.S., Guimaraes, G.B., Fruchting, A., 2009. Gamma-spectrometric surveys in differentiated granites. I: A review of the method, and of the geochemical behavior of K, Th and U\rLevantamentos gamaespectrometricos em granitos diferenciados. I: Revisao da metodologia e do comportamento geoquimico dos el. Geol. USP - Ser. Cient. 9, 33–53.

Valaee, M., Ayoubi, S., Khormali, F., Lu, S.G., Karimzadeh, H.R., 2016. Using magnetic susceptibility to discriminate between soil moisture regimes in selected loess and loess-like soils in northern Iran. J. Appl. Geophys. 127, 23–30. https://doi.org/10.1016/j.jappgeo.2016.02.006

van Dam, R.L., Hendrickx, J.M., Harrison, B., Borchers, B., Norman, D.I., Ndur, S., Jasper, C., Niemeyer, P., Nartey, R., Vega, D.N., Calvo, L., Simms, J.E., 2004. Spatial variability of magnetic soil properties. Detect. Remediat. Technol. Mines Minelike Targets IX 5415, 665. https://doi.org/10.1117/12.540693

Vandenhove, H., Van Hees, M., Wouters, K., Wannijn, J., 2007. Can we predict uranium bioavailability based on soil parameters? Part 1: Effect of soil parameters on soil solution uranium concentration. Environ. Pollut. 145, 587–595. https://doi.org/10.1016/j.envpol.2006.04.011

Viscarra Rossel, R.A., Webster, R., Kidd, D., 2014. Mapping gamma radiation and its uncertainty from weathering products in a Tasmanian landscape with a proximal sensor and random forest kriging. Earth Surf. Process. Landforms 39, 735–748. https://doi.org/10.1002/esp.3476

W.K. Jung, N.R. Kitchen, S.H. Anderson, E.J.S., 2007. Crop management effects on water infiltration for claypan soils. J. Soil Water Conserv. 62, 55–63.

Wang, X., Li, Z., Cai, C., Shi, Z., Xu, Q., Fu, Z., Guo, Z., 2012. Effects of rock fragment cover on hydrological response and soil loss from Regosols in a semi-humid environment in South-West China. Geomorphology 151–152, 234–242. https://doi.org/10.1016/j.geomorph.2012.02.008

Wilford, J., 2012. A weathering intensity index for the Australian continent using airborne gamma-ray spectrometry and digital terrain analysis. Geoderma 183–184, 124–142. https://doi.org/10.1016/j.geoderma.2010.12.022

Wilford, P.N., Bierwirth, J.R., Craig, M.A., 1997. Application of airborne gamma-ray spectrometry in soiVregolith mapping and Applied Geomorphology 17.

Yates, F., 1934. The Analysis of Multiple Classifications with Unequal Numbers in the Different Classes. J. Am. Stat. Assoc. 29, 51–66. https://doi.org/10.1080/01621459.1934.10502686

Zhou, L.P., Oldfield, F., Wintle, A.G., Robinson, S.G., Wang, J.T., 1990. Partly pedogenic origin of magnetic variations in Chinese loess. Nature 346, 737–739. https://doi.org/10.1038/346737a0

Zolfaghari, Z., Mosaddeghi, M.R., Ayoubi, S., 2015. ANN-based pedotransfer and soil spatial prediction functions for predicting Atterberg consistency limits and indices from easily available properties at the watershed scale in western Iran. Soil Use Manag. 31, 142–154. https://doi.org/10.1111/sum.12167

2. SOILS NATURAL RADIOLOGICAL CHARACTERIZATION AND ITS RELATION WITH PEDOGENESIS, PEDOGEOMORPHOLOGICAL AND PEDOGEOCHEMICAL PROCESSES IN THE TROPICAL ENVIRONMENT

Danilo César de Mello[1], José Alexandre Melo Demattê[1]*, Fellipe Alcantara de Oliveira Mello[1], Raul Roberto Poppiel[1], Nélida Elizabet Quiñonez Silvero[1], José Lucas Safanelli[1], Arnaldo Barros e Souza[1], Luis Augusto Di Loreto Di Raimo[1], Rodnei Rizzo[1], Maria Eduarda Bispo Rezende[1]

[1] Department of Soil Science, "Luiz de Queiroz" College of Agriculture, University of São Paulo, Av. Pádua Dias, 11, CP 9, Piracicaba, SP 13418-900, Brazil; emails: daniloc.demello@gmail.com; jamdemat@usp.br*; fellipeamello@usp.br; raulpoppiel@gmail.com; neliquinhonez92@gmail.com; jose.lucas.safanelli@usp.br; arnaldo_bsouza@hotmail.com; luis.diloreto@hotmail.com; rodnei.rizzo@gmail.com; eduardaresende@usp.br
* Corresponding author

Abstract

The understanding of pedogeochemical, pedogeomorphological processes and their relationship with soil attributes can provide data that optimize land use and management. Geophysical methods such as proximal gamma spectrometry have high potential to provide information for understanding the processes that occur in the pedosphere and some pedological attributes. Therefore, this research was undertaken aiming at understanding and recognizing landscape dynamics, pedogenesis processes, soil attributes, as well as, the use of gamma-spectrometry. The study was carried out in southeastern Brazil. Soil samples were physico-chemical analyzed at 89 locations (0 - 20 cm). At these sites, surface gamma-spectrometric data were collected, which gives information about radionuclides such as uranium, thorium and potassium. The data were analyzed and geoprocessed using *R*, *SAGA GIS* and *ArcGIS* softwares. Radionuclides were analyzed in four topossequences and related to geology, relief and soil classes considering pedogeochemical aspects. The concentration of radionuclides in the soil has a direct relationship with the contents present in the parent material and, consequently, with the rocks and sediments mineralogy. In addition, the geochemical behavior and weathering of each radionuclide determines its permanence or its removal in the soil. Denudation processes that occur along each topossequence determine the distribution of radionuclides along the relief. The radionuclide contents in certain soil class is related to pedogenesis processes, mainly claying for more evolved soil classes and / or those with argic horizon, whereas in less evolved soil classes the parent material exerts a more significant effect than pedogenesis. There was a negative correlation between uranium and altitude, indicating greater mobility of this element in relation to thorium which, in turn presented a negative correlation with sandy texture and positive with clay. Potassium presented a positive correlation with soil CEC and clayey texture. The gamma-spectrometric sensor detected significant variations in certain parts of the topossequences, that were not detected in traditional soil survey. This may indicate changes from one soil class to another or the continuity of a particular soil class, demonstrating the potential of this tool for digital mapping and pedogeochemical, pedogeomorphological and pedogenesis processes studies.

Keywords: Soil; Gamma-ray spectrometry; Radionuclide; Digital soil mapping; Radioactivity mapping; Pedogenesis; Pedogeomorphology; Geochemistry; Geology

2.1. INTRODUCTION

Soil is the substrate for all agroforestry activities, being an essential environmental component for the maintenance of human life, through the production of food, fiber and wood (Robinson et al. 2017). According to FAOSTAT (2003), approximately 95% of world agriculture depends on the soil. Some studies suggest that food production will have to be nearly doubled to meet the demand of 9 billion people by 2050 (Godfray et al. 2010). As a result, agriculture has been expanding to new frontiers, causing losses of native vegetation, biodiversity and impacts on the hydrological cycle, carbon emission and soil degradation (Silvério et al. 2015; Barlow et al. 2016; Baumann et al. 2017).

The soil composes the pedosphere, which in turn, interfaces with the hydrosphere, lithosphere, atmosphere and biosphere, directly affecting the dynamics of all aquatic and terrestrial ecosystems. There are many processes occurring in pedosphere, which in turn affects other environmental spheres. Some of important processes are: pedogeomorphological referring to geomorphological effects like erosional and depositional processes on soil (Atalay, 2018); Pedogeochemical is the geochemical processes on mineral formation and some soil attributes (Paisani et al. 2013); Pedogenesis refers to geochemical and biological processes that result in specific soil classes formation and / or horizons (Van Breemen and Buurman, 2003).

To mitigate or prevent soil degradation, land planning is needed, throughout the knowledge of processes, attributes and their distribution on the landscape. Soil spatial information is important to the efficient use of resources, once it allow a better decision making and consequently a sustainable management of soils (Foley, 2011). Land surveys provide information on the spatial distribution of soil classes and attributes for a given area. However, according to Hartemink et al. (2013), few countries have detailed soil maps that, despite of provide useful information, do not attend the necessity of pedologists due to widespread information (Arrouays et al. 2014). In Brazil, the RADAMBRASIL project carried out in the 1970s produced pedological maps on the scale 1: 1,000,000 or less (McBratney et al. 2003), However, it provides only a general information about the soil variability.

Traditional soil mapping is expensive and time-consuming. Usually, it provides limited information (Soil Survey Staff, 2017), and in some cases, do not allow field incursions

(Kempen et al. 2012). Nevertheless, in recent years, new technologies have emerged allowing Earth observation, being remote sensing one of the most important for soil data acquisition (Soil Survey Staff, 2017). According to McBratney et al (2003), the proximal remote sensing can be used to soil attributes mapping. Among the techniques, the reflectance spectroscopy is one of most used to extract soil information. However, these techniques have limitations in time to prepare samples (Demattê et al. 2015).

Recently, geophysical methods such as gamma-spectrometry, so far used for geological prospecting, have great potential for soil studies (Schuler et al. 2011; Beamish, 2013; Reinhardt and Herrmann, 2019). Herrmann et al. (2010) highlighted the distinction of soil and relief classes in Thailand using this technique. Moonjun et al. (2017), emphasized the importance of the technique to understand soil formation processes. These authors, combine gamma spectrometry to digital elevation model and generated pedological maps.

Gamma spectrometry is a geophysical technique that generates data from gamma radiation emitted by naturally occurring radionuclides in rocks, minerals, soils and sediments (Minty, 1988). Radionuclides are natural radioactive elements, mainly by thorium, uranium and potassium, that emit radiation and are governed by the law of radioactive decay, a process that generates gamma rays and are of short wavelength electromagnetic spectrum.

The quantification and understanding of the radionuclides distribution (eTh, eU and K) in rocks, sediments, soils and on the landscape can provide insights about pedogeomorphological processes. It also indicate chemical composition of rock constituent minerals and mineralogical composition which may describes secondary minerals weathering products (Wilford et al. 1997). However, due to the complexity of the quantities and distribution of radionuclides in soils and landscape, for each environment, a conceptual model of behavior and understanding of radionuclides, as well as they relationship with environmental variables should be elaborated, due to the particular geological and pedogeochemical differences of each environment.

Recent researches has been carried out using the gamma-spectrometric technique with emphasis on the prediction of soil attributes such as texture and hydraulic properties (Beamish, 2013; Priori et al. 2014; Heggemann et al. 2017; Read et al. 2018; Pinheiro et al. 2019; Morais et al. 2019), precision agriculture (Dierke and Werban, 2013; Dennerley et al. 2018; Meyer, 2019) and digital soil mapping (Herrmann et al., 2010). However, the results of most studies show the limitations of sensors and technique for prediction and correlation with certain soil attributes, digital soil mapping and understanding of landscape dynamics, due to the poor information about how radionuclides are distributed in the environment and the natural processes that determine this distribution (Laubenstein et al., 2013). Therefore, to advances in gamma-spectrometry technique applied to soil science, it is necessary to go forward on understand of the radionuclide variation along landscape and its relationship with environmental processes in pedosphere, as well as the relationship with soil attributes and their applications.

The radionuclides present in soil parent material, after release in soil solution by weathering, it can have many pathways in soil profile and on landscape. The behavior of radionuclides dependent of geochemical proprieties of each element. Due to this, the hypothesis of this research assumes that the concentration and distribution of radionuclides on the landscape has a direct relation with geomorphological, geochemical and pedogenetic processes that occur in the pedosphere and some of its attributes.

Given the above, the present research aims to underline the fundamentals of emitted gamma radiation along relief, by pedogeomorphological, pedogeochemical and physicochemical point of view, as well as its relationship with some soil attributes. We expect to provide a basis for understanding the distribution and concentration of radionuclides in the relief and the integrated soil processes evolved, allowing improves in soil attribute prediction modeling, pedogeoenvironmental reconstruction, geological infers, geochemical history, pedogenesis processes related to soil classes and digital soil mapping. With this information, it is possible to determine the appropriate use and management of soil in order to achieve sustainable land use.

2.2. MATERIAL AND METHODS

2.2.1. Study area, soil sampling and physicochemical analysis

The study area has 183 hectares and is located in Raffard County, São Paulo State, southwest of Brazil, between the geographic coordinates 23º 0’ 31.37” to 22º 58’ 53.97” S and 53º 39’ 47.81” to 53º 37’ 25.65” W, in the Capivari river basin, Tietê sub-basin **(Fig. 1)**, with the predominance of sugarcane cultivation. Geomorphologically, this area is inserted in the Paulista Peripheral Depression, with predominance of ancient Paleozoic sedimentary rocks, relatively less resistant to weathering and erosion, than the formations of the oldest neighboring plateaus (Atlantic Plateau to the east and Western Plateau to the west). The altitude and slope range from 474 to 567 meters and 0 to 35%, respectively **(Fig. 2a and 2d).**

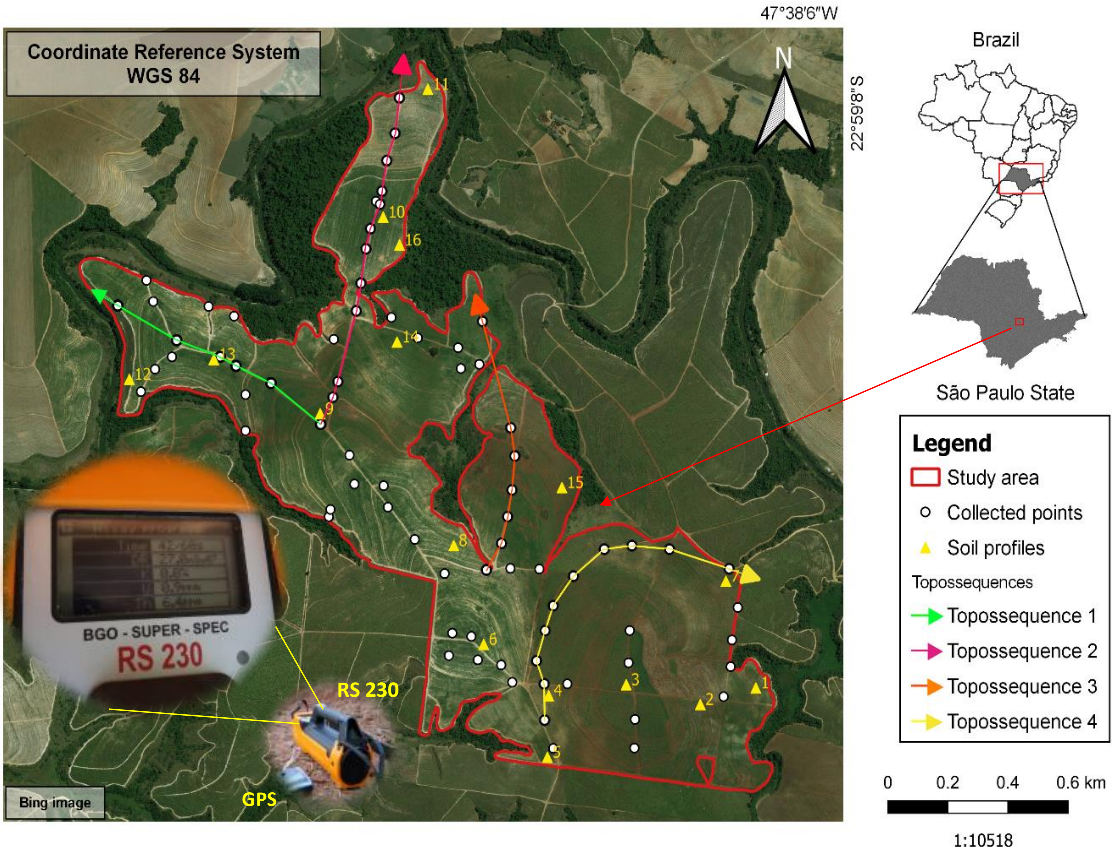

Figure 1. a) Study area, collected points and selected topossequences and Gamma-ray spectrometer (RS 230) reading soil surface and GPS attached to sensor.

The geology pertaining to Itararé formation (Tubarão group), which is composed by siltstone and metamorphic siltstones, as well as, intrusive diabase dykes of the Serra Geral Formation (São Bento group) and fluvial sediments deposited by the Capivari River in ancient fluvial terraces **(Fig. 2b)**. According to the Köppen classification, the region's climate is subtropical mesothermal (Cwa), with average winter temperatures of 18 ° C (July) and summer temperatures of 22 ° C (February). Regarding the average annual precipitation, the volumes vary between 1100 and 1700 mm (Alvares et al., 2013; Nanni and Demattê, 2006).

Due to geological complexity and heterogeneous relief, the soils that occur in the area (**Fig. 2c**) were allocated into several classes. For soil classification, 16 profiles were evaluated (**Fig. 1**), and were classified according to (Bazaglia Filho et al. 2013; Nanni and Demattê, 2006) in: Cambisols, Phaeozems, Nitisols, Acrisols e Lixisols (IUSS Working Group WRB, 2015). In addition to the profiles, soil samples were collected for the physicochemical analyzes, through augers, in 89 points (0 - 20 cm layer), distributed according to **Fig. 1**.

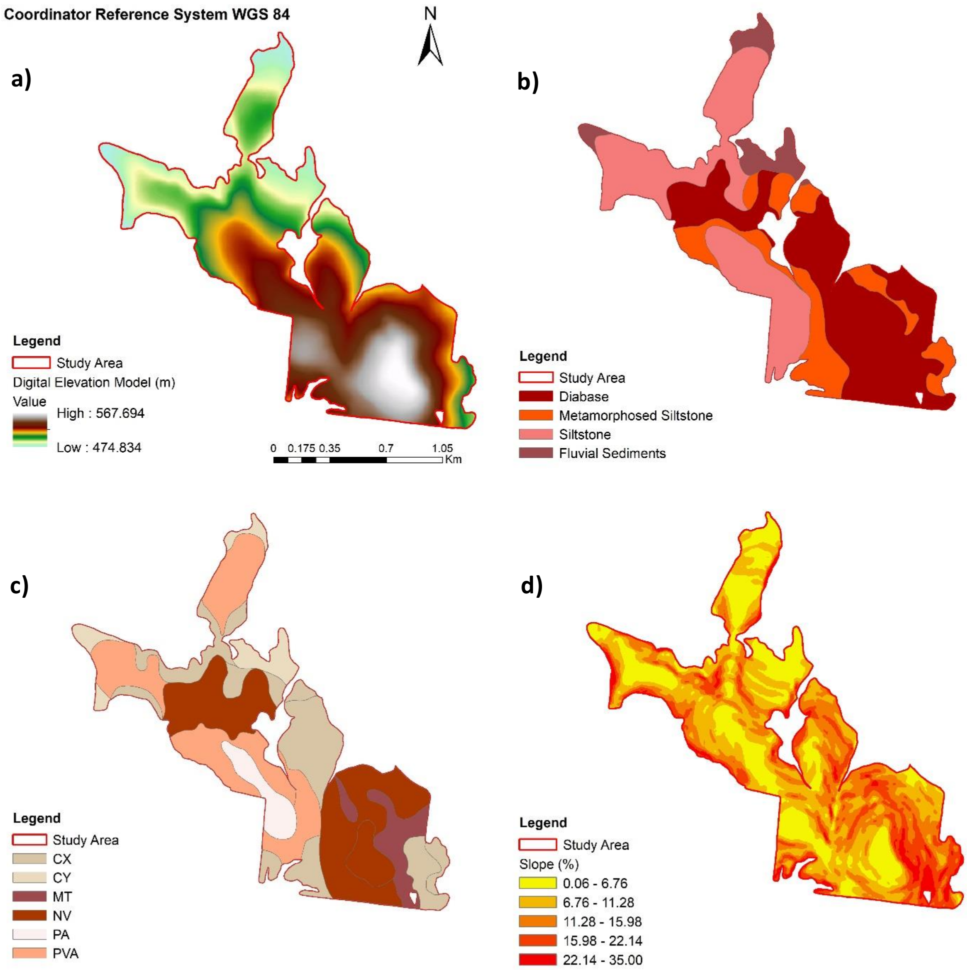

Figure 2. a) Digital elevation model. b) Geological compartments of landscape. c) Soil classes: CX: Haplic Cambisols, CY: Fluvic Cambisols, MT: Luvic Phaozem, NV: Rhodic Nitisol: PA: Xanthic Acrisol, PVA: Rhodic Lixisol. The geological and Soil classes maps were adapted from Bazaglia Filho et. al. (2012). d) Slope.

The sand, silt and clay contents were determined by the densimeter method, according to Camargo, et al. (1986) and the textural groups following EMBRAPA, (2011). The dry and wet color of the samples was determined using the Munsell color chart. For the determination of exchangeable cations, Calcium (Ca), Magnesium (Mg), Potassium (K) and sum of bases (SB), as well as, the other chemical attributes, base saturation (V%), aluminum saturation (m%), electrical conductivity (ECC), pH in water and KCl, total and effective acidity and organic matter content were determined according to EMBRAPA, (2017).

2.2.2. Geophysical data collection

Game-spectrometric measurements were performed using the near-gamma-spectrometer (GM) model Radiation Solution RS 230 (**Fig. 1**). The main captured energy by sensor originates from soil depth of 30 to 60 cm, depending on bulk density and wetness (Wilford et al. 1997; Taylor et al. 2002; Beamish, 2015). Automatic GM calibration was performed by switching on and leaving the sensor on the ground surface for approximately 5 minutes until the readings of the eU, eTh and K contents were stable, where the mean values are graphically demonstrated and the sensor outputs, which a beep, indicating that the device is properly calibrated (Radiation Solutions, 2009). Measurements were taken in the 'assay-mode', the highest precision, which radionuclide contents are quantified in parts per million (ppm) for eU and eTh, whereas for K the unit of measurement is in percent (%). Gamma-spectrometric readings of eU, eTh and K contents, were maintained during the interval of 2 minutes by each point, allowing enough time to establish a stable spectrum (**Fig. 1)**. The GM has an own GPS that was coupled to the equipment, which allowed georeferencing with altimetric dimensions of the collected points. The collected data were stored in the memory of the equipment itself, where they were later transferred to a computer, where tables were generated, in a format compatible with the geoprocessing software and, where these data were concatenated with their respective information from the physicochemical analyzes of all collection points for later geoprocessing.

2.2.3. Generation of digital elevation model, slope and maps

The digital elevation model (DEM) and slope (S) models were extracted from the database, crated from GPS data and tabulated on the computer, using the SAGA GIS (2.1.2) software and the *terrain analysis* tool. In order to analyze the behavior of radionuclide contents distributions in relation to geology, soil classes and relief, four topossequences were also established, using ArcGIS 10.3 software (ESRI, 2011), with length ranging from 850 m to 1180 m and altitudes ranging from 550 m to 477.2 m (**Fig. 1**), spanning four geological compartments and six soil classes (**Fig. 2a 2b and 2c, respectively**).

2.2.4. Statistical analysis

Descriptive statistical analysis was performed using the software *R* (R Core Team, 2015), *boxplot* function *corrplot* package, where the values of maximum, minimum, mean, median, standard deviation (SD) and coefficient of variation (CV) were obtained for radionuclide contents in relation to geology, topossequences and soil classes. Also, a *Pearson* correlation analysis was performed between all soil attributes and radionuclide contents. Analysis of variance (ANOVA) with *type III error* was performed by comparing radionuclide contents between lithology and soil classes (**Fig. 4 b and c**). At this stage, the *R emmeans*

(Estimated Marginal Means) package was also used to consider the averaging for unbalanced levels. The ANOVA was performed using *the sums of squares type III* proposed by (Fisher, 1925) and described by (Yates, 1934). Subsequently, the means were compared using the *Simultaneous Inference in General Parametric Models* (*R*) *multcomp* package, to verify statistically significant differences between radionuclide concentrations over the lithological compartments and soil classes using marginal contrasts adjusted by *Tukey*.

The interpolations of the three radionuclides were performed aiming to compare the punctual values and analyses the spatial distribution on study area, using the software ArcGIS 10.3 (ESRI, 2011) and the *interpolation tool (IDW),* inverse square of distance method.

2.3. RESULTS AND DISCUSSION

2.3.1. Distribution of radionuclides and relationship with geology, mineralogy and pedogeochemical processes

The mean contents of the radionuclides eU, eTh and K, on the lithological compartments, diabase, metamorphosed siltstone, siltstone and fluvial sediments are shown in **Table 1**.

Table 1. Descriptive statistics for the analyzed radionuclides by geological compartments

Summary Statistics	***eU*** [1]				***eTh*** [2]				***K*** [3]			
	D	**MS**	**S**	**FS**	**D**	**MS**	**S**	**FS**	**D**	**MS**	**S**	**FS**
Mean	2.28	2.93	2.95	2.94	6.70	7.49	6.97	6.81	0.33	0.76	0.21	0.38
Standard deviation	0.72	0.58	0.71	0.61	1.62	1.94	2.71	2.51	0.25	0.42	0.16	0.16
Minimum	1.1	2	1.9	2.1	3	3.8	3.5	4.5	0	0.3	0	0.1
Maximum	3.6	3.8	5.1	3.8	10	12.1	17.2	10.2	1.1	1.4	0.8	0.5
Count	24	15	31	5	24	15	31	5	24	15	31	5

[1] Equivalent Uranium. [2] Equivalent Thorium. [3] Equivalent Potassium. D: Diabase, MS: Metamorphosed Siltstone, S: Siltstone, FS: Fluvial sediments.

The highest contents of the eU and eTh radionuclides (**Table 1**) were observed on the areas located on sedimentary rocks (metamorphic siltstone and siltstone) and fluvial sediments. These results disagree with those obtained by Berkowitz et al. (2008), Dickson & Scott, (1997) and Sturchio, (2003), who observed the lowest contents of these elements on sedimentary rocks. This behavior can be explained by the nature of these rocks. In this case, the particles from sedimentary rocks were originated from pre-weathered sediments. Consequently, they tend to have lower levels of these radionuclides, compared to igneous and metamorphic rocks. The higher levels of eU and eTh radionuclides on sedimentary rocks can be explained by the fact that the concentrations of each radionuclide primarily reflect the mineralogy of each rock or sediment in the landscape. Metamorphosed siltstone and siltstone consist, mineralogically, in quartz, feldspar and micas, which in turn have trace minerals, torite ($ThSiO_4$), uranite (UO_2), thorogummite [Th (SiO_4) 1-X (OH) 4X] and zirconium ($ZrSiO_4$) (Mernagh and Miezitis, 2008). These minerals are rich in the silicon element which is related to higher U and Th contents (Guagliardi et al. 2013). In fact, Dickson & Scott (1997), Wilford et al. (1997) and Arnedo et al. (2017) found a positive correlation between radionuclide contents and silicon concentration in igneous rocks (**Fig. 5a**). This also explains the lower levels of eU and eTh radionuclides on diabase, which have low contents of these elements due to their mineralogy (Dickson & Scott. 1997; Mernagh and Miezitis, 2008; Silva et al. 2010 and Arnedo et al. 2017).

The radionuclide K concentrations were low in all geological compartments (**Table 1**). This radionuclide is present in greater quantity in the silicate minerals such as feldspars and micas that constitute the metamorphic siltstones. Therefore, K concentrations are higher on these rocks compared to diabase, with lower silicate mineral contents. These results are also corroborated by works by Dickson & Scott, (1997) who demonstrated low K contents in mafic igneous rocks.

The U has higher solubility and mobility compared to Th under oxidizing conditions (Wilford, 2012), consequently, there was a depletion in the contents of the first and an enrichment of the second in the geological compartment corresponding to the metamorphosed siltstone (**Table 1**). Similar results were reported by Ribeiro et al. (2018), when they investigated the levels of radionuclides eU, eTh and K in the igneous-metamorphic pedogeoenvironment in Rio de Janeiro, Brazil. It is important to highlight that, in addition to geology, the geochemical events that occurred in the area of each radionuclide act in determining its concentration and distribution on the landscape (Dickson & Scott, 1997). In fact, according to Wilford et al. (1997), in a tropical environment with highly chemically weathered soils, moderately acidic pH and free drainage, the radionuclide K has high mobility and is easily leached from the system and a small part is retained in soil CEC, contributing to lower concentration and distribution of this element in the area. With respect to eU and eTh, they present low mobility and are more stable during the weathering process, being adsorbed to iron, aluminum and titanium oxides, tending to concentrate in soil waste materials (Dickson & Scott, 1997; Wilford, 2012).

Regarding fluvial sediments, the mean eU and eTh contents were 2.94 and 6.81 ppm, respectively, while the K content was 0.38% (**Table 1**). The low K and moderate eU and eTh contents can be explained by the higher Capivari river transport of sediments which are derived from sedimentary rocks. Additionally, a smaller fraction of sediments derived from igneous and metamorphic rocks, since this region would have been covered by Resende Formation sediments where in a later and more recent geomorphological event, the river carved out crystalline rocks (Ab'Sáber, 1957; Oliveira and Santos, 2008). These results agree with those obtained by Wilford et al. (1997), who reported a higher presence of zircon mineral in the old sandy river deposits and high levels of eU and eTh, while the levels of K were low. Boyle (1982) also found eU levels ranging from 0.5 to 5 ppm in fluvial sediments, which according to Taylor et al. (2002) is due to the presence of weathering-resistant minerals.

The **Fig. 4** shows mean comparison test and boxplot for radionuclides and environmental variables. According to the Tukey test (**Fig. 4a**) the significant statistical differences were for radionuclides K and U, on the different lithological compartments. This probably is due to the high mobility of K and lower mobility of eTh, in addition to mineralogical composition of lithology, as explained above (Dickson & Scott, 1997).

2.3.2. Variability of radionuclides on landscape and pedogeomorphological processes

Analyzing topossequence 1 (T1) (**Fig. 3**), the highest levels of eU and eTh (3.8 and 9.1 ppm, respectively) occur at an altitude of 496.2 m (P3), where there was a slight depression in relation to surrounding relief and, situated on the siltstone geological compartment. In addition, the highest K contents (0.6%) occur in the lower part of T1, at P6 (513.4 m). Radionuclides contents and distribution on the landscape depend of many factors. The most important ones are the parent material, the balance and intensity of weathering and pedogenesis processes, as well as landscape denudation processes (Wilford et al. 1997). Higher levels of eU and eTh on the depression along T1 can be explained by erosive processes, where materials containing these elements were eroded and transported from the highest parts and deposited on this depression, thus, the landscape denudation is higher active in relation to weathering and pedogenesis. Schuler et al. (2011), found similar results when studied the behavior of U, Th and K in soil classes in Thailand, where in a depressed area there was an increase in the levels of these radionuclides. These researchers explained the phenomenon by the selective transport of materials containing these elements. Thus, erosive and depositional geomorphological phenomena were more relevant to determine the levels and distribution of eU and eTh at this point than lithology. Similarly, Cattle et al. (2003) explained how the erosive and depositional processes in Australian soils, affect the distribution of radionuclides on the landscape. The low K content at this point P3 (0.1%) can be explained by the high leaching rates, and on a micro scale can be considered depositional and stable surface. Similarly, Bierwirth et al. (1996) and Wilford et al. (1997), studied radionuclide contents in soils derived from meta sedimentary rocks with low K contents in highly weathered environment and stable geomorphic surface. The authors justified the lower levels of this radionuclide by the high K mobility in this environment in relation to eU and eTh.

The null value of eTh (0 ppm) at altitude 496.8 m (T1 - P4) (**Fig. 3**) over siltstone explains the discrepancy from the mean value of the boxplot (**Fig. 4b**). This point is a slight elevation from the left and right micro-depression of the rest of the topossequence and is an area of erosive material loss, a phenomenon that may explain the null value of eTh.

The highest K contents in the lower parts (0.6%) at P5 and P6 and, the lowest K content in the highest parts P1, P2, P3 and P4 (varying between 0.1 - 0.2%) of T1 (**Fig. 3**) can be explained either by the mineralogy of the silt-rich parent material (minerals containing K feldspars and micas), or by transporting this element through erosion or leaching to the landscape lower parts (Broschat, 1995; Sharma, 1998). These results are also reported by Khan and Fenton, (2010) who found a depletion of the K contents in the higher parts of the landscape and higher levels in the lower parts. They attributed these results to the different intensities of weathering at each part of the landscape.

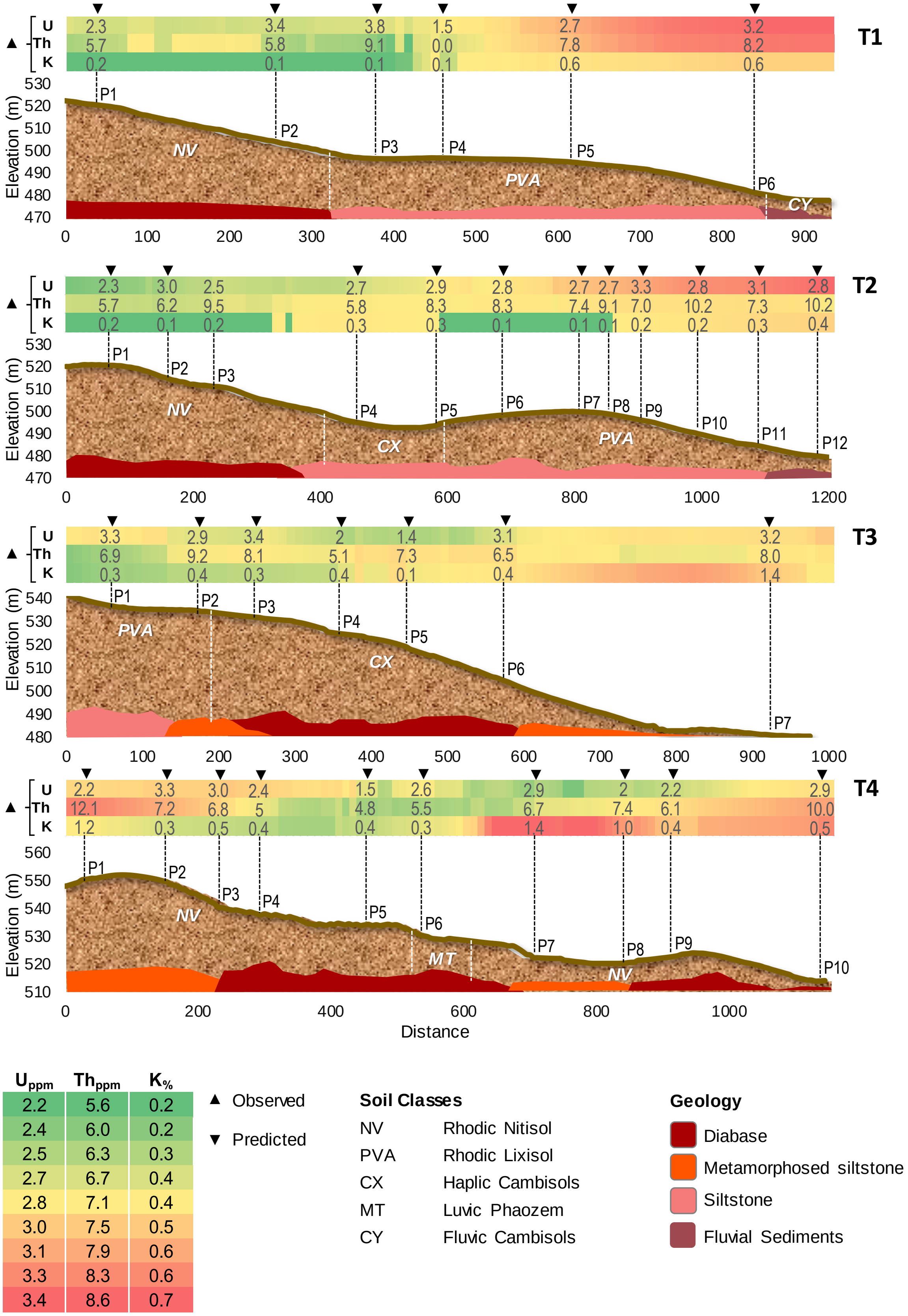

Figure 3. Distribution and concentration of radionuclides (uranium, thorium and potassium) throughout the four topossequences and correspondent soil classes and geological compartment for each collected point. T1: topossequences 1. T2: topossequences 2. T3: topossequences 3. T4: topossequences 4.

Similar to T1, T2 presented higher concentrations of eU (3.3 ppm) occurring at an approximate altitude of 496.9 m (P9), also on siltstone (**Fig. 3**). In relation to eTh the highest concentrations (10.2 ppm) occur in the lower parts of the landscape (489.4 and 477.2 m) at P10 and P12, on siltstone and fluvial sediments, respectively. Higher K concentration (0.3 and 0.4%), occurs in the lower parts of the landscape at P11 and P12 (483.7 and 477.2 m, respectively), on siltstone and fluvial sediments. The high levels of eU and eTh are governed mainly by pedogenesis processes that are associated with the Lixisol class. In this case there is formation and translocation of clay (argilluviation) from superficial horizons to subsurface horizons, mainly at the top of B horizon. Such process result in greater adsorption of these radionuclides to clay minerals. According to Dickson & Scott, (1997), both uranium and thorium released in the weathering process are adsorbed to silicate and/or oxide clayey colloids. Herrmann et al. (2010) found similar results when studying the behavior of radionuclides in Thai Acrisols. The authors observed an increase in U and Th contents and a reduction in K, as the soil was weathered and oxide and clay minerals formation occurred in Lixisols and Ferralsols. Studying the behavior of radionuclides in Australia soils, Dickson & Scott, (1997), reported redistribution of Th and U within the soil profile. The authors described an increase in the concentration of eTh and eU at the top of B horizon in soils. According to them, this is due to increases in the clay content on this horizon and attributed this behavior to the adsorption of these radionuclides to the surface of the silicate and oxide clay mineral colloids.

Points located at 493 and 493.4 m altitude at P4 and P5 (**Fig. 3**), had slight depression in relation to the surrounding relief. Different from T1, in these points the erosion processes are more intensified and the area corresponding to the points are under Cambisol, shallow soil and less pedogenetically evolved. Thus, the levels of U, Th and K are closely related to the mineralogy of the parent material (siltstone), which justifies, for example, an abnormal pattern for the contents of K (0.3%). Wilford et al. (1997) report that in soils poorly evolved and thin, such as Cambisols and Leptosols, the gamma-spectrometric response is directly associated with rock mineralogy, especially the K response.

The higher eU (3.3 ppm) (P9) and lower eU (2.3 ppm) (P1) at T2 (**Fig. 3**) explain the *out layers* in the statistical analysis. This is related to the area of material loss (point corresponding to the lowest value) and the area of onset of accumulation, resulting this wide range variation from one point to another along T2.

At T3 (**Fig. 3**) the highest eU (P1) and eTh (P2) contents (3.3 and 9.2 ppm, respectively) were found at the highest altitudes (535.2 and 534.4 m, respectively), with eU over siltstone and eTh over metamorphosed siltstone. The diabase lithology presented the lowest eU contents (1.4 ppm – P5) at the intermediate altitude of the topossequence (516.7 m). On the other hand, the highest K values (1.4%) were found in the lower part (486.15 m – P7) on fluvial sediments. The high levels of eU and eTh, similarly to T2 can be explained by the action of the top of the landscape with lower erosion rates. Both points are over the area of Lixisol, which due to clayey the top of B horizon presents higher clay contents capable of adsorbing these radionuclides increasing its concentration. Similar results were obtained by Dickson & Scott, (1997) when studying the behavior of radionuclides in depth in argic horizons.

The top of the landscape in T3 (**Fig. 3**) tends to flat and erosion rates are lower than those of pedogenesis and weathering. The relatively low K values at these higher altitude points are also evidence of the high weathering rates. However, it is important to realize the parent material has higher potassium-containing minerals in its chemical composition and, as a result the levels of K are not too overly low. Wilford et al. (1997), explain the association of U and Th with silicate and sesquioxide clay minerals where these elements tend to concentrate in weathered soils due to the formation of fine particles, while depleting K contents due to leaching. Furthermore, this behavior of radionuclides in relation to pedogenesis and weathering was observed by Koons et al. (1980) and Wilford, (2012).

The higher K contents in lower parts of T2 (0.3, 0.4% - P11 and P12, respectively) and T3 (1.4% - P7) (**Fig.3**) can also be explained by the fact that these points are located on a more recent depositional surface of the Capivari river, where these sediments, also come from the higher parts of the landscape. The sediments carried by the Capivari River, which flows in a sedimentary environment, are rich in silt and sand, which in turn, contain K-rich minerals, such as feldspar and muscovite, contributing to the higher levels of this radionuclide in the fluvial depositional environment. Erosion and leaching of highland water flows also carry this element through both erosion and leaching, and K tends to settle and/or precipitate into river deposits. According to Wilford et al. (1997), on active depositional surfaces weathering rates occurs at a lower intensity and its influence on radionuclide distribution decreases. On the other hand, depositional processes govern the distribution of radionuclides, being the most important for K in this environment.

Regarding topossequence 4 (T4) (**Fig. 3**), the highest values of eU (P2) and eTh (P1) (3.3 and 12.1 ppm, respectively) were found in the highest parts of the landscape (550.6 m eTh and 548.9 m eU), similar to T3. Differently to the others topossequences, the highest K values (1.4 and 1% - P7 and P8, respectively) are associated with the intermediate altitudes of

522 m and 518.5 m, respectively, and on metamorphosed siltstone, which is a slight depression, as in T1 and T2. The highest values of eU and eTh are related to the geology and mineralogy of the parent material of soil (diabase), as well as to the pedogenesis (nitidization) processes with formation and translocation of clays and iron oxides in the formation of the *nitic* B horizon, associated with the class of the Nitisols (Wispelaere et al. 2015). At these points the highest levels of eU and eTh were recorded, possibly due to the adsorption of these elements to clays and iron oxides (Wilford et al. 1997; Herrmann et al., 2010; Wilford, 2012).

In relation to the higher K contents at intermediate altitudes at T4 (1.4% - P7) (**Fig. 3**), these values may be associated with surface transport through erosive processes and deposited in this micro depression in the relief. In fact, the lithology below is the diabase and this rock has minerals with low levels of this element, it being insufficient to explain higher levels of K, compared to neighboring points that present low levels in this radionuclide. It is possible to observe this wide variation in the K contents (**Fig. 3c**), due to the higher contents in that point, where the high values create a variation too different from the average of the K content. On the other hand, at P10, the low K concentration (0.5%) and high eU (2.9 ppm) eTh (10 ppm) contents at the lower T4 (513.4 m) may indicate that the deposition processes are smaller than weathering rates and that the Capivari River may have changed its course. According to studies by Ab'Sáber, (1957) and Oliveira and Santos, (2008), this occurred by a process of river capture or impact of a meteorite.

The **Fig. 4b** shows the Boxplot for topossequences for three radionuclides. It is possible to realize that the main variation occurred for K between the four topossequences. Also, the great variability was observed for U. It is probably due to geochemical behavior of each radionuclide and more or less parent material influence along each topossequence (Dickson & Scott, 1997).

2.3.3. Relationship between eU, eTh and K contents and distribution with weathering and pedogenesis processes

The descriptive statistics of the levels of eU, eTh and K for main soil classes are presented in **Table 2**. For Haplic Cambisols (CX) and Fluvic Cambisols (CY), the mean, maximum and minimum values, reflect the mineralogy of the original rock (metamorphosed siltstone, siltstone, diabase or fluvial sediments), since these soils are shallow, weathered and pedogenetically evolved, where erosive processes predominate over the pedogenetic ones. These values in radionuclide contents are outside the maximum and minimum limits found by Schuler et al. (2011) in Cambisols derived from limestone in Thailand, due to the different parent materials. These authors reported gradual increases in the levels of the three radionuclides in poorly evolved soils following the change of the parent material. Wilford et al. (1997) confirm these results by explaining that the radionuclide response on unstable geomorphic surfaces with active erosion is directly correlated with the parent material mineralogy and geochemistry.

The **Fig. 4c** demonstrates the differences by mean comparison test for the three radionuclides and soil classes. The main differences could be highlighted for K and U, due to the greater mobility during pedogenesis processes, mainly in more evolved soil classes.

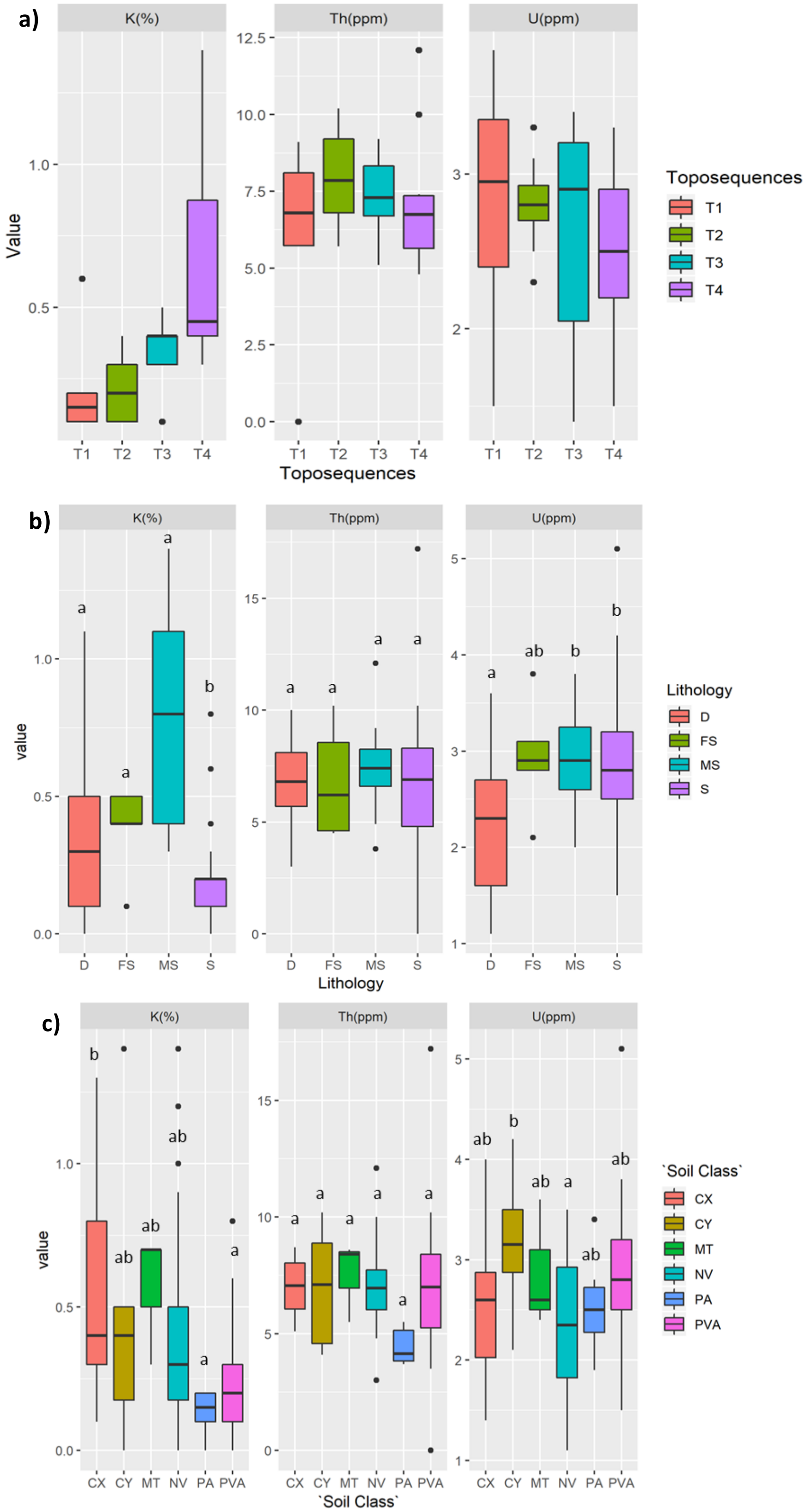

Figure 4. a) Multi comparison test for lithology for significant at the 0.1 significance level (b) *Boxplot* for topossequences (c) Multi comparison test for significant at the 0.1 significance level. Geology abbreviation; D: diabase, FS: fluvial sediments, MS: metamorphosed siltstone, S: siltstone. Soil classes abbreviation: CX: Haplic Cambisols, CY: Fluvic Cambisols, MT: Luvic Phaozem, NV: Rhodic Nitisol: PA: Xanthic Acrisol, PVA: Rhodic Lixisol.

In CY, located in alluvial deposits the mean K content (0.45%) was higher compared to CX (0.30%) (**Table 2**). According to Moonjun et al. (2017), this is related to recent depositional areas, where higher K contents are associated with silt and clay particle mineralogy rich in this element. These results are also supported by Dickson & Scott, (1997) and Rawlins et al. (2007) by studying the behavior of radionuclides in soils developed on recent colluvial sediments.

The values of the average radionuclide contents found in the soils of Rhodic Lixisol (PVA) and Rhodic Nitisol (NV) classes (**Table 2**) may be associated with the intense action of chemical weathering and pedogenesis, mainly on the U and Th (**Fig. 3e**) that redistribute these elements in the landscape (Cook et al., 1996). For the Lixisol class, these values were similar for K and lower for eU and eTh found Schuler et al. (2011). These authors studied radionuclides in soils in Thailand. They attributed this difference to the parent material (limestone). According to Viscarra Rossel et al. (2014), Nitisols originated from mafic rock on stable geomorphic has weathering favored. As a result, it has low gamma radiation emissions by radionuclides due to intense weathering mantle and K leaching. For PVA and NV, the predominant pedogenetic processes are the formation of clays and clayey with formation of iron oxides. These pedogenetic processes alter the concentrations and distribution of the three radionuclides in the soil and make the concentrations of eU, eTh and K not present similar levels to those found in the parent material. These results are corroborated by Moonjun et al. (2017), who explain the inconsistencies between the radionuclide levels found in soils and rocks, due to the action and interaction of weathering and pedogenesis processes.

Table 2. Descriptive statistics for the analyzed radionuclides by soil classes

Summary Statistics	***eU*** [1]				***eTh*** [2]				***K*** [3]			
	CX	***CY***	***PVA***	***NV***	***CX***	***CY***	***PVA***	***NV***	***CX***	***CY***	***PVA***	***NV***
Mean	2.48	2.45	3.03	2.52	6.75	9.375	8.23	7.15	0.30	0.45	0.24	0.54
Standard deviation	0.94	0.49	0.35	0.50	1.28	1.17	1.07	2.15	0.14	0.07	0.16	0.40
Minimum	1.4	2.1	2.7	1.5	5.1	8.55	6.9	4.8	0.1	0.4	0.1	0.1
Maximum	3.4	2.8	3.8	3.3	8.1	10.2	10.2	12.1	0.4	0.5	0.6	1.4
Count	4	2	11	13	4	2	11	13	4	2	11	13

[1] Equivalent Uranium. [2] Equivalent Thorium. [3] Equivalent Potassium. CX: Cambisol, CY: Fluvic Cambisol, PVA: Rhodic Lixisol, NV: Rhodic Nitisol.

The **Fig. 5** demonstrates the behavior of radionuclides according to mineralogy of soil parent material and weathering/pedogenesis processes. The **Fig. 5c** demonstrates the general behavior of U, Th and K according to variability of weathering and pedogenesis processes by soil classes. It is possible to realize that, increases in weathering and pedogenesis process, result in soil classes evolution and increases in U, Th content, whereas K decreases. According to Dickson & Scott, (1997), the formation and claying of oxide clays during pedogenesis, favors adsorption and accumulation of U and Th in these clay minerals, especially at the top of the textural B horizon (argic horizon) (Santos-Francés et al., 2018). It is important to realize that, both PVA and NV are on a stable geomorphic surface (**Fig. 3**), which favors weathering and pedogenetic processes of clay and oxide formation, where U and Th contents tend to increase by the action of pedogenesis while the K levels decrease by the action of weathering and leaching, as proposed by Schuler et al. (2011) (**Fig. 5b**). Herrmann et al. (2010); Schuler et al. (2011) and Moonjun et al. (2017) fond similar results for K depletion when studying soils developed on stable terraces in Thailand where in this environment intense K leaching and claying occurred.

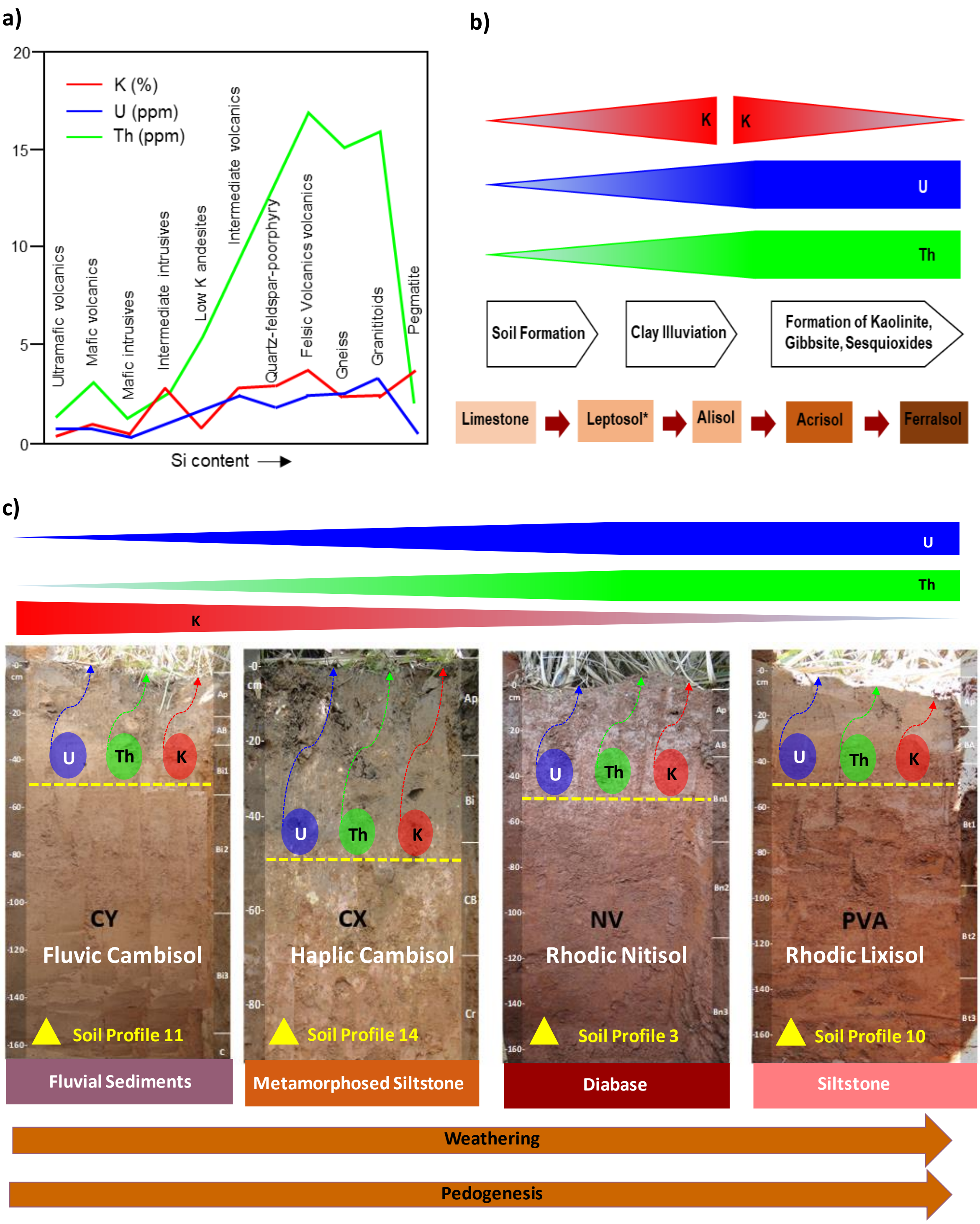

Figure 5. a) Variation in average K, U & Th content for igneous rocks with increasing acidity (Si content), adapted from Dickson and Scott, 1997. b) K, U, and Th distribution in Limestone and its derived soils (referred to the complete *solum*), adapted from Schuler et al. (2011). c) General variability of radionuclides by soil classes according to weathering and pedogenesis intensity. The yellow discontinuous lines indicate the gamma sensor reading depth (approximately 50cm).

2.3.4. Relationship between radionuclides and soil attributes

There is a significant negative correlation (-0.32) between eU and altitude (**Fig. 6**). This negative correlation was expected due to the fact that the highest levels occur at the lowest points of the landscape and the lowest levels at the highest parts (**Fig. 7a**). Besides, these results agree with the geology (**Fig. 7b**), since the highest levels of eU are located on the lithological compartments metamorphosed siltstone and siltstone.

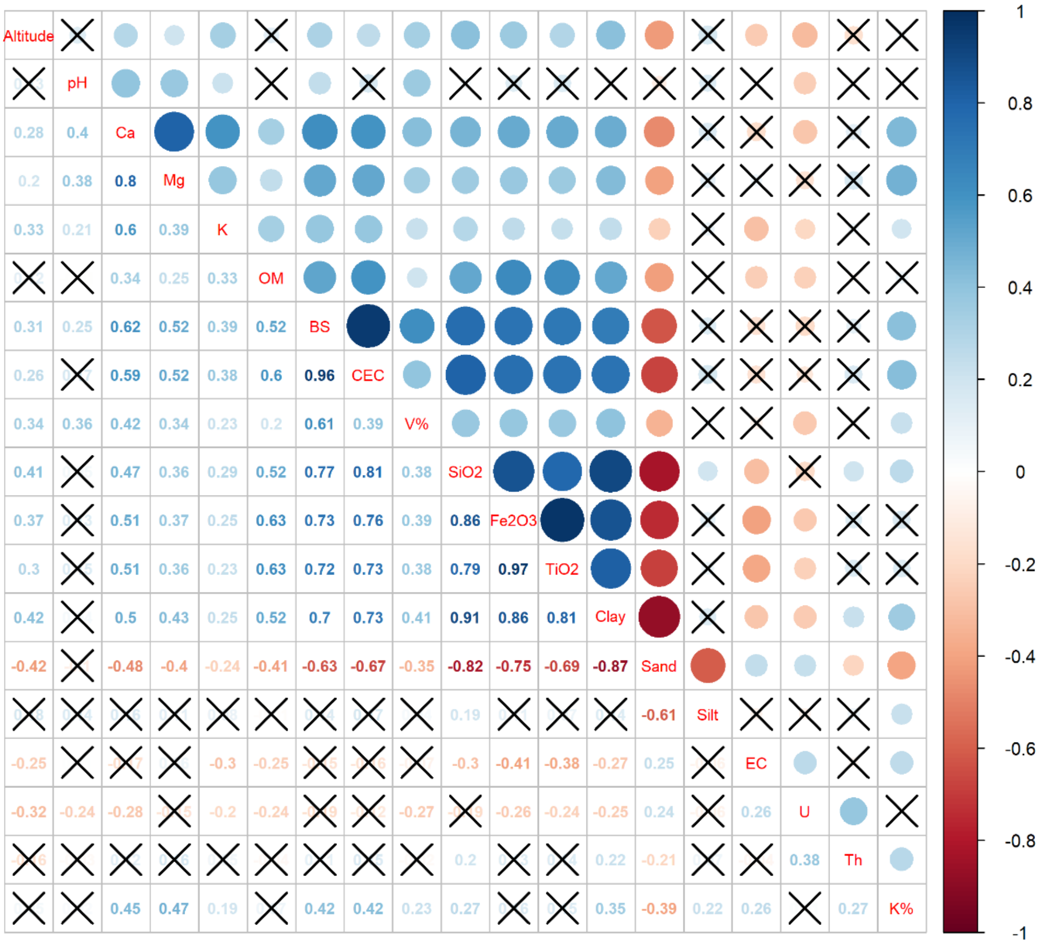

Figure 6. Pearson's correlation coefficient for soil physical and chemical attributes, magnetic susceptibility and radionuclides (uranium, thorium and potassium). Values overlapped with an "X" are not statistically significant at the 0.1 significance level.

The eTh presented negative correlation with sand (-0.21) and significant and positive correlation with clay (0.22) (**Fig. 6**). These results agree with those of Becegato et al. (2019) who found correlation for eTh (0.86) and eU (0.92) with the clay content. The eTh is the least mobile among radionuclides and, due to this, it was probably adsorbed to clay minerals and iron oxides (Filistovič et al. 2015; Santos-Francés et al. 2018) formed mainly in the pedogenesis processes, especially on textured soils to very clayey PVA and NV (**Fig.7c**). Schuler et al. (2011), when studying the behavior of radionuclides on Acrisols in Thailand, found similar results with eU and eTh enrichment due to the incorporation of these elements into the oxidic clay minerals that were formed by pedogenesis.

In relation to K, there was a significant and positive correlation with base saturation (BS) and CEC (both 0.42) (**Fig. 6**). This correlation was expected since K tends to occupy and become adsorbed on soil CEC as well as calcium and magnesium. This theory is corroborated by the correlation between K and clay (0.35) and sand (-0.39), where the higher the clay content, the higher the soil CEC. These results agree with those obtained by Schuler et al. (2011) who analyzed the correlation of K with CEC and obtained a r = 0.59 and a negative correlation between K and eU and K and eTh. In addition, it is possible to observe in **Fig. 7e**, that higher K contents are distributed over clayey soils and higher CEC (Nitisols and Lixisols). The high K levels on Cambisols (**Fig. 7e**), in turn, can be explained by the greater presence of weatherable primary minerals and less to do with texture, according to the model proposed by (Wilford et al. 1997) on the behavior of radionuclides in geomorphic processes on the landscape.

Although the correlations (**Fig. 6**) were not high, it allowed to satisfactorily correlate the contents of eTh and K with the soil texture. In fact, according to Ferreira et al. (2018), the concentrations of eTh and K along the profiles and in the landscape are also correlated with other soil attributes.

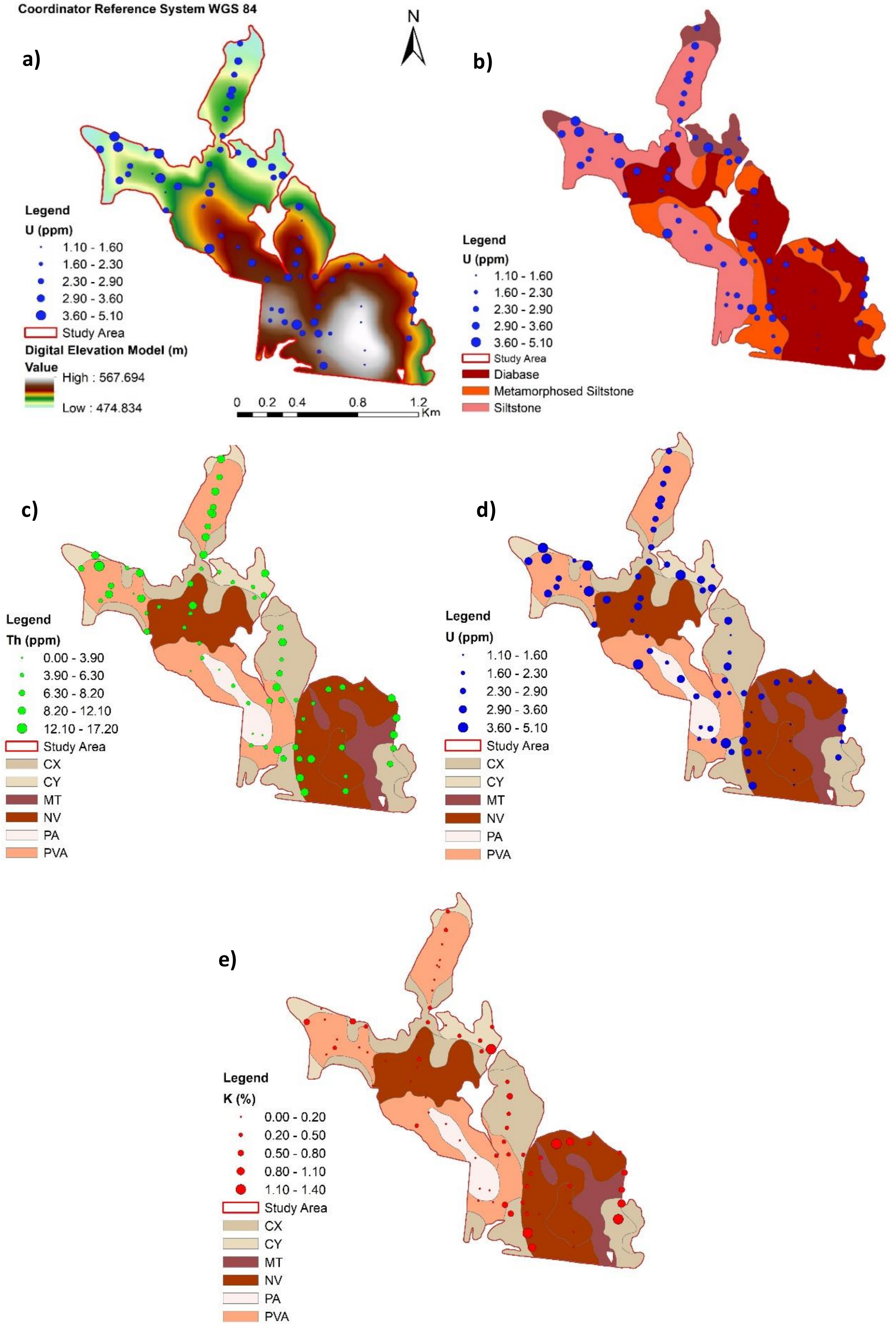

Figure 7. a) Digital elevation model and uranium concentration/distribution. b) Geological compartments and uranium concentration/distribution. c) Magnetic susceptibility concentration/distribution. d) Soil classes and Th concentration/ distribution. e) Soil classes and eU concentration/ distribution. f) Soil classes and K concentration/distribution.

2.3.5. Concentrations of eU, eTh and K and pedological digital mapping

According to **Fig. 4c**, significant variations can be observed by the mean comparison test for K and eU contents between distinct soil classes and practically zero variation for eTh contents. The biggest differences for K contents may be related to the great solubility and mobility of this element in the soil profile. Uranium, in turn, depends beyond the clay and iron oxide content, on the hydrodynamics of the soil, because under reducing conditions U predominates in the insoluble and low mobility form U^{4+} (Wilford, 2012). In CX, PA (Xanthic Lixisol), PVA and MT (Luvic Phaozem) soils, water infiltrates and tends to saturate the topsoil due to some subsurface impediment such as argic horizon (Jung et al. 2007) or poor effective soil depth, and consequently water flow (Wang et al. 2012). In this way the U^{6+} (soluble and mobile) is reduced to U^{4+}, making this element longer in some soil classes, which may explain part of the differences found.

At T1 it is possible to observe that there was a sudden variation in eTh content from 5.8 ppm to 9.1 ppm from point 2 (P2) to point 3 (P3), respectively, concomitant with the change of soil class (NV to PVA) and geology (from diabase to siltstone) (**Fig. 2b**). The sensor reading detected this sudden radionuclide variation, indicating that some environmental factor/soil formation, changed at this point and affected the concentration of eTh. Since the climate does not vary on a micro scale, neither the vegetation, there are two factors which can be considered: relief and the parent material. The relief did not show significant variations for the change point in radionuclide content (493.4 m to 493 m, leaving only the lithological variation, corresponding to the parent material and originating NV and PVA.

For T2 (**Fig. 3**), two points draw attention to significant changes in eTh values. The change from point 4 (P4) to point 5 (P5) from 5.8 ppm to 8.3 ppm, and the change from point 11 (P11) to point 12 (P12) from 7.3 ppm to 10.2 ppm. In the transition between P4 and P5 both are under the same parent material and under the indifferent action of the other soil formation factors, and in P5, probably the pedogenesis processes that led to the formation of silicate and/or oxide clay and minerals and eTh retention. This fact, leads us to question whether really at this point (P5), still according to traditional soil mapping carried out in the area, predominates the soil class CX, which is characterized by its poor pedogenetic evolution and under the strong influence of the parent material. This same fact would lead us to dispute the occurrence of more intense pedogenetic processes, the high eTh content in the transition corresponding to P12 (10.2 ppm) too high for fluvial sediments. According to Reinhardt and Herrmann, (2019), this anomaly can be explained due to the lower sensor accuracy in the quantification of radionuclides on developed over transported sediments relative to *insitu* developed soils. These results are in agreement with those obtained by Alomari et al. (2019) who obtained the lowest radionuclide readings in soils developed over unconsolidated sediments over Jordan geological formations.

With respect to T3, a significant variation in eTh levels occurred in the transition from point 3 (P3) to point 4 (P4) from 8.1 ppm to 5.1 ppm (**Fig. 3**), corresponding to the Cambisol area, over diabase lithology. Since for mafic rocks the expected levels of eTh are low (Dickson & Scott, 1997), the high content in P3 could indicate a higher pedogenetic evolution of this soil, which does not corroborate the current classification in the order of the Cambisols, where perhaps the soil class would still be a continuation of the Lixisol or a transitional area between the soil classes. This is a high potential and higher sensor accuracy in soil class delimitation, especially those where argilluviation processes occur and/or identification of transition areas helping the delimitation between one soil classes (Herrmann et al., 2010; Reinhardt and Herrmann, 2019).

Finally, at T4 (**Fig. 3**), significant variations in eTh contents occurred at the transitions between point 1 (P1) and 2 (2), and between points 9 (P9) and 10 (P10). From P1 to P2 eTh values were 12.1 to 7.2 ppm, respectively, and from P9 to P10 from 6.1 to 10 ppm. In the first case, both points P1 and P2 are located on the same geology (metamorphosed siltstone) and soil class (Nitisol) (**Fig. 2b**). Too high eTh levels in P1 may have occurred due to the formation of this Nitisol from a Ferralsol, according to the model proposed by Cooper et al. (2010). This manner, the high levels of residual eTh in the Nitisol would be an inheritance of the parent material (Ferralsol). It is also possible to verify a higher K content (1.4%), which is not expected in mafic rocks derived Nitisol (Dickson & Scott, 1997). With respect to the points 9 and 10, the geological bases change between the points of diabase (P9) to fluvial sediments (P10). Therefore, changes in radionuclide contents are expected. The sudden change in eTh levels between points may indicate a different soil class on fluvial sediments, not corresponding to the order of the Nitisols, similar to what may be occurring in the first case.

It is important to realize that, gamma sensor detected variations between transitions of some soil classes, which were not considered in traditional pedological mapping (**Fig. 3**). Thus, gamma spectrometry has a high potential for distinguishing some soil classes, being a useful and promising tool for digital soil mapping, especially when associated with other field sensors. Schuler et al. (2011) and Moonjun et al. (2017) highlight the potential and importance of the technique in pedological digital mapping. However, these researchers warned to limitation of the sensor to a depth of 30 cm to 40 cm and little understanding of the concentration and distribution of radionuclides in the landscape, as well as, the factors that affecting this distribution and concentrations, which was the main objective of this research. Reinhardt and Herrmann, (2019) suggest the detection capability of the gamma sensor at depths of up to 60 cm in mineral soils and 1 m in organic soils. On the other hand, (Rossel et al. 2007) reinforces the importance and ability of the sensor to predict soil attributes in this surface layer (0-15 cm and 15–50 cm), which contribute to the pedological digital mapping. According to Viscarra Rossel et al. 2014) another sensor limitation would be that for soils formed over environments with wide geological variation, the prediction of attributes becomes more difficult, especially in areas where there have been no previous studies on the distribution and distribution and concentration of radionuclides. Furthermore, these authors report that radionuclide sources in the soil are still poorly explored for pedological mapping purposes.

2.4. CONCLUSIONS

The pedogeoenvironmental variable that most contributed to the levels and distribution of eU, eTh and K were lithology, especially in soils such as Cambisols, poorly evolved.

Pedogeomorphological processes associated with landscape denudation and river deposition contributed to the distribution and differentiation of radionuclides, mainly for soils located in relief micro depressions and in the lower parts of the landscape.

More weathered and evolved soils (Lixisols and Nitisols), did not present good compatibility with geology due to redistribution of radionuclides caused by pedogeochemical and pedogenesis processes, mainly K leaching by the first process and retention to U and Th silicate and oxidized clay minerals for the second one.

Correlations between radionuclide contents and soil attributes were low, but it was sufficient to explain the texture relationship for eTh and K.

Nearby gamma spectrometry is a promising tool to be used for pedological digital mapping, especially if associated with other field sensors. For each area, it is necessary to establish a specific theoretical model that represents the distribution and concentration of radionuclides in the landscape, associated with other environmental factors such as geology, geochemical history, microclimate, soil class and relief.

ACKNOWLEDGEMENTS

We would like to thank the National Council for Scientific and Technological Development (CNPq) for the first author scholarship (grant No. 134608/2015-1); the São Paulo Research Foundation (FAPESP) (grant No. 2014-22262-0) for providing essential resources to the Laboratory of Remote Sensing Applied to Soils from “Luiz de Queiroz” College of Agriculture (ESALQ/USP); and the Geotechnologies in Soil Science group (GeoSS – website http://esalqgeocis.wixsite.com/english) for the support.

REFERENCES

A. R. Fisher, 1925. No Title Statistical Methods for Research Workers. Oliver Boyd.

Ab’Sáber, 1957. Geomorfologia do Sítio Urbano de São Paulo.

Abbaszadeh Afshar, F., Ayoubi, S., Besalatpour, A.A., Khademi, H., Castrignano, A., 2016. Integrating auxiliary data and geophysical techniques for the estimation of soil clay content using CHAID algorithm. J. Appl. Geophys. 126, 87–97. https://doi.org/10.1016/j.jappgeo.2016.01.015

Alastair Ruffell, J.M., 2008. Geoforensics, in: Geoforensics. p. 288.

Alomari, A.H., Saleh, M.A., Hashim, S., Alsayaheen, A., 2019. Investigation of natural gamma radiation dose rate (GDR) levels and its relationship with soil type and underlying geological formations in Jordan. J. African Earth Sci. 155, 32–42. https://doi.org/10.1016/j.jafrearsci.2019.04.006

Alvares, C.A., Stape, J.L., Sentelhas, P.C., De Moraes Gonçalves, J.L., Sparovek, G., 2013. Köppen’s climate classification map for Brazil. Meteorol. Zeitschrift 22, 711–728. https://doi.org/10.1127/0941-2948/2013/0507

Arnedo, M.A., Rubiano, J.G., Alonso, H., Tejera, A., González, A., González, J., Gil, J.M., Rodríguez, R., Martel, P., Bolivar, J.P., 2017. Mapping natural radioactivity of soils in the eastern Canary Islands. J. Environ. Radioact. 166, 242–258. https://doi.org/10.1016/j.jenvrad.2016.07.010

Arrouays, D., Grundy, M.G., Hartemink, A.E., Hempel, J.W., Heuvelink, G.B.M., Hong, S.Y., Lagacherie, P., Lelyk, G., McBratney, A.B., McKenzie, N.J., Mendonca-Santos, M. d. L., Minasny, B., Montanarella, L., Odeh, I.O.A., Sanchez, P.A., Thompson, J.A., Zhang, G.-L., 2014. GlobalSoilMap: Toward a Fine-Resolution Global Grid of Soil Properties, in: Advances in Agronomy 125. pp. 93–134. https://doi.org/10.1016/B978-0-12-800137-0.00003-0

Asgari, N., Ayoubi, S., Demattê, J.A.M., 2018. Soil drainage assessment by magnetic susceptibility measures in western Iran. Geoderma Reg. 13, 35–42. https://doi.org/10.1016/j.geodrs.2018.03.003

Atalay, İ.C.S.S.K.M.E., 2018. Pedogeomorphology, in: The Soils of Turkey. Springer, Cham, pp. 75–103.

Aydin, A., Ferré, E.C., Aslan, Z., 2007. The magnetic susceptibility of granitic rocks as a proxy for geochemical composition: Example from the Saruhan granitoids, NE Turkey. Tectonophysics 441, 85–95. https://doi.org/10.1016/j.tecto.2007.04.009

Ayoubi, S., Abazari, P., Zeraatpisheh, M., 2018. Soil great groups discrimination using magnetic susceptibility technique in a semi-arid region, central Iran. Arab. J. Geosci. 11. https://doi.org/10.1007/s12517-018-3941-4

Ayoubi, S., Adman, V., 2019. Iron Mineralogy and Magnetic Susceptibility of Soils Developed on Various Rocks in Western Iran. Clays Clay Miner. 67, 217–227. https://doi.org/10.1007/s42860-019-00020-5

Ayoubi, S., Adman, V., Yousefifard, M., 2019. Use of magnetic susceptibility to assess metals concentration in soils developed on a range of parent materials. Ecotoxicol. Environ. Saf. 168, 138–145. https://doi.org/10.1016/j.ecoenv.2018.10.024

Ayoubi, S., Mirsaidi, A., 2019. Magnetic susceptibility of Entisols and Aridisols great groups in southeastern Iran. Geoderma Reg. 16, e00202. https://doi.org/10.1016/j.geodrs.2018.e00202

Barlow, J., Lennox, G.D., Ferreira, J., Berenguer, E., Lees, A.C., Nally, R. Mac, Thomson, J.R., Ferraz, S.F.D.B., Louzada, J., Oliveira, V.H.F., Parry, L., Ribeiro De Castro Solar, R., Vieira, I.C.G., Aragaõ, L.E.O.C., Begotti, R.A., Braga, R.F., Cardoso, T.M., Jr, R.C.D.O., Souza, C.M., Moura, N.G., Nunes, S.S., Siqueira, J.V., Pardini, R., Silveira, J.M., Vaz-De-Mello, F.Z., Veiga, R.C.S., Venturieri, A., Gardner, T.A., 2016. Anthropogenic disturbance in tropical forests can double biodiversity loss from deforestation. Nature 535, 144–147. https://doi.org/10.1038/nature18326

Baumann, M., Gasparri, I., Piquer-Rodríguez, M., Gavier Pizarro, G., Griffiths, P., Hostert, P., Kuemmerle, T., 2017. Carbon emissions from agricultural expansion and intensification in the Chaco. Glob. Chang. Biol. 23, 1902–1916. https://doi.org/10.1111/gcb.13521

Bazaglia Filho, O., Rizzo, R., Lepsch, I.F., Prado, H. do, Gomes, F.H., Mazza, J.A., Demattê, J.A.M., 2013. Comparison between detailed digital and conventional soil maps of an area with complex geology. Rev. Bras. Ciência do Solo 37, 1136–1148. https://doi.org/10.1590/s0100-06832013000500003

Beamish, D., 2015. Relationships between gamma-ray attenuation and soils in SW England. Geoderma 259–260, 174–186. https://doi.org/10.1016/j.geoderma.2015.05.018

Beamish, D., 2013. Gamma ray attenuation in the soils of Northern Ireland, with special reference to peat. J. Environ. Radioact. 115, 13–27. https://doi.org/10.1016/j.jenvrad.2012.05.031

Becegato, V.A., Becegato, V.R., Baum, C.A., Lavnitcki, L., Paulino, A.T., 2019. Multivariate statistical analysis correlating 238 U, 232 Th, and 40 K equivalent activities in soil to geochemical data from an agricultural area. J. Soils Sediments 19, 1901–1910. https://doi.org/10.1007/s11368-018-2161-6

Berkowitz, B., Dror, I., Yaron, B., 2008. Contaminant Geochemistry, Contaminant Geochemistry. https://doi.org/10.1007/978-3-540-74382-8

Binley, A., Hubbard, S.S., Huisman, J.A., Revil, A., Robinson, D.A., Singha, K., Slater, L.D., 2015. The emergence of hydrogeophysics for improved understanding of subsurface processes over multiple scales. Water Resour. Res. 1–30. https://doi.org/10.1002/2015WR017016.Received

Blundell, A., Dearing, J.A., Boyle, J.F., Hannam, J.A., 2009. Controlling factors for the spatial variability of soil magnetic susceptibility across England and Wales. Earth-Science Rev. 95, 158–188. https://doi.org/10.1016/j.earscirev.2009.05.001

Brevik, E.C., Calzolari, C., Miller, B.A., Pereira, P., Kabala, C., Baumgarten, A., Jordán, A., 2016. Soil mapping, classification, and pedologic modeling: History and future directions. Geoderma 264, 256–274. https://doi.org/10.1016/j.geoderma.2015.05.017

Broschat, T.K., 1995. Nitrate, phosphate, and potassium leaching from container-grown plants fertilized by several methods. HortScience 30, 74–77.

Camargo, O.A.; Moniz, A.C.; Jorge, J.A. & Valadares, J.M.A.S., 1986. Métodos de análise química, mineralógica e física de solos do Instituto Agronômico do estado de São Paulo. Bol. técnico 106, 94.

Camargo, L.A., Marques Júnior, J., Pereira, G.T., Bahia, A.S.R. de S., 2014. Clay mineralogy and magnetic susceptibility of Oxisols in geomorphic surfaces. Sci. Agric. 71, 244–256. https://doi.org/10.1590/S0103-90162014000300010

Cervi, E.C., Maher, B., Poliseli, P.C., de Souza Junior, I.G., da Costa, A.C.S., 2019. Magnetic susceptibility as a pedogenic proxy for grouping of geochemical transects in landscapes. J. Appl. Geophys. 169, 109–117. https://doi.org/10.1016/j.jappgeo.2019.06.017

Coey, J.M.D., 1987. Magnetic order in trioctahedral sheet silicates: A review, in: Proceedings of the International Clay Conference, Denver, 1985, The Clay Minerals Society, Bloomington,. pp. 261–266.

Cook, S.E., Corner, R.J., Groves, P.R., Grealish, G.J., 1996. Use of airborne gamma radiometric data for soil mapping. Aust. J. Soil Res. 34, 183–194. https://doi.org/10.1071/SR9960183

Cooper, M., Vidal-Torrado, P., Grimaldi, M., 2010. Soil structure transformations from ferralic to nitic horizons on a toposequence in southeastern Brazil. Rev. Bras. Ciência do Solo 34, 1685–1699. https://doi.org/10.1590/s0100-06832010000500021

Coulouma, G., Caner, L., Loonstra, E.H., Lagacherie, P., 2016. Analysing the proximal gamma radiometry in contrasting Mediterranean landscapes: Towards a regional prediction of clay content. Geoderma 266, 127–135. https://doi.org/10.1016/j.geoderma.2015.12.006

Curi, N., Franzmeier, D.P., 1984. Toposequence of Oxisols from the Central Plateau of Brazil. Soil Sci. Soc. Am. J. 48, 341–346. https://doi.org/10.2136/sssaj1984.03615995004800020024x

D. A. Clarck & D. W. Emerson, 1991. Notes on rock magnetization characteristics in applied geophysical studies. Explor. Geophys. 22, 547–555.

Da Costa, A.C.S., Bigham, J.M., Rhoton, F.E., Traina, S.J., 1999. Quantification and characterization of maghemite in soils derived from volcanic rocks in southern Brazil. Clays Clay Miner. 47, 466–473. https://doi.org/10.1346/CCMN.1999.0470408

Dahlkamp, F.J., 1993. Uranium Ore Deposits. Springer.

Damaceno, J.G., de Castro, D.L., Valcácio, S.N., Souza, Z.S., 2017. Magnetic and gravity modeling of a Paleogene diabase plug in Northeast Brazil. J. Appl. Geophys. 136, 219–230. https://doi.org/10.1016/j.jappgeo.2016.11.006

De Jong, E., Pennock, D.J., Nestor, P.A., 2000. Magnetic susceptibility of soils in different slope positions in Saskatchewan, Canada. Catena 40, 291–305. https://doi.org/10.1016/S0341-8162(00)00080-1

De Wispelaere, L., Marcelino, V., Regassa, A., De Grave, E., Dumon, M., Mees, F., Van Ranst, E., 2015. Revisiting nitic horizon properties of Nitisols in SW Ethiopia. Geoderma 243–244, 69–79. https://doi.org/10.1016/j.geoderma.2014.12.021

Dearing, J.A., 1999. Environmental Magnetic Susceptibility., 2 nd. ed, Using the Bartington MS2 system. Chi Publishing, Kenilworth, UK.

Dearing, J.A., 1994. Environmental magnetic susceptibility, using the Bartington MS2 system.

Dearing, J.A., Hay, K.L., Baban, S.M.J., Huddleston, A.S., Wellington, E.M.H., Loveland, P.J., 1996. Magnetic susceptibility of soil: An evaluation of conflicting theories using a national data set. Geophys. J. Int. 127, 728–734. https://doi.org/10.1111/j.1365-246X.1996.tb04051.x

Demattê, J.A.M., Araújo, S.R., Fiorio, P.R., Fongaro, C.T., Nanni, M.R., 2015. Espectroscopia VIS-NIR-SWIR na avaliação de solos ao longo de uma topossequência em Piracicaba (SP). Rev. Cienc. Agron. 46, 679–688. https://doi.org/10.5935/1806-6690.20150054

Deng, D.N., 2015. A comparative study of hand-held magnetic susceptibility instruments. M.Sc. Thesis 207.

Dennerley, C., Huang, J., Nielson, R., Sefton, M., Triantafilis, J., 2018. Identifying soil management zones in a sugarcane field using proximal sensed electromagnetic induction and gamma-ray spectrometry data. Soil Use Manag. 34, 219–235. https://doi.org/10.1111/sum.12410

Dickson, B.L.; Scott, K.M., 1997. Interpretation of aerial gamma-ray surveys – adding the geochemical factors. J. Aust. Geolology Geophys. 17, 187–200.

Dierke, C., Werban, U., 2013. Relationships between gamma-ray data and soil properties at an agricultural test site. Geoderma 199, 90–98. https://doi.org/10.1016/j.geoderma.2012.10.017

Domra Kana, J., Djongyang, N., Raïdandi, D., Njandjock Nouck, P., Dadjé, A., 2015. A review of geophysical methods for geothermal exploration. Renew. Sustain. Energy Rev. 44, 87–95. https://doi.org/10.1016/j.rser.2014.12.026

Egmond, F.M. Van, Veeke, S. Van Der, Knotters, M., Koomans, R.L., Limburg, J., 2018. Mapping soil texture with a gamma-ray spectrometer : comparison between UAV and proximal measurements and traditional sampling. WOt-technical Rep. 137, 58p.

EMBRAPA, 2017. Manual de metodos de analises, Manual de métodos de análise de solo.

EMBRAPA, 2011. Documentos 132 Manual de Métodos de. Embrapa 230.

Fabris, J.D., De Jesus Filho, M.F., Coey, J.M.D., Mussel, W.D.N., Goulart, A.T., 1997. Iron-rich spinels from Brazilian soils. Hyperfine Interact. 110, 23–32. https://doi.org/10.1023/A:1012619331408

Falco, N., Wainwright, H., Dafflon, B., Léger, E., Peterson, J., Steltzer, H., Wilmer, C., Rowland, J.C., Williams, K.H., Hubbard, S.S., 2019. Investigating Microtopographic and Soil Controls on a Mountainous Meadow Plant Community Using High-Resolution Remote Sensing and Surface Geophysical Data. J. Geophys. Res. Biogeosciences 124, 1618–1636. https://doi.org/10.1029/2018JG004394

FAOSTAT, 2003. Food and Agriculture Organization of the United Nations, Statistical Databases.

Ferreira, A., Daraktchieva, Z., Beamish, D., Kirkwood, C., Lister, T.R., Cave, M., Wragg, J., Lee, K., 2018. Indoor radon measurements in south west England explained by topsoil and stream sediment geochemistry, airborne gamma-ray spectroscopy and geology. J. Environ. Radioact. 181, 152–171. https://doi.org/10.1016/j.jenvrad.2016.05.007

Filho, B., 2012. Universidade de São Paulo Escola Superior de Agricultura " Luiz de Queiroz " Comparação entre mapas de solos obtidos pelos métodos convencional e digital numa área complexa Osmar Bazaglia Filho Piracicaba. Master Diss. Soils Plant Nutr. 190 p.

Filistovič, V., Maceika, E., Tarasiuk, N., Lukšiene, B., Konstantinova, M., Buivydas, Š., Koviazina, E., Puzas, A., 2015. Model of Non-equilibrium Multiphase Contaminant Transport in Lake Water-Sediment System. Water. Air. Soil Pollut. 226. https://doi.org/10.1007/s11270-015-2455-x

Fine, P., Singer, M.J., Verosub, K.L., 1992. Use of magnetic-susceptibility measurements in assessing soil uniformity in chronosequence studies. Soil Sci. Soc. Am. J. 56, 1195–1199. https://doi.org/10.2136/sssaj1992.03615995005600040032x

Foley, 2011. Sustain the Planet ? Sci. Am. 305, 60–65.

Fontes, M.P.F., De Oliveira, T.S., Da Costa, L.M., Campos, A.A.G., 2000. Magnetic separation and evaluation of magnetization of Brazilian soils from different parent materials. Geoderma 96, 81–99. https://doi.org/10.1016/S0016-7061(00)00005-7

Ghilardi, M., Kunesch, S., Styllas, M., Fouache, E., 2008. Reconstruction of Mid-Holocene sedimentary environments in the central part of the Thessaloniki Plain (Greece), based on microfaunal identification, magnetic susceptibility and grain-size analyses. Geomorphology 97, 617–630. https://doi.org/10.1016/j.geomorph.2007.09.007

Gholamzadeh, M., Ayoubi, S., Shahrivar, F.S., 2019. Using magnetic susceptibility measurements to differentiate soil drainage classes in central Iran. Stud. Geophys. Geod. 63, 465–484. https://doi.org/10.1007/s11200-018-0679-0

Gillot, P.Y., Hildenbrand, A., Lefèvre, J.C., Albore Livadie, C., 2006. The K/Ar dating method: principle, analytical techniques, and application to holocene volcanic eruptions in Southern Italy. Acta Vulcanol. 18, 55–66.

Godfray, H.C.J., Beddington, J.R., Crute, I.R., Haddad, L., Lawrence, D., Muir, J.F., Pretty, J., Robinson, S., Thomas, S.M., Toulmin, C., 2010. Food Security: The Challenge of Feeding 9 Billion People. Science (80-.). 327, 812 LP – 818. https://doi.org/10.1126/science.1185383

Govedarica, D.D., Gavrilov, M.B., Zeremski, T.M., Govedarica, O.M., Hambach, U., Tomić, N.A., Sentić, I., Marković, S.B., 2019. Relationships between heavy metal content and magnetic susceptibility in road side loess profiles: A possible way to detect pollution. Quat. Int. 502, 148–159. https://doi.org/10.1016/j.quaint.2018.01.020

GRANT, U.S., 1900. Contact metamorphism of a basic igneous rock. Geol. Soc. Am. Bull. 11, 503–510. https://doi.org/10.1130/gsab-11-503

Grimley, D.A., Arruda, N.K., Bramstedt, M.W., 2004. Using magnetic susceptibility to facilitate more rapid, reproducible and precise delineation of hydric soils in the midwestern USA. Catena 58, 183–213. https://doi.org/10.1016/j.catena.2004.03.001

Grimley, D.A., Vepraskas, M.J., 2000. Magnetic susceptibility for use in delineating hydric soils. Soil Sci. Soc. Am. J. 64, 2174–2180. https://doi.org/10.2136/sssaj2000.6462174x

Grison, H., Petrovsky, E., Kapicka, A., Stejskalova, S., 2016. Magnetic and chemical parameters of andic soils and their relation to selected pedogenesis factors. Catena 139, 179–190. https://doi.org/10.1016/j.catena.2015.12.005

Guagliardi, I., Buttafuoco, G., Apollaro, C., Bloise, A., De Rosa, R., Cicchella, D., 2013. Using gamma-ray spectrometry and Geostatistics for assessing geochemical behaviour of radioactive elements in the lese catchment (southern Italy). Int. J. Environ. Res. 7, 645–658.

Hanesch, M., Rantitsch, G., Hemetsberger, S., Scholger, R., 2007. Lithological and pedological influences on the magnetic susceptibility of soil: Their consideration in magnetic pollution mapping. Sci. Total Environ. 382, 351–363. https://doi.org/10.1016/j.scitotenv.2007.04.007

Hartemink, A.E., Krasilnikov, P., Bockheim, J.G., 2013. Soil maps of the world. Geoderma 207–208, 256–267. https://doi.org/10.1016/j.geoderma.2013.05.003

Heggemann, T., Welp, G., Amelung, W., Angst, G., Franz, S.O., Koszinski, S., Schmidt, K., Pätzold, S., 2017. Proximal gamma-ray spectrometry for site-independent in situ prediction of soil texture on ten heterogeneous fields in Germany using support vector machines. Soil Tillage Res. 168, 99–109. https://doi.org/10.1016/j.still.2016.10.008

Herrmann, L., Schuler, U., Rangubpit, W., Erbe, P., Surinkum, A., Zarei, M., Stahr, K., 2010. The potential of gamma-ray spectrometry for soil mapping. 19th World Congr. Soil Sci. 117–120.

Hooper, R.L., 1987. Factors affecting the magnetic susceptibility of baked rocks above a burned coal seam. Int. J. Coal Geol. 9, 157–169.

IUSS Working Group WRB, 2015. World reference base for soil resources 2014. International soil classification system for naming soils and creating legends for soil maps, World Soil Resources Reports No. 106. https://doi.org/10.1017/S0014479706394902

Ivanovich, M., Harmon, R.S., 1982. Uranium series disequilibrium: applications to environmental problems. Oxford University Press, USA.

J. A. Quaggio, Raij, B., 2001. Determination of pH in calcium chloride and total acidity. Chem. Anal. Fertil. Eval. Trop. Soils. Inst. Agronômico Campinas, Campinas 181–188.

Jiménez, C., Benavides, J., Ospina-Salazar, D.I., Zúñiga, O., Ochoa, O., Mosquera, C., 2017. Relationship between physical properties and the magnetic susceptibility in two soils of Valle del Cauca Relación entre propiedades físicas y la susceptibilidad magnética en dos suelos del Valle del Cauca. Cauca. Rev. Cienc. Agri 34, 33–45. https://doi.org/10.22267/rcia.173402.70

Johansson, M., Åkerman, H.J., 2008. Thawing Permafrost and Thicker Active Layers in Sub-arctic Sweden. Permafr. Periglac. Process. 19, 279–292. https://doi.org/10.1002/ppp

Jordanova, N., Jordanova, D., Mokreva, A., Ishlyamski, D., Georgieva, B., 2019. Temporal changes in magnetic signal of burnt soils – A compelling three years pilot study. Sci. Total Environ. 669, 729–738. https://doi.org/10.1016/j.scitotenv.2019.03.173

Jordanova, N., Jordanova, D., Petrov, P., 2016. Soil magnetic properties in Bulgaria at a national scale-Challenges and benefits. Glob. Planet. Change 137, 107–122. https://doi.org/10.1016/j.gloplacha.2015.12.015

Kelly, J.M., Resources, N., Lafayette, W., 1977. Acid precipitation effects on soil pH and base saturation of exchangeable sites 1, 401–408.

Kempen, B., Brus, D.J., Stoorvogel, J.J., Heuvelink, G.B.M., de Vries, F., 2012. Efficiency Comparison of Conventional and Digital Soil Mapping for Updating Soil Maps. Soil Sci. Soc. Am. J. 76, 2097. https://doi.org/10.2136/sssaj2011.0424

Khan, F.A., Fenton, T.E., 2010. Factors Affecting Potassium Status of Alluvial-Derived Soils of Western Iowa. Soil Sci. Soc. Am. J. 60, 836. https://doi.org/10.2136/sssaj1996.03615995006000030023x

Koch-Steindl, H., Pröhl, G., 2001. Considerations on the behaviour of long-lived radionuclides in the soil. Radiat. Environ. Biophys. 40, 93–104. https://doi.org/10.1007/s004110100098

Koons, R.D., Helmke, P.A., Jackson, M.L., 1980. Association of Trace Elements with Iron Oxides During Rock Weathering1. Soil Sci. Soc. Am. J. 44, 155. https://doi.org/10.2136/sssaj1980.03615995004400010032x

Lancmuir, D., Herman, J.S., 2002. 1-S2.0-0016703780902264-Main 44, 1–14.

Laubenstein, M., Plastino, W., Povinec, P.P., Fabbri, V., Aprili, P., Balata, M., Bella, F., Cardarelli, A., De Deo, M., Gallese, B., Ioannucci, L., Nisi, S., Antonecchia, D., Del Pinto, C., Giarrusso, G., 2013. Radionuclide mapping of the Molise region (Central Italy) via gamma-ray spectrometry of soil samples: Relationship with geological and pedological parameters. J. Radioanal. Nucl. Chem. 298, 317–323. https://doi.org/10.1007/s10967-012-2353-2

Li, J., Heap, A.D., 2008. A Review of Spatial Interpolation Methods for Environmental Scientists. Aust. Geol. Surv. Organ. GeoCat# 68, 154. https://doi.org/http://www.ga.gov.au/image_cache/GA12526.pdf

Lim, C.H., Jackson, M.L., 1986. Dissolution for total elemental analysis, in: Madison (Ed.), Methods of Soil Analysis. Part 2: Chemical and Microbiological Properties. American Society of Agronomy, pp. 1–12.

Lindon, J.C.G.E.T.D.W.K., 2016. Encyclopedia of Spectroscopy and Spectrometry, 3 edition. ed. Elsevir.

Lourenço, A.M., Sequeira, E., Sant’Ovaia, H., Gomes, C.R., 2014. Magnetic, geochemical and pedological characterisation of soil profiles from different environments and geological backgrounds near Coimbra, Portugal. Geoderma 213, 408–418. https://doi.org/10.1016/j.geoderma.2013.07.035

Lu, S., Wang, H., Bai, S., 2009. Heavy metal contents and magnetic susceptibility of soils along an urban - Rural gradient in rapidly growing city of eastern China. Environ. Monit. Assess. 155, 91–101. https://doi.org/10.1007/s10661-008-0420-5

Luque, E.C.L., 2008. Propiedades magnéticas de los óxidos de hierro en suelos mediterráneos. Universidad de Córdoba, Córdoba.

Maher, B.A., 1998. Magnetic properties of modern soils and quaternary loessic paleosols: Paleoclimatic implications. Palaeogeogr. Palaeoclimatol. Palaeoecol. 137, 25–54. https://doi.org/10.1016/S0031-0182(97)00103-X

Maher, B.A., Taylor, R.M., 1988. Formation of ultrafine-grained magnetite in soils. Nature 336, 368–370. https://doi.org/10.1038/336368a0

Marques, J., Siqueira, D.S., Camargo, L.A., Teixeira, D.D.B., Barrón, V., Torrent, J., 2014. Magnetic susceptibility and diffuse reflectance spectroscopy to characterize the spatial variability of soil properties in a brazilian haplustalf. Geoderma 219–220, 63–71. https://doi.org/10.1016/j.geoderma.2013.12.007

Mathé, V., Lévêque, F., 2003. High resolution magnetic survey for soil monitoring: Detection of drainage and soil tillage effects. Earth Planet. Sci. Lett. 212, 241–251. https://doi.org/10.1016/S0012-821X(03)00241-3

Maxbauer, D.P., Feinberg, J.M., Fox, D.L., 2016. Magnetic mineral assemblages in soils and paleosols as the basis for paleoprecipitation proxies: A review of magnetic methods and challenges. Earth-Science Rev. 155, 28–48. https://doi.org/10.1016/j.earscirev.2016.01.014

McBratney, A.B., Mendonça Santos, M.L., Minasny, B., 2003. On digital soil mapping, Geoderma. https://doi.org/10.1016/S0016-7061(03)00223-4

McFadden, M., Scott, W.R., 2013. Broadband soil susceptibility measurements for EMI applications. J. Appl. Geophys. 90, 119–125. https://doi.org/10.1016/j.jappgeo.2013.01.009

Mernagh, T.P., Miezitis, Y., 2008. A Review of the Geochemical Processes Controlling the Distribution of Thorium in the Earth ' s Crust and Australia ' s Thorium Resources 48.

Meyer, S. et al, 2019. Creating soil texture maps for precision liming using electrical resistivity and gamma ray mapping, 19th ed.

Michel, F.M., Barrón, V., Torrent, J., Morales, M.P., Serna, C.J., Boily, J.F., Liu, Q., Ambrosini, A., Cismasu, A.C., Brown, G.E., 2010. Ordered ferrimagnetic form of ferrihydrite reveals links among structure, composition, and magnetism. Proc. Natl. Acad. Sci. U. S. A. 107, 2787–2792. https://doi.org/10.1073/pnas.0910170107

Minty, B.R.S., 1997. GA1687.pdf.

Minty, B.R.S., 1988. A Review of Airborne Gamma-Ray Spectrometric Data-Processing Techniques. Aust. Gov. Publ. Serv.

Mokhtari Karchegani, P., Ayoubi, S., Lu, S.G., Honarju, N., 2011. Use of magnetic measures to assess soil redistribution following deforestation in hilly region. J. Appl. Geophys. 75, 227–236. https://doi.org/10.1016/j.jappgeo.2011.07.017

Moonjun, R., Shrestha, D.P., Jetten, V.G., van Ruitenbeek, F.J.A., 2017. Application of airborne gamma-ray imagery to assist soil survey: A case study from Thailand. Geoderma 289, 196–212. https://doi.org/10.1016/j.geoderma.2016.10.035

Morais, P.A. de O., Souza, D.M. de, Carvalho, M.T. de M., Madari, B.E., de Oliveira, A.E., 2019. Predicting soil texture using image analysis. Microchem. J. 146, 455–463. https://doi.org/10.1016/j.microc.2019.01.009

Muhammad Aqeel Ashraf;Mohd Jamil MaahMohd Jamil Maah; Ismail Bin YusoffIsmail Bin Yusoff, 2011. Introduction to Remote Sensing of Biomass. https://doi.org/10.5772/16462

Mullins, C.E., 1977. Magnetic Susceptibility of the Soil and Its Significance in Soil Science – a Review. J. Soil Sci. 28, 223–246. https://doi.org/10.1111/j.1365-2389.1977.tb02232.x

Nanni, M.R., Demattê, J.A.M., 2006. Spectral Reflectance Methodology in Comparison to Traditional Soil Analysis. Soil Sci. Soc. Am. J. 70, 393. https://doi.org/10.2136/sssaj2003.0285

Nico Van Breemen and Peter Buurman, 2003. Soil Formation, 2 nd. ed, KLUWER ACADEMIC PUBLISHERS. Laboratory of Soil Science and Geology, NEW YORK, BOSTON, DORDRECHT, LONDON, MOSCOW. https://doi.org/10.1017/CBO9781107415324.004

Oliveira, D. De, Santos, A.H.B. dos, 2008. Trajetórias do rio Capivari : implicações de um impacto meteorítico na drenagem no reverso. Geografias 04, 69–76.

P. Driessen, J. Deckers, O. Spaargaren, F.N., 2001. Lecture notes on the major soils of the world.

Paisani, J.C., Pontelli, M.E., de Barros Corrêa, A.Ô.C., Rech Rodrigues, R.A., 2013. Pedogeochemistry and micromorphology of oxisols - A basis for understanding etchplanation in the Araucárias Plateau (Southern Brazil) in the Late Quaternary. J. South Am. Earth Sci. 48, 1–12. https://doi.org/10.1016/j.jsames.2013.07.011

Pansu, M., Gautheyrou, J., 2006. Handbook of Soil Analysis – Mineralogical, Organic and Inorganic Methods. Springer, Netherlands.

Parasnis, D.S., 1986. Principles of Applied Geophysics, 4ª. ed.

Parker, R., Ruffell, A., Hughes, D., Pringle, J., 2010. Geophysics and the search of freshwater bodies: A review. Sci. Justice 50, 141–149. https://doi.org/10.1016/j.scijus.2009.09.001

Phil Bierwirth,Paul Gessler, McKane, and D., 1996. Proceedings of the 8th Australasian Remote Sensing Conference. Proc. 8th Australas. Remote Sens. Conf. 1–3.

Pinheiro, E.A.R., de Jong van Lier, Q., Inforsato, L., Šimůnek, J., 2019. Measuring full-range soil hydraulic properties for the prediction of crop water availability using gamma-ray attenuation and inverse modeling. Agric. Water Manag. 216, 294–305. https://doi.org/10.1016/j.agwat.2019.01.029

Priori, S., Bianconi, N., Costantini, E.A.C., 2014. Can γ-radiometrics predict soil textural data and stoniness in different parent materials? A comparison of two machine-learning methods. Geoderma 226–227, 354–364. https://doi.org/10.1016/j.geoderma.2014.03.012

R W Boyle, 1982. Geochemical prospecting for thorium and uranium deposits. Elsevier Scientific Publishing Company, Amsterdan.

Rahimi, M.R., Ayoubi, S., Abdi, M.R., 2013. Magnetic susceptibility and Cs-137 inventory variability as influenced by land use change and slope positions in a hilly, semiarid region of west-central Iran. J. Appl. Geophys. 89, 68–75. https://doi.org/10.1016/j.jappgeo.2012.11.009

Randall Schaetzel and Sharon Anderson, 2005. Soil Genesis and Geomorphology.

Rawlins, B.G., Lark, R.M., Webster, R., 2007. Understanding airborne radiometric survey signals across part of eastern England. Earth Surf. Process. Landforms 32, 1503–1515. https://doi.org/10.1002/esp.1468

Read, C.F., Duncan, D.H., Ho, C.Y.C., White, M., Vesk, P.A., 2018. Useful surrogates of soil texture for plant ecologists from airborne gamma-ray detection. Ecol. Evol. 8, 1974–1983. https://doi.org/10.1002/ece3.3417

Reinhardt, N., Herrmann, L., 2019. Gamma-ray spectrometry as versatile tool in soil science: A critical review. J. Plant Nutr. Soil Sci. 182, 9–27. https://doi.org/10.1002/jpln.201700447

Ribeiro, F.C.A., Silva, J.I.R., Lima, E.S.A., do Amaral Sobrinho, N.M.B., Perez, D. V., Lauria, D.C., 2018. Natural radioactivity in soils of the state of Rio de Janeiro (Brazil): Radiological characterization and relationships to geological formation, soil types and soil properties. J. Environ. Radioact. 182, 34–43. https://doi.org/10.1016/j.jenvrad.2017.11.017

Robinson, D.A., Panagos, P., Borrelli, P., Jones, A., Montanarella, L., Tye, A., Obst, C.G., 2017. Soil natural capital in Europe; A framework for state and change assessment. Sci. Rep. 7, 1–14. https://doi.org/10.1038/s41598-017-06819-3

Rochette, P., Jackson, M., Aubourg, C., 1992. Rock magnetism andn the interpretation of magnetic susceptibility. Rev. Geophys. 30, 209–226.

Rodríguez Martín, J.A., Arias, M.L., Grau Corbí, J.M., 2006. Heavy metals contents in agricultural topsoils in the Ebro basin (Spain). Application of the multivariate geoestatistical methods to study spatial variations. Environ. Pollut. 144, 1001–1012. https://doi.org/10.1016/j.envpol.2006.01.045

Roman, S.A., Johnson, W.C., Geiss, C.E., 2013. Grass fires-an unlikely process to explain the magnetic properties of prairie soils. Geophys. J. Int. 195, 1566–1575. https://doi.org/10.1093/gji/ggt349

Romero-Ruiz, A., Linde, N., Keller, T., Or, D., 2018. A Review of Geophysical Methods for Soil Structure Characterization. Rev. Geophys. 56, 672–697. https://doi.org/10.1029/2018RG000611

Rossel, R.A.V., Taylor, H.J., McBratney, A.B., 2007. Multivariate calibration of hyperspectral γ-ray energy spectra for proximal soil sensing. Eur. J. Soil Sci. 58, 343–353. https://doi.org/10.1111/j.1365-2389.2006.00859.x

Rutherford and Soddy, 1902. The cause and nature of radioactivity - Part I, Journal of African Earth Sciences. https://doi.org/10.1016/j.jafrearsci.2017.04.031

Rutherford, E., Soddy, F., 1902. XLI. The cause and nature of radioactivity .—Part I . London, Edinburgh, Dublin Philos. Mag. J. Sci. 4, 370–396. https://doi.org/10.1080/14786440209462856

S. R. Cattle, S. N. Meakin, P.R. and R.G.C., 2003. Using radiometric data to identify æolian dust additions to topsoil of the Hillston district, western NSW. Aust. J. Soil Res.

Santos-Francés, F., Gil Pacheco, E., Martínez-Graña, A., Alonso Rojo, P., Ávila Zarza, C., García Sánchez, A., 2018. Concentration of uranium in the soils of the west of Spain. Environ. Pollut. 236, 1–11. https://doi.org/10.1016/j.envpol.2018.01.038

Santos, H.L., Júnior, J.M., Matias, S.S.R., Siqueira, D.S., Pereira, G.T., 2011. Suscetibilidade magnética na identificação de compartimentos da paisagem em uma vertente. Rev. Bras. Ciencias Agrar. 6, 710–716. https://doi.org/10.5039/agraria.v6i4a1347

Sarmast, M., Farpoor, M.H., Esfandiarpour Boroujeni, I., 2017. Magnetic susceptibility of soils along a lithotoposequence in southeast Iran. Catena 156, 252–262. https://doi.org/10.1016/j.catena.2017.04.019

Sawyer, E.W., 1986. The influence of source rock type, chemical weathering and sorting on the geochemistry of clastic sediments from the Quetico Metasedimentary Belt, Superior Province, Canada. Chem. Geol. 55, 77–95. https://doi.org/10.1016/0009-2541(86)90129-4

Schuler, U., Erbe, P., Zarei, M., Rangubpit, W., Surinkum, A., Stahr, K., Herrmann, L., 2011. A gamma-ray spectrometry approach to field separation of illuviation-type WRB reference soil groups in northern Thailand. J. Plant Nutr. Soil Sci. 174, 536–544. https://doi.org/10.1002/jpln.200800323

Schwertmann, U., 1988. Occurrence and formation of iron oxides in various pedoenvironments. Iron soils clay Miner. 267–308. https://doi.org/10.1007/978-94-009-4007-9_11

Shenggao, L., 2000. Lithological factors affecting magnetic susceptibility of subtropical soils, Zhejiang Province, China. Catena 40, 359–373. https://doi.org/10.1016/S0341-8162(00)00092-8

Shenggao, L., 1998. Magnetic properties and iron oxide mineralogy of subtropical soils and environmental implications. Zhejiang University, China.

Silva, S.M.P. da, Crósta, A.P., Ferreira, F.J.F., Beurlen, H., Silva, A.M., Santos, L.F. dos, 2010. Espectrometria de raios gama de granitos pegmatíticos da Província Pegmatítica da Borborema (PPB), nordeste do Brasil. Rev. Bras. Geofísica 28, 673–690. https://doi.org/10.1590/s0102-261x2010000400011

Silvério, D. V., Bustamante, M., Brando, P.M., Macedo, M.N., Coe, M.T., Beck, P.S.A., 2015. Agricultural expansion dominates climate changes in southeastern Amazonia: The overlooked non-GHG forcing. Environ. Res. Lett. 10. https://doi.org/10.1088/1748-9326/10/10/104015

Singer, M.J., Fine, P., 1989. Pedogenic factors affecting magnetic susceptibility of northern California soils. Soil Sci. Soc. Am. J. 53, 1119–1127. https://doi.org/10.2136/sssaj1989.03615995005300040023x

Singer, M.J., Verosub, K.L., Fine, P., TenPas, J., 1996. A conceptual model for the enhancement of magnetic susceptibility in soils. Quat. Int. 34–36, 243–248. https://doi.org/10.1016/1040-6182(95)00089-5

Siqueira, D.S., Marques, J., Matias, S.S.R., Barrón, V., Torrent, J., Baffa, O., Oliveira, L.C., 2010. Correlation of properties of Brazilian Haplustalfs with magnetic susceptibility measurements. Soil Use Manag. 26, 425–431. https://doi.org/10.1111/j.1475-2743.2010.00294.x

Smith, R.C., Rose, A.W., 1975. Geology and Geochemistry of Triassic Diabase in Pennsylvania. Bull. Geol. Soc. Am. 86, 943–955. https://doi.org/10.1130/0016-7606(1975)86<943:GAGOTD>2.0.CO;2

Snnecker, J.P., 2000. Materiais Magnéticos Doces e Materiais Ferromagnéticos Amorfos. Rev. Bras. Ensino Física 22, 396–405.

Solutions, R., 2009. Spectrum stabilization and calibration for the RSI RS-125 and RS-230 handheld spectrometers.

Souza Junior, I.G. de, Costa, A.C.S. da, Vilar, C.C., Hoepers, A., 2010. Mineralogia e susceptibilidade magnética dos óxidos de ferro do horizonte B de solos do Estado do Paraná. Ciência Rural 40, 513–519. https://doi.org/10.1590/s0103-84782010000300003

Spassov, S., Egli, R., Heller, F., Nourgaliev, D.K., Hannam, J., 2004. Magnetic quantification of urban pollution sources in atmospheric particulate matter. Geophys. J. Int. 159, 555–564. https://doi.org/10.1111/j.1365-246X.2004.02438.x

Staff, S.S., 2017. Soil Survey Manual - Soil Taxonomy, Soil Survey Manual.

Sturchio, N.C., 2003. Uranium-series disequilibrium: Applications to Earth, Marine, and environmental sciences. Geochim. Cosmochim. Acta 57, 4327–4328. https://doi.org/10.1016/0016-7037(93)90331-p

Taylor, M J, Smettem, K., Pracilio, G., Verboom, W., 2002. Relationships between soil properties and high-resolution radiometrics, central eastern Wheatbelt, Western Australia. Explor. Geophys. 33, 95–102.

Taylor, Miranda J, Smettem, K., Smettem, K., Pracilio, G., Verboom, W., 2002. Relationships between soil properties and high-resolution radiometrics , central eastern Relationships between soil properties and high-resolution radiometrics , central eastern Wheatbelt , Western Australia 33, 95–102. https://doi.org/10.1071/EG02095

Thompson, R., Oldfield, F., 1986. Environmental Magnetism. Allen and, 227.

Triantafilis, J., Gibbs, I., Earl, N., 2013. Digital soil pattern recognition in the lower Namoi valley using numerical clustering of gamma-ray spectrometry data. Geoderma 192, 407–421. https://doi.org/10.1016/j.geoderma.2012.08.021

U. C. Sharma, 1998. Influence of soil texture and rainfall on leaching of potassium and its recovery by potato (Solonum tuberosum). Indian J. Agric. Sci. 59, 713–717.

Ulbrich, H.H.G.J., Ulbrich, M.N.C., Ferreira, F.J.F., Alves, L.S., Guimaraes, G.B., Fruchting, A., 2009. Gamma-spectrometric surveys in differentiated granites. I: A review of the method, and of the geochemical behavior of K, Th and U\rLevantamentos gamaespectrometricos em granitos diferenciados. I: Revisao da metodologia e do comportamento geoquimico dos el. Geol. USP - Ser. Cient. 9, 33–53.

Valaee, M., Ayoubi, S., Khormali, F., Lu, S.G., Karimzadeh, H.R., 2016. Using magnetic susceptibility to discriminate between soil moisture regimes in selected loess and loess-like soils in northern Iran. J. Appl. Geophys. 127, 23–30. https://doi.org/10.1016/j.jappgeo.2016.02.006

van Dam, R.L., Hendrickx, J.M., Harrison, B., Borchers, B., Norman, D.I., Ndur, S., Jasper, C., Niemeyer, P., Nartey, R., Vega, D.N., Calvo, L., Simms, J.E., 2004. Spatial variability of magnetic soil properties. Detect. Remediat. Technol. Mines Minelike Targets IX 5415, 665. https://doi.org/10.1117/12.540693

Vandenhove, H., Van Hees, M., Wouters, K., Wannijn, J., 2007. Can we predict uranium bioavailability based on soil parameters? Part 1: Effect of soil parameters on soil solution uranium concentration. Environ. Pollut. 145, 587–595. https://doi.org/10.1016/j.envpol.2006.04.011

Viscarra Rossel, R.A., Webster, R., Kidd, D., 2014. Mapping gamma radiation and its uncertainty from weathering products in a Tasmanian landscape with a proximal sensor and random forest kriging. Earth Surf. Process. Landforms 39, 735–748. https://doi.org/10.1002/esp.3476

W.K. Jung, N.R. Kitchen, S.H. Anderson, E.J.S., 2007. Crop management effects on water infiltration for claypan soils. J. Soil Water Conserv. 62, 55–63.

Wang, X., Li, Z., Cai, C., Shi, Z., Xu, Q., Fu, Z., Guo, Z., 2012. Effects of rock fragment cover on hydrological response and soil loss from Regosols in a semi-humid environment in South-West China. Geomorphology 151–152, 234–242. https://doi.org/10.1016/j.geomorph.2012.02.008

Wilford, J., 2012. A weathering intensity index for the Australian continent using airborne gamma-ray spectrometry and digital terrain analysis. Geoderma 183–184, 124–142. https://doi.org/10.1016/j.geoderma.2010.12.022

Wilford, P.N., Bierwirth, J.R., Craig, M.A., 1997. Application of airborne gamma-ray spectrometry in soiVregolith mapping and Applied Geomorphology 17.

Yates, F., 1934. The Analysis of Multiple Classifications with Unequal Numbers in the Different Classes. J. Am. Stat. Assoc. 29, 51–66. https://doi.org/10.1080/01621459.1934.10502686

Zhou, L.P., Oldfield, F., Wintle, A.G., Robinson, S.G., Wang, J.T., 1990. Partly pedogenic origin of magnetic variations in Chinese loess. Nature 346, 737–739. https://doi.org/10.1038/346737a0

Zolfaghari, Z., Mosaddeghi, M.R., Ayoubi, S., 2015. ANN-based pedotransfer and soil spatial prediction functions for predicting Atterberg consistency limits and indices from easily available properties at the watershed scale in western Iran. Soil Use Manag. 31, 142–154. https://doi.org/10.1111/sum.12167

3. SOIL MAGNETISM AND ITS RELATIONSHIP WITH PEDOSPHERE NATURALLY OCCURRING PROCESSES, SOIL ATTRIBUTES AND SURVEY, IN HETEROGENEOUS TROPICAL ENVIRONMENT

Danilo César de Mello[1], José A. M. Demattê[1]*, Nélida E. Q. Silvero[1], Luís A. D. L. Di Raimo[1], Raul R. Poppiel[1], Fellipe A. O. Mello[1], Arnaldo B. Souza[1], José L. Safanelli[1], Maria E. B. Rezende[1], Rodnei Rizzo[1]

[1] Department of Soil Science, "Luiz de Queiroz" College of Agriculture, University of São Paulo, Av. Pádua Dias, 11, CP 9, Piracicaba, SP 13418-900, Brazil; emails: daniloc.demello@gmail.com; jamdmat@usp.br*; neliquinhonez92@gmail.com; luis.diloreto@hotmail.com; raulpoppiel@gmail.com; fellipeamello@usp.br; arnaldo_bsouza@hotmail.com; jose.lucas.safanelli@usp.br; eduardaresende@usp.br; rodnei.rizzo@gmail.com
* Corresponding author.

Abstract

The soil magnetic susceptibility (MS) has potential to be used as a pedoenvironmental indicator from which mineralogy, pedogeochemical, pedogeomorphological and pedogenesis processes can be inferred. It can be used in pedosphere studies, as an auxiliary information for appropriate and sustainable soil use and management. This research was performed aiming to analyze how pedogenesis and geochemical processes can affect the soil magnetic susceptibility and some of its attributes, as well as the potential use in soil great group discrimination, following the digital soil mapping approach. The study is located in a site at São Paulo State - Brazil. Soil samples were physico-chemical analyzed at 89 locations (0 - 20 cm). At these sites, MS were collected with KT 10 – Terraplus (portable field instrument) and analyzed in function of geology, relief and soil classes. The results showed that geology strongly affects MS, mainly on diabase segment, followed by metamorphosed siltstone and siltstone. On fluvial sediments, the MS has different behavior due to different sediments deposited by the Capivari river. In less evolved soil class, such as Cambisols, lithology has more important contribution than pedogenesis. In more evolved soil classes, nitidization increases MS, whereas argilluviation reduce it. The MS values did not decrease significantly or even increase downslope, due to presence of diabase on the lower parts. It was found difference of MS between diabase west and diabase east in study area, indicating major influence of geomorphic processes than lithology. With respect to soil attributes, it was found positive correlation between MS and Base Saturation, Cation Exchange Capacity, Organic Matter, and Fe_2O_3 and clay content, whereas a negative correlation was found to MS and sand content. The MS has identified changes in lithology and soil classes compartments on landscapes demonstrating to be a potential tool on the discriminating soil great group classes and digital soil mapping.

Keywords: magnetic susceptibility, pedosphere processes, soil classes, digital soil mapping, remote sensing.

3.1. INTRODUCTION

The world population will achieve more than 9 billion people by 2050, and the production of food and fiber to meet this demand is expected to nearly double (Godfray et al. 2010). Knowing that worldwide agroforestry activities depend on the soil resource as a means of production (FAOSTAT, 2003), its recognition as an environmental component for the maintenance of human life and support, the production of fiber and food, is fundamental (Robinson et al. 2017).

There is a tendency to expand agricultural frontiers to new areas, with consequent environmental impact and degradation of agroecosystems (Godfray et al. 2010). The main environmental processes that occur in pedosphere system are pedogeomorphological, pedogeochemical and pedogenesis. Pedogeomorphological are processes related to landscape evolution (Atalay, 2018). Pedogeochemical is the geochemical pathways that result in mineral formation and soil profile features (Paisani et al. 2013). Pedogenesis is related to geochemical and biological pathways resulting in different soil classes or horizons differentiation (Van Breemen and Buurman, 2003). Therefore, knowledge of soil attributes, as well as the pedogenetic, pedogeomorphological and biogeochemical processes that occur in the pedosphere, is essential to determine the soils capacity for a proper land use and management, with the consequent mitigation or prevention of environmental degradation (Li and Heap, 2008; Foley, 2011).

Among soil attributes, magnetic susceptibility (MS) is one of the closest related to pedogenesis processes (Singer et al. 1996; Sarmast et al. 2017), geology (Lu et al., 2000), texture and organic carbon (Camargo et al. 2014; Jiménez et al. 2017), soil degradation (Mokhtari Karchegani et al. 2011), water balance (Valaee et al. 2016) and soil survey (Grimley et al. 2004). Thus, pedologists have used soil magnetism studies to understand pedogenetic and pedogeomorphological processes along the soil evolution (McFadden and Scott, 2013; Sarmast et al., 2017).

Magnetization is strong and significantly important for a high percentage of Brazilian soils, especially in areas over basaltic spills (Costa et al. 1999). MS allow the quantification of the magnetization intensity of iron-containing minerals in rocks, soils and sediments, quickly, safely and non-destructively (Dearing, 1994). The minerals can be classified into: ferromagnetic, ferrimagnetic, paramagnetic and anti-ferromagnetic (Dearing, 1999). This classification has been established according to how they respond to an applied magnetic field in relation to their relative susceptibility ranging from 10^{-5} to 10^{-6} *SI* (Snnecker, 2000).

Magnetic properties of the soil determined by geophysical techniques reflect the presence of ferrimagnetic minerals from the clay and sand fraction, such as maghemite and magnetite, respectively, as well as other minerals such as ferrihydrite and hematite. (Valaee et al. 2016). It also allows inference to the soil formation processes and source material (Mullins, 1977; De Jong et al. 2000). MS technique is applied to geosciences and environmental sciences efficiently to detect presence of ferrimagnetic minerals (Ayoubi and Mirsaidi, 2019). The geology and consequently the mineralogy of rocks and sediments that originate the soils, are the main conditioners of its magnetic properties (Ayoubi et al. 2018). Moreover, in the pedosphere there are many environmental variables acting on the MS, such as the stage of landscape evolution, soil formation processes, source material, biological activity, soil hydrology, physical chemical properties and human activities (Spassov et al. 2004). In tropical environments such as Brazil, the climate, temperature and soil water regime act concurrently with geology to determine magnetic properties by converting ferrimagnetic to paramagnetic minerals or the opposite (De Jong et al. 2000; Grimley et al. 2004; Gholamzadeh et al. 2019).

Some works were carried out with the objective to identify soil magnetic signatures, still using laboratory methods (Van Dam et al., 2004; Grimley et al., 2004; Siqueira et al., 2010; Camargo et al., 2014; Marques et al., 2014; Jordanova et al., 2016; Jiménez et al., 2017; Kanu et al., 2019). In addition, the most studies focus on results of MS without relate to naturally occurring processes in pedosphere (pedogeochemical, pedogeochemical and pedogeomorphological) (Cervi et al., 2019). There is also a paucity of research demonstrating how MS can be used as a tool in soil classification and digital mapping (Sarmast et al. 2017; Cervi et al. 2019). By contributing to this knowledge gap, it is possible to improve MS applications in soil science (Grunwald et al. 2011; Brevik et al. 2016). So, it is necessary more researches to verify the potential use of soil magnetic signatures, using field methods, in the variety lithology and its relation to pedosphere processes, soil classes and water regimes (Cervi et al. 2019).

The hypothesis of this research is based on naturally occurring processes in pedosphere affect the soil MS and the attributes related to, as well as different parent material and relief. Besides, we hypothesis if the field sensor (proximal remote sensing) detected satisfactorily the variety of soil MS according to different pedoenvironment.

Given this, the research was carried out with the purpose of analyzing the relationship with pedogenesis and pedogeomorphological processes that occur in pedosphere, considering the influence of geochemical comportment of minerals, lithology and relief in

MS, in different pedological classes using field sensor. In addition, we analyzed the potentiality of the MS by proximal remote sensing to discriminate soil attributes and large groups of soils classes, contributing to the digital soil mapping. This research may provide the basis for improving the technique in surveying and digital soil mapping (Cervi et al. 2019), understanding of pedogenetic, biogeochemical and pedogeomorphological processes that occur in the soil, as well as environmental studies such as identification of heavy metals (Rahimi et al. 2013; Govedarica et al. 2019; Ayoubi et al. 2019), metal prediction modeling work in intelligent artificial neural network systems, machine learning, decision trees (Zolfaghari et al. 2015), algorithm CHILD (Abbaszadeh Afshar et al. 2016).

3.2. MATERIAL AND METHODS

3.2.1. Study area characterization and sample collection for physical chemical analysis.

The study site is geomorphologically inserted in the Peripheral Depression of São Paulo, in the Capivari River watershed, located in the interior of São Paulo State, Brazil. The area has 183 hectares currently cultivated with sugar-cane. **(Fig. 1).** The lithology is composed of sedimentary rocks (metamorphic siltstones and siltstones), diabase intrusive dikes and river sediments (**Fig. 2a**). The relief is quite heterogeneous, with altitudes ranging from 474.83 m to 567.69 m and a maximum slope of 35%. The climate of the region, according to the Köppen classification, is subtropical mesothermal (Cwa), with an average annual precipitation volume of 1200 mm (Alvares et al. 2013), with average temperatures of 18 °C in winter and 22 ° C in the summer.

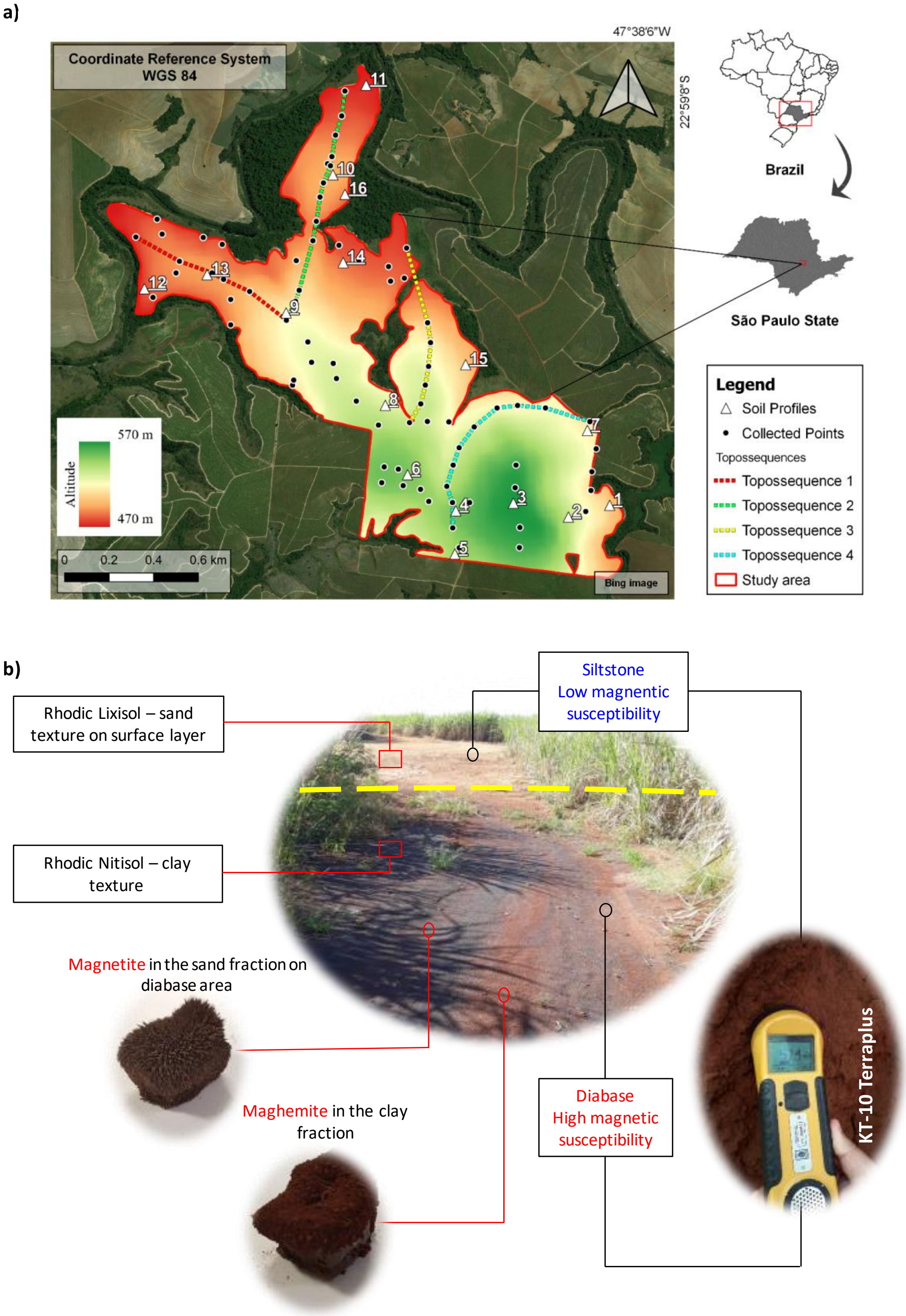

Figure 1. a) Study area, collected points and selected topossequences. b) Susceptibilimeter (KT-10 Terraplus) reading soil surface and some of soil classes and minerals magnetically quantified.

Due to lithological variability and heterogeneous relief, there is an important diversity of soils in the area that fall into several taxonomic classes, which in previous works were classified as: Acrisols, Lixisols, Nitisols, Cambisols and Phaeozems (IUSS Working Group WRB, 2015) (**Fig. 2d**). We used a detailed soil class map as reference for investigating the relationship between soil classes distribution and MS patterns.

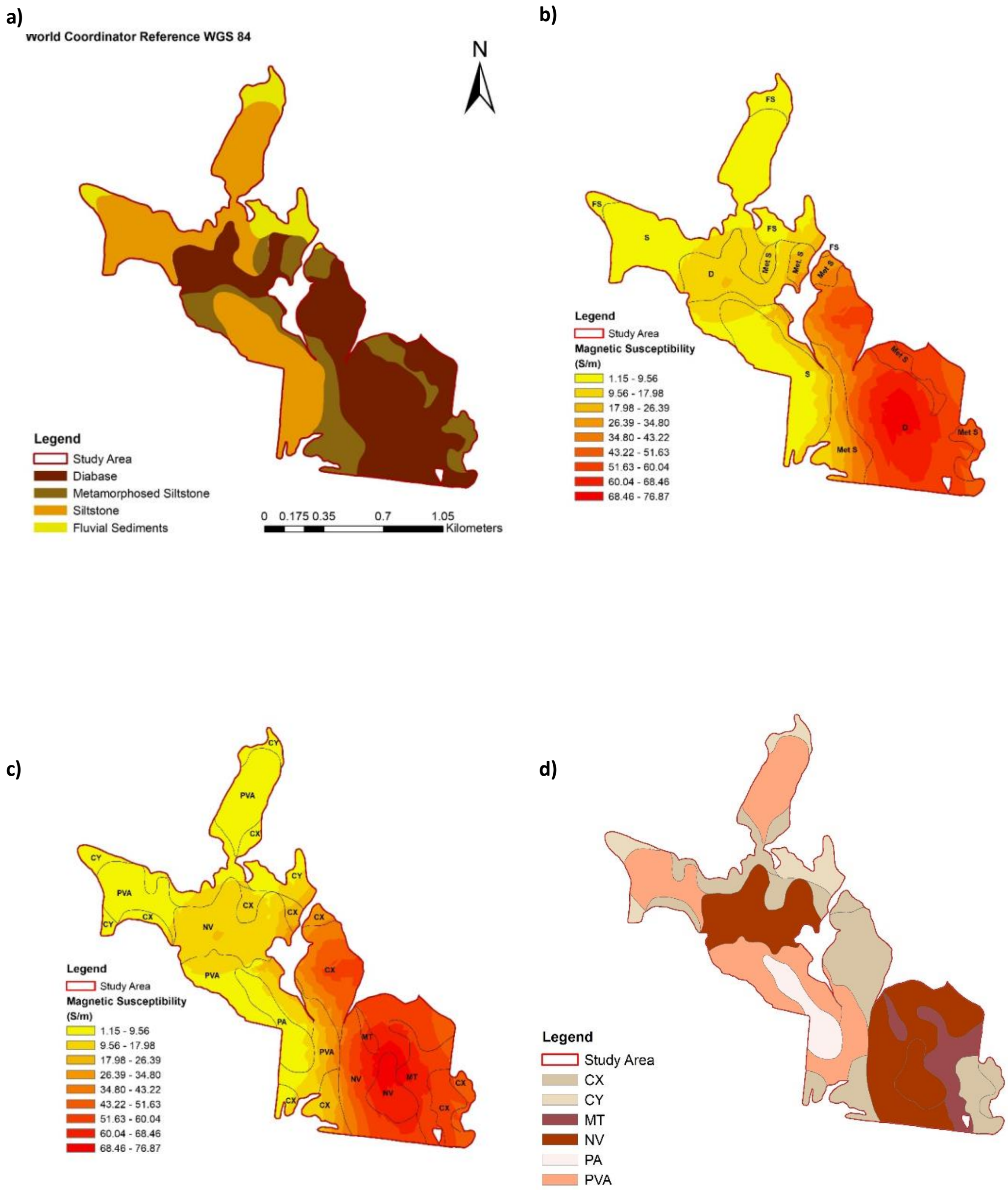

Figure 2. a) Geological compartments. b) Magnetic Susceptibility and Geology: D: Diabase; Met S: Metamorphosed Siltstone; S: Siltstone; FS: Fluvial sediments. c) Magnetic Susceptibility and soil classes: CX: Haplic Cambisols, CY: Fluvic Cambisols, MT: Luvic Phaozem, NV: Rhodic Nitisol: PA: Xanthic Acrisol, PVA: Rhodic Lixisol. The geological and Soil classes maps were adapted from Bazaglia Filho et. al. (2012).

For the physical and chemical analysis, soil samples were collected at a depth of 0-20 cm in 89 points, using an auger, distributed in the area (**Fig. 1**). Each point was georrefered. The particle size analysis was performed by the densimeter method following the methodology proposed by Camargo, (1986) wherein the samples were previously air dried, ground and passed through a 2 mm sieve. Subsequently the definitions of the textural groups was determined according to EMBRAPA, (2011). The wet and dry color of the samples was determined using the Munsell chart. Exchangeable cations, magnesium (Mg), calcium (Ca) and aluminum (Al^{3+}) were determined by atomic absorption spectrophotometer after extraction with 1M KCl solution. Regarding potassium cation (K^{+}), quantification was performed via Mehlich-1 using a flame photometer (EMBRAPA, 2017). Potential acidity ($H^{+} + Al^{3+}$) was determined by the SMP method Quaggio and Raij, (2001), whereas the pH in water by the methodology (EMBRAPA, 2017). The organic matter (OM) content was determined following the Walkley-Black methodology proposed by Pansu and Gautheyrou, (2006). Iron (Fe_2O_3) contents were determined by sulfuric digestion (Lim and Jackson, 1986). Silicon (SiO_2) and titanium (TiO_2) contents were determined following the methodology (EMBRAPA, 2017). Subsequently, the parameters were calculated, base sum (SB) base saturation (V%), aluminum saturation (m%) and cation exchange capacity (CTC), using the analytical data obtained.

3.2.2. Magnetic susceptibility data collection

At the 89 points (**Fig.1**), surface readings were performed with a near geophysical susceptibility sensor (SC), for easy, rapid and high precision of measurements, model *KT10 - Terraplus* (**Fig. 1b**), which measures the MS to a depth of 2 cm from the ground of the minerals that constitute rocks and sediments, with precision *10^{-6} SI.*

The sensor was properly calibrated by determining the frequency of the outdoor oscillator, then determining the frequency with the SC directly above ground and finally measuring the frequency again in the open air. This procedure is necessary since the operating principle of the device is based on the difference between the material MS (ground) and the outdoor measurement. From there the scanner mode readings were applied, which uses the best geometric correlation to the direct MS readings providing fast and accurate quantification. The readings were made in triangulation around the auger collection points, obtaining three readings that noted in a spreadsheet and the average of these three readings was used. This procedure was performed to reduce noise.

3.2.3. Digital elevation model generation and maps

In the SAGA GIS (2.1.2) software (*Terrain analysis tool*), the digital elevation model (DEM) was created from the tabulated database, using altitude and georreferenced points. Four toposequences were defined and plotted (**Fig. 1a**), using the software ArcGIS 10.3 (ESRI, 2011), where the lithology, soil classes and relief information were concatenated, in order to analyze the distribution of MS considering the landscape.

3.2.4. Statistical analysis

Statistical analyzes were performed aiming to identify significant differences between the MS values by lithology compartment and soil classes (more and less evolved). To evaluate that, analysis of variance and mean comparison by Tukey test ($p < 0.05$) was carried out in R software (R Core Team, 2015). The analysis of variance was performed considering *type III error* to verify statistical differences between MS on lithological compartments and soil classes. In this step, the *R emmeans* (*Estimated Marginal Means*) package was used to consider estimations for unbalanced data. The Tukey test was performed using *multcomp* (*Simultaneous Inference in General Parametric Models*) package. Additionally, descriptive statistics of MS maximum, minimum, mean, median, standard deviation (SD) and coefficient of variation (CV) were calculated considering MS, lithology and soil classes. Person's correlation analysis was carried out between all MS and soil attributes to analyze their relations. Thus, the statistical results assisted to relate the MS spatial distribution with known soil physico chemical attributes, classes and pedogenesis processes related to ferralitizattion (Nitisols) and argilluviation (Lixisols).

In ArcGIS 10.3 software (ESRI, 2011), the interpolation of the MS values (Fig. 3 and toposequences with predicted values) was performed by the *Spatial analyst* - *Interpolation* - Kriging method. The experimental semivariogram was estimated follow:

$$\gamma(h) = \frac{1}{2N(h)} \sum_{i=1}^{N(h)} [z(x_i) - z(x_i + h)]^2$$

$\gamma(h)$: semivariance;

$N(h)$: number of pair of points separated by the distance

h; $z(x_i)$: value of z in the position x_i;

$z(x_i + h)$: value of z in the position $x_i + h$.

After semivariogram performance, the interpolation was undertaken by ordinary kriging, estimated as:

$$\hat{z}(x_0) = \sum_{i=1}^{N} \lambda_i \, z(x_i)$$

$\hat{z}(x_0)$ is the kriging estimator at the x_0 point;

$z(x_i)$ represents the measured value at the x_i point;

λ_i is the kriging weight attributed to closest $z(x_i)$ values to estimate $\hat{z}(x_0)$.

3.3. RESULTS AND DISCUSSION

3.3.1. Relationship of magnetic susceptibility with lithology and mineralogy

The summary statistics of MS values demonstrated significant differences in function of lithology (**Tab. 1 and Fig. 3a**). The mean value of MS for diabase is four times higher than the second highest mean MS, i.e. for metamorphosed siltstone. These discrepancies was also reported by Sarmast et al. (2017), in a landscape of Iran, which explained that the differences occurred due to varying mineralogical and chemical compositions. The decrease of MS from diabase to the other lithological compartments (**Fig. 3a**) can be explained by the higher occurrence of ferrimagnetic minerals in diabase (mafic igneous rock) (Mullins, 1977), as well as the strong influence of the iron minerals of this rock on the surrounding metamorphosed siltstone (Sawyer, 1986), followed by the lower ferrimagnetic mineral content in siltstone and river sediments (**Fig. 1a**).

Table 1. Descriptive statistics for the analyzed magnetic susceptibility by lithological compartments

Summary Statistics	***MS***			
	D	***Met. S***	***S***	***FS***
Mean	60.65	13.69	3.37	6.24
Standard deviation	30.72	17.11	6.40	5.34
Minimum	21.9	0.42	0.35	0.63
Maximum	113	44.67	24.36	14.6
Count	20	12	28	5

MS: Magnetic Susceptibility. D: Diabase. Met. S: Metamorphosed Siltstone. S: Siltstone. FS: Fluvial Sediments.

Some of *outliers*, can be observed with values above average of MS on the siltstone (**Fig. 3a**). It can be explained by deposition and concentration of magnetite derived from diabase in higher altitudes to lower altitudes, which was observed in field. In addition, it could be occurred due to the variability of transported sediments that originated this rock in the past, along the sedimentary cycle. There was probably higher concentration of ferrimagnetic minerals in specific erratic points of this rock, still formation of magnetite and hematite by hydrothermal alterations (Hooper, 1987).

a)

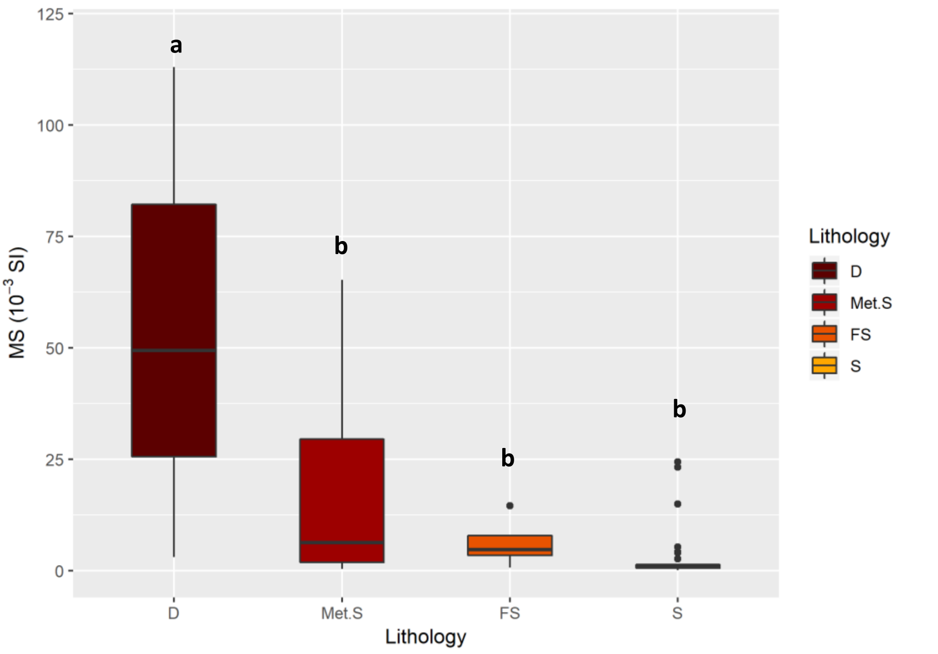

b)

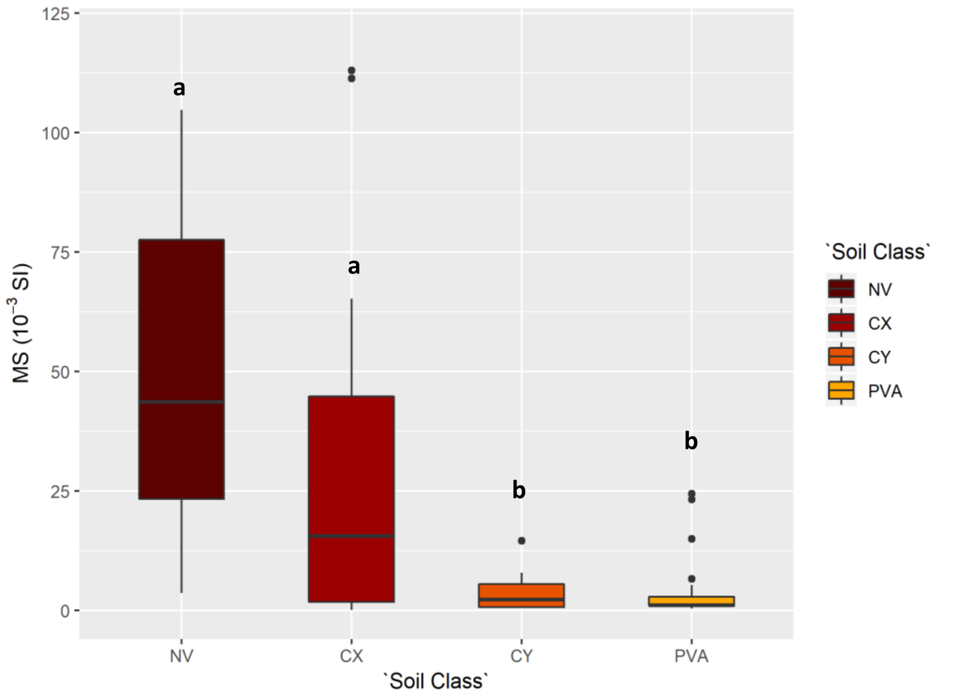

Figure 3. Boxplot for magnetic susceptibility. Multi comparison test for lithology (a) and soil classes (b), significant at the 0.1 significance level., respectively. Geology abbreviation; D: diabase, FS: fluvial sediments, MS: metamorphosed siltstone, S: siltstone. Soil classes abbreviation: CX: Haplic Cambisols, CY: Fluvic Cambisols, NV: Rhodic Nitisol, PVA: Rhodic Lixisol.

It can be observed that the highest mean values of MS (60.65) (**Tab. 1**) occurred over the areas of diabase. These results are corroborated by Ayoubi and Adman (2019), who found higher MS values in basic rocks compared to sedimentary rocks in Iranian soils. Singer and Fine, (1989), Shenggao, (2000) and Damaceno et al. (2017), analyzed MS in soils derived from different source materials and also found higher values in soils derived from this same mafic basic rock. This is because mafic rocks are rich in ferromagnesian minerals (Aydin et al. 2007) and, it releases iron into the system through weathering (De Jong et al. 2000; Cervi et al. 2019), and free and hot drainage environment, favoring the formation of ferrimagnetic minerals such as magnetite and maghemite (Schwertmann, 1988; Grimley and Vepraskas, 2000; Maxbauer et al. 2016).

In addition, according to Dearing et al. (1996) the climate associated with iron release rate, under the weathering action and pedoclimate control on a regional scale, are determining factors in soil MS variability due to the formation of pedogenic ferrimagnetic minerals such as magnetite and maghemite (Shenggao, 2000), on soils settled in the same lithology. However, the interpolated map (**Fig. 2b**) shows discrepancies between the east and west diabase areas, which can be observed also in the descriptive statistics by the mean, minimum and maximum values (**Tab. 2**). The explanation for this difference is probably related to persistence of ferrimagnetic minerals and / or variables in soil formation factors (Lourenço et al. 2014; Grison et al. 2016), different mineralogical composition of diabases or ferralitization operating in different rates (Smith and Rose, 1975).

Table 2. Descriptive statistics for the analyzed magnetic susceptibility by two diabase areas (east and west)

Summary Statistics	***MS***	
	Diabase east	***Diabase west***
Mean	65.77	19.94
Standard deviation	30.91	17.76
Minimum	9.2	2.99
Maximum	113	49.4
Count	17	6

Intermediate mean value of MS (13.69) (**Tab. 1**) was found on metamorphosed siltstone. This value may be related to the influence of diabase intrusion in the siltstone metamorphism process, where iron-rich minerals may have been enriched due to the mobility of this element during metamorphism (Sawyer, 1986) and repositioning on metamorphic rocks (Hooper, 1987) and/or magnetite formation from metamorphosed rocks (Grant, 1900).

According to Hooper, (1987) this iron enrichment occurs as a mixed mass of magnetite and hematite that line fractures in metamorphic rocks. In addition, according to Schwertmann, (1988), Roman et al. (2013) and Jordanova et al. (2019) maghemite and magnetite can be formed in soils derived from low iron materials through past fires that are common in tropical regions where high temperatures and the presence of OM allow the formation of pedogenic iron oxides with high MS.

The lower MS values (3.37) (**Tab. 1**) in soils over siltstones is due to the non-influence of diabase on this lithological compartment (Sawyer, 1986), associated with the absence or low content of ferrimagnetic minerals in the parent material or their non-persistence in the soil by environmental factors, or the complete alteration via pedogenetic processes (Fontes et al. 2000). The low MS values reaffirm the silica rich mineralogy and low iron content, because the lower readings are associated with minerals with low magnetizable iron content and, consequently higher silicate minerals like feldspars, micas and quartz. On the other hand, on diabase geological compartment occurs the opposite, due to this rock be rich in ferrimagnetic minerals (magnetite and maghemite, for example) where the highest MS values were recorded. Second Souza Junior et al. (2010), soil MS indicates the presence of ferrimagnetic minerals such as magnetite and maghemite and that according to Santos et al. (2011) MS values may indicate evolution of pedogenetic processes in different soil fractions, which may act by decreasing MS if the pedoenvironmental conditions favor the formation of antiferrimagnetic minerals.

In relation to fluvial sediments, the mean value of MS was 6.24 (**Tab. 1**), little high than siltstone mean value. In fluvial depositional environments, there is a combination of concentrated and dispersed sources of magnetic minerals from different source materials, which explains mean nonconforming values of MS on this landscape segment, which according to results obtained by Sarmast et al., (2017), the MS value decrease with altitude (Ghilardi et al. 2008).

3.3.2. Magnetic susceptibility variability in toposequence and altitude affect by pedogeomorphological processes

In toposequence 1 (T1) (**Fig. 4**) an abrupt change in the MS values between points P2(11.23 x 10^{-3} *SI*) and P3 (0.58 x 10^{-3} *SI*) can be observed. This wide variation is attributed to changes in lithology (diabase / siltstone) and / or soil classes Rhodic Nitisol to Rhodic Lixisol (NV / PVA), since there was little variation in altitude and distance between these points. On the other hand, point 2 (altitude 496.2 m) consists of a slight depression in relation to neighboring points, being an active depositional environment. In this place the pedogenetic processes of magnetite and maghemite neoformation are lower than the deposition rates of new species and, there is no enough time to form ferrimagnetic pedogenic minerals. The neoformation of ferrimagnetic minerals through the release of iron from the source material via weathering and neoformation of secondary minerals via pedogenesis is dependent on the time of action of these processes on geomorphic surfaces (Shenggao, 2000; Spassov et al. 2004; Camargo et al. 2014). Moreover, Curi and Franzmeier (1984), highlight the importance in geochemical processes throughout the landscape that affect the crystallinity of iron oxides and consequently their MS, where on geomorphic surfaces that favor leaching in tropical environments, occurs the weathering of magnetite and maghemite, resulting in lower values of MS.

Regarding toposequence 2 (T2) (**Fig. 4**), it can be observed that the MS values tend to decrease from the top of the landscape to the lower parts. These results are in agreement with those obtained by De Jong et al. (2000); Blundell et al. (2009); Sarmast et al. (2017), who analyzed the influence of relief on the variation of MS. The fact is related to the variation of two factors along the toposequence, drainage (Mathé and Lévêque, 2003) and particle transport (Rahimi et al. 2013). The top of the landscape (**Fig. 1a**), flatter, predominant deep soil and good infiltration Rhodic Nitisol (NV), favors higher infiltration rate and better drainage On the other hand, the downstream water flow goes to lower parts over Cambissols areas (CX) and Lixisols (PVA), shallow and restricted drainage soils as a function of limited effective depth and textural gradient, respectively. Grimley and Vepraskas (2000) and Maxbauer et al. (2016) emphasize that for formation of magnetite and pedogenic maghemite, good drainage conditions are necessary, a fact that occurs only in the upper relief. In addition, Mullins, (1977) stresses that under restricted drainage conditions, the occurrence of a hypoxic environment is favored and, consequently, iron is bio-reduced and impairs the formation of ferrimagnetic minerals, a fact that would explain the lower values in the lower parts of toposequence.

De Wispelaere et al. (2015), stated that, weak temporary recurrent hydromorphism in some soil classes, resulted in redistribution of Fe-Mn oxides, and this also would contribute to reduction of MS. At the same time, the transport and redistribution of particles throughout erosion, where the fines tend to be carried to the watercourse and the sand fraction tends to accumulate in the lower parts of the landscape, MS values contribute to minor MS values. This fact contributes to the explanation of the lower values of MS in the landscape in the lower parts of the landscape, because although MS ferrimagnetic minerals exist in the sand fraction, the contents are higher in the clay fraction (Mullins, 1977; Maher and Taylor, 1988; Zhou et al. 1990).

It is possible to observe a significant and positive correlation of 0.39 between MS and altitude (**Fig. 5a**). Although the results agree with those obtained by De Jong et al. (2000) and Sarmast et al. (2017), disagree with those obtained by Thompson and Oldfield (1986) who found higher susceptibility levels in the lower parts of the landscape. The likely explanation is the greatest influence of geology, which according to com Ayoubi et al. (2018) is the main determining factor of MS. The representative soil class profile in different altitudes (**Fig. 5b**), correspond to correlation map between MS and Digital Model Elevation. The relationship between these variables is not always directly proportional. At various points on the map, high MS values are observed in the lower parts of the landscape, resulting in an inversely proportional correlation between these quantities. This may be due to the fact that the lower altitude area is over the diabase (west) lithology, where geology and / or pedogenesis processes exerted the greatest influence on the formation and permanence of ferrimagnetic minerals (Lu et al. 2009).

In toposequence 3 (T3) and toposequence 4 (T4) (**Fig. 4**) the elevation and relief variations little explained the variations in the MS values along the landscape. In T3, significant variations in MS values occurred between points P1 / P2, P2 / P3, P5 / P6 and P6 / P7 (**Fig. 4**), concurrently with changes in lithology, identifying the transition points between a geological compartment and another. In T4, in turn, the largest variations occurred between the points P2 / P3, P6 / P7, P8 / P9 and P9 / P10, also indicating the lithological transitions (Fig. 3). These results reaffirm the conclusions of Shenggao, (2000); Vepraskas, (2000); Grimley and Hanesch et al. (2007); Camargo et al. (2014); Sarmast et al. (2017); Ayoubi and Adman, (2019) that geology is one of the factors that most affect soil MS. In addition, for certain sites, especially in T4 (on NV), pedogenetic processes such as argilluviation may have strongly influenced the MS values along these toposequences (Zhou et al. 1990; Shenggao, 1998; Asgari et al. 2018). In T3, the predominant soil is CX, with little expression of pedogenesis and greater influence of lithology. Importantly, it is difficult to separate which factor (lithology or pedogenetic processes) most influences MS, as previously reported in Hanesch et al. (2007) studying the effects of lithology and pedogenesis on MS in soils in Austria.

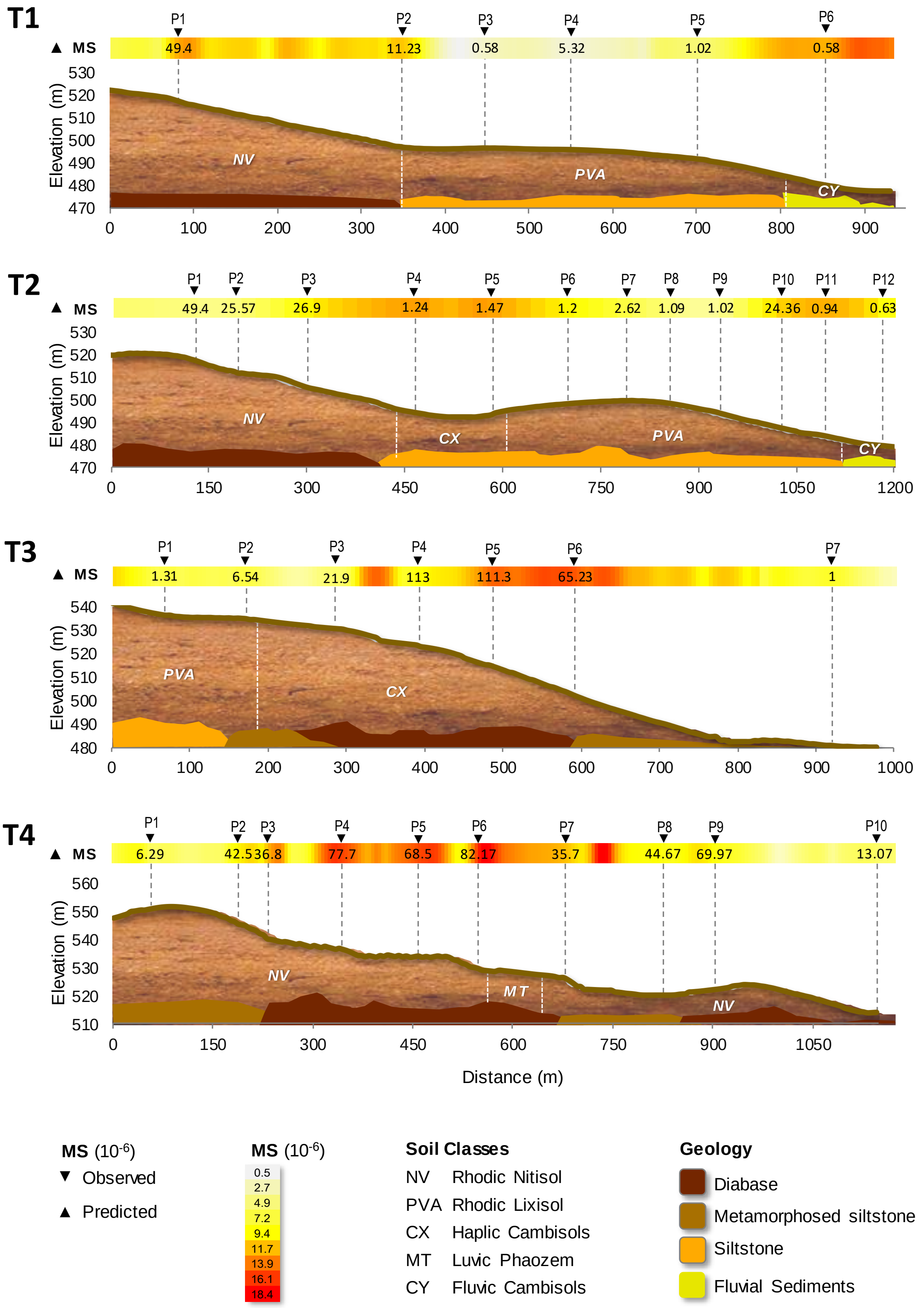

Figure 4. Magnetic susceptibility variability throughout the four topossequences and correspondent soil classes and geological compartment for each collected point. T1: topossequences 1. T2: topossequences 2. T3: topossequences 3. T4: topossequences 4.

3.3.3. Pedogenesis processes, soil classes and magnetic susceptibility

The highest values were found for Rhodic Nitisols (NV), followed by the Haplic Cambisols (CX), both located mostly over the diabase lithological compartment (**Tab. 3**). Smaller MS values were found for the Fluvic Cambisol (CY) and Rhodic Lixisol (PVA) soils classes (**Tab. 3**). The mean comparison test (**Fig. 3b**) demonstrates this difference, where NV and CX belong to the same group and CY and PVA to another. Importantly, the soils NV and CX are clayey in texture while CY and PVA are sandy in texture (PVA in the upper layers). According to Grimley et al. (2004) Soil MS, among other factors, is affected by the surface texture of the soil. Thus, processes that lead to clay formation and clay texture, from source materials rich in ferromagnesian minerals where NV and CX occur, contribute to higher MS values.

Table 3. Descriptive statistics for the analyzed magnetic susceptibility by soil classes

Summary Statistics	***CX***	***CY***	***PVA***	***NV***
Mean	17.97	4.68	4.16	52.84
Standard deviation	21.82	5.10	6.79	31.9
Minimum	0.07	0.6	0.35	6.29
Maximum	65.23	14.6	24.36	104.8
Count	12	7	24	20

MS: Magnetic Susceptibility. CX: Haplic Cambisol, CY: Fluvic Cambisol, PVA: Rhodic Lixisol. NV: Rhodic Nitisol.

The pedogenetic processes that occur in the superficial layers of the soil, lead to the formation of autogenic ferrimagnetic minerals and exert greater influence on MS values. In evolved and weathered soils such as NV, ferrimagnetic minerals are not directly derived from the source material but by pedogenesis processes such as the secondary neoformation of magnetite and maghemite, which increase the MS values (Shenggao, 2000; Ayoubi et al. 2018). Besides, ferralitization occur in this soil class and likely affect the distribution of magnetic minerals in soil profile, due to accumulation of iron oxides on the soil aggregates (Driessen et al, 2001). On the other hand, in the clay texture CX, the ferrimagnetic minerals derived directly from the parent material, influenced the highest MS values (Shenggao, 2000), since this soil is poorly evolved and there is less expression of pedogenesis of secondary ferrimagnetic minerals.

In the Rhodic Lixisol (PVA) class soils (**Tab. 3**), the pedogenetic process that had the greatest influence on MS was argilluviation. According to Breemen and Buurman, (2003), in these soils, besides inheritance of the source material, translocation of clay from superficial to superficial layers occurs, prevailing the surface sandy texture and lower DM values (Ayoubi et al. 2018). These results are corroborated by works of Fine et al. (1992) and Singer and Fine, (1989), reported differences in MS values related to claying processes, like argilluviation and ferralitization. In CY, in turn, the sandy texture prevails due to the deposition of different river sediments, with different ferrimagnetic materials, which is not related to pedogenesis processes but rather to depositional processes. In this soil, magnetite probably predominates in the sand fraction, so the mean values (**Tab. 3**) are higher than those of PVA.

Analyzing toposequences T1 (between points P2 / P3), T2 (P3 / P4) and T3 (P2 / P3; P6 / P7) (**Fig. 4**) transitions occur between lithologies, soil classes, pedogenetic processes, degree of evolution and texture variations. Thus, identifying transitional boundaries between soil classes, MS has a high potential to contribute, in addition to soil classification, to pedological digital mapping. In fact, Jordanova et al. (2016) used MS data quantitatively to improve soil classification and field pedological recognition in Bulgarian soils and obtained satisfactory results. Moreover, Marques et al. (2014) separated large groups of soils using MS and concluded that the technique can reproduce with high accuracy the spatial distribution of soil physical and chemical attributes. Pedogenesis processes, mainly argilluviation and ferralitization had greater influence than lithology in more evolved soils, where the MS values were higher, where these processes acted on the variations of ferrimagnetic mineral types in these soil classes, which allows the separation of some taxonomic groups. Ayoubi et al. (2018) reached the same conclusion after examining the possibility of stratifying large soil groups in Iran via MS.

3.4 Relationship between soil attributes and magnetic susceptibility

It was found a positive correlation of MS with clay (0.62) and Fe_2O_3 (0.77) (**Fig. 5a**). These results express correlation values close to those obtained by Siqueira et al. (2010) to clay (0.68) and Fe_2O_3 (0.82), where this correlation was expected due to the soils of most of the area being highly weathered, originated from materials of iron rich origin, where pedogenesis processes and relief conditions favored the permanence and formation of ferrimagnetic minerals via mineral formation of colloidal particles (maghemite) or ferrihydrite but not goethite (Michel et al. 2010), mainly in the clay fraction.

For sand, the negative correlation found (-0.55) (**Fig. 5a**) may indicate a higher presence of quartz minerals with low ferrimagnetic mineral contents, in other words, low magnetite content in the silt and sand fraction. Besides, Siqueira et al. (2010), further explains that surface pedogenic ferrimagnetic minerals may have their MS suppressed by the effects of pedogenic ferrimagnetic minerals or, magnetite crystals in the sand-silt fraction may be directly oxidized to antiferrimagnetic minerals, lowering the MS values (Fabris et al. 1997).

There was a positive correlation between MS and BS (0.57) (**Fig. 5a**). These values are concatenated with the correlation values between Ca, Mg and K and MS (0.66, 0.39 and 0.5, respectively). In fact, as exchangeable cations (Ca, Mg and K) increase, the BS value also increases (Kelly et al.1977). On the other hand, the significant and positive correlation between CEC and MS (0.56) (Fig. 5a) is associated with the correlation between clay and MS (0.62). The higher the clay content in the soil, the higher the CEC, due to the larger specific surface and there is a tendency for higher amounts of ferrimagnetic minerals in the clay (maghemite) fraction, originating from the source material (De Jong et al. 2000) or pedogenesis processes (Ayoubi et al. 2018). These results are similar to those obtained by Maher, (1998) and Siqueira et al. (2010), who reported a positive correlation between MS and CEC, and obtained correlation values of 0.68 and 0.62, respectively.

The significant and positive correlation with OM (0.53) (**Fig. 5a**) was not geochemically expected since, according to Schwertmann (1988) high OM levels favor iron complexation and consequently reduce the formation of ferrimagnetic minerals or their precursors. This tends to form antiferrimagnetic minerals such as goethite if conditions are higher (Schaetzel and Anderson, 2005). These results disagree with those obtained by Ayoubi and Adman, (2019), which obtained negative correlation values for soil organic carbon (SOC) and MS, attributing this fact to the diamagnetic character of OM reducing the values of MS. However, Ayoubi et al. (2019) found positive correlation values between MS and SOC, which second Rodríguez Martín et al. (2006), this can be explained by the higher CEC of OM and high adsorption of some ferrimagnetic metals.

a)

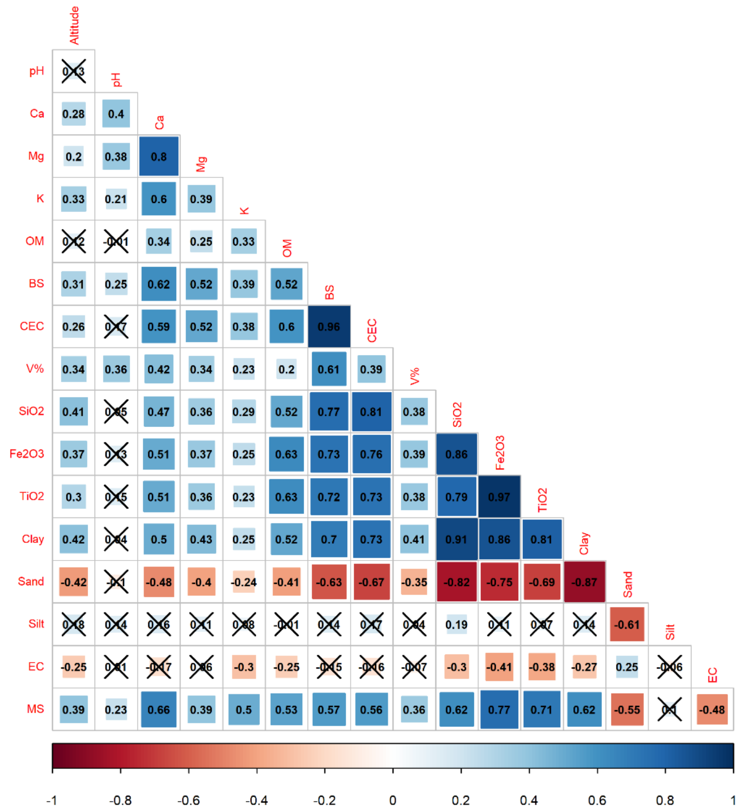

b)

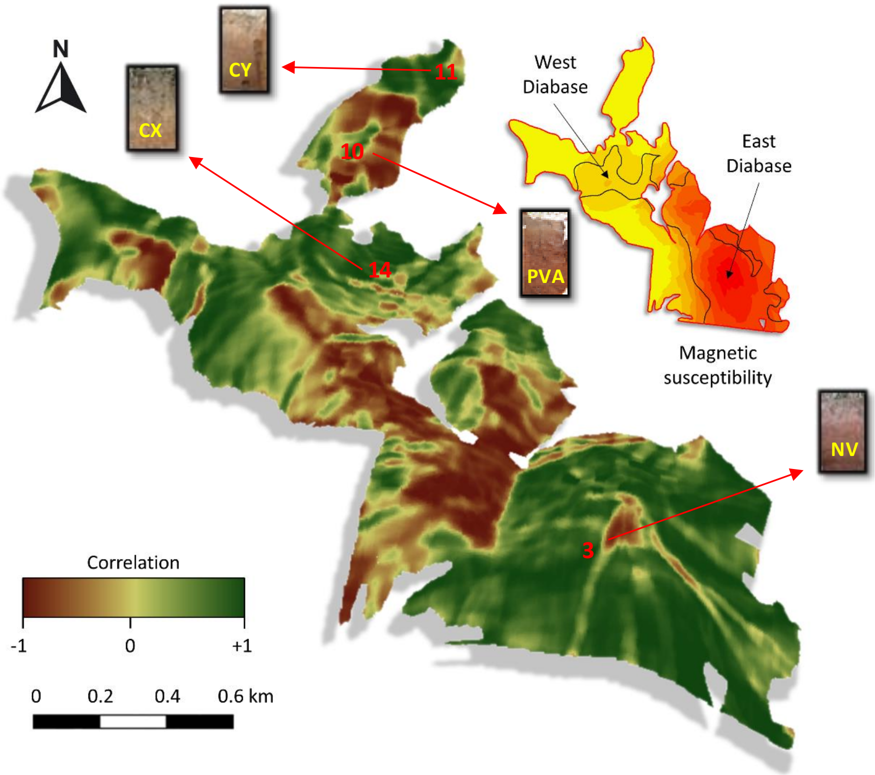

Figure 5. a) Pearson's correlation coefficient for soil physical and chemical attributes and magnetic susceptibility. Values overlapped with an "X" are not statistically significant at the 0.1 significance level. b) Correlation map between magnetic susceptibility and digital model elevation and representative soil profiles: CX: Haplic Cambisol (soil profile 10), CY Cambisol: Fluvic (soil profile 11), NV: Rhodic Nitisol (soil profile 3): PVA: Rhodic Lixisol (soil profile 10).

The magnetic characterization on soil surface, throughout geophysical techniques present low cost, simple execution and precise. Despite of sensors detect ferrimagnetic minerals on soil surface, it is possible to infer soil depth attributes and processes, once the processes and environmental factor (as lithology, relief, mineralogy etc.) that affect them is known, which in turn was the purpose of this research.

The understanding of which and how environmental processes in pedosphere affect the MS in different soil classes, can provides information about soil attributes. This information can be used in soil mapping, farming planning and appropriate land use and management in a sustainable way, as well as attribute prediction modeling works and map generation.

3.4. CONCLUSIONS

It was not possible to consider each pedoenvironmental factor isolated to study soil MS, which lithology, relief, pedogenesis, in addition to geochemical comportment of iron element and minerals. All of them act concomitantly to determine soil MS.

The geology and consequently the mineralogy of the source material exerted the greatest influence on MS in the less evolved soil classes (Fluvic and Haplic Cambisols), while for the more evolved classes (Rhodic Nitisol and Lixisol) pedogenesis processes had the greatest influence.

The ferralitization and argilluviation processes (NV and PVA, respectively), probably had more influence in these more evolved soil classes, in addition to pedogenesis of ferrimagnetic minerals pathway.

Geology affected MS by providing ferrimagnetic minerals directly from the source material via weathering, while pedogenesis by the neoformation of ferrimagnetic minerals, as well as their redistribution on the soil surface.

Relief variations act on the distribution of granulometric fractions containing ferrimagnetic minerals on the soil surface and the points of greatest slope, exerted less influence on geology and pedogenetic processes in the determination of MS.

MS identified the transition areas between soil classes along the toposequences and is an important tool for delimiting and classifying soils in large groups, contributing to the pedological digital mapping.

MS had valuable significant correlation with soil texture, CEC and Fe_2O_3, which can help to discriminate soil great groups in soil mapping processes.

The field sensor detected satisfactorily variations in soil MS, allowing to identify soil classes and lithology variations, it being a potential tool for digital soil mapping.

For each particular environment a conceptual model to interpret soil MS and its relation with pedosphere processes, need to be stablish, once many variables, with different characteristics affect MS values.

ACKNOWLEDGEMENTS

We would like to thank the National Council for Scientific and Technological Development (CNPq) for the first author scholarship (grant No. 134608/2015-1); the São Paulo Research Foundation (FAPESP) (grant No. 2014-22262-0) for providing essential resources to the Laboratory of Remote Sensing Applied to Soils from "Luiz de Queiroz" College of Agriculture (ESALQ/USP); and the Geotechnologies in Soil Science group (GeoSS – website http://esalqgeocis.wixsite.com/english) for the support.

REFERENCES

A. R. Fisher, 1925. No Title Statistical Methods for Research Workers. Oliver Boyd.

Ab'Sáber, 1957. Geomorfologia do Sítio Urbano de São Paulo.

Abbaszadeh Afshar, F., Ayoubi, S., Besalatpour, A.A., Khademi, H., Castrignano, A., 2016. Integrating auxiliary data and geophysical techniques for the estimation of soil clay content using CHAID algorithm. J. Appl. Geophys. 126, 87–97. https://doi.org/10.1016/j.jappgeo.2016.01.015

Alastair Ruffell, J.M., 2008. Geoforensics, in: Geoforensics. p. 288.

Alomari, A.H., Saleh, M.A., Hashim, S., Alsayaheen, A., 2019. Investigation of natural gamma radiation dose rate (GDR) levels and its relationship with soil type and underlying geological formations in Jordan. J. African Earth Sci. 155, 32–42. https://doi.org/10.1016/j.jafrearsci.2019.04.006

Alvares, C.A., Stape, J.L., Sentelhas, P.C., De Moraes Gonçalves, J.L., Sparovek, G., 2013. Köppen's climate classification map for Brazil. Meteorol. Zeitschrift 22, 711–728. https://doi.org/10.1127/0941-2948/2013/0507

Arnedo, M.A., Rubiano, J.G., Alonso, H., Tejera, A., González, A., González, J., Gil, J.M., Rodríguez, R., Martel, P., Bolivar, J.P., 2017. Mapping natural radioactivity of soils in the eastern Canary Islands. J. Environ. Radioact. 166, 242–258. https://doi.org/10.1016/j.jenvrad.2016.07.010

Arrouays, D., Grundy, M.G., Hartemink, A.E., Hempel, J.W., Heuvelink, G.B.M., Hong, S.Y., Lagacherie, P., Lelyk, G., McBratney, A.B., McKenzie, N.J., Mendonca-Santos, M. d. L., Minasny, B., Montanarella, L., Odeh, I.O.A., Sanchez, P.A., Thompson, J.A., Zhang, G.-L., 2014. GlobalSoilMap: Toward a Fine-Resolution Global Grid of Soil Properties, in: Advances in Agronomy 125. pp. 93–134. https://doi.org/10.1016/B978-0-12-800137-0.00003-0

Asgari, N., Ayoubi, S., Demattê, J.A.M., 2018. Soil drainage assessment by magnetic susceptibility measures in western Iran. Geoderma Reg. 13, 35–42. https://doi.org/10.1016/j.geodrs.2018.03.003

Atalay, İ.C.S.S.K.M.E., 2018. Pedogeomorphology, in: The Soils of Turkey. Springer, Cham, pp. 75–103.

Aydin, A., Ferré, E.C., Aslan, Z., 2007. The magnetic susceptibility of granitic rocks as a proxy for geochemical composition: Example from the Saruhan granitoids, NE Turkey. Tectonophysics 441, 85–95. https://doi.org/10.1016/j.tecto.2007.04.009

Ayoubi, S., Abazari, P., Zeraatpisheh, M., 2018. Soil great groups discrimination using magnetic susceptibility technique in a semi-arid region, central Iran. Arab. J. Geosci. 11. https://doi.org/10.1007/s12517-018-3941-4

Ayoubi, S., Adman, V., 2019. Iron Mineralogy and Magnetic Susceptibility of Soils Developed on Various Rocks in Western Iran. Clays Clay Miner. 67, 217–227. https://doi.org/10.1007/s42860-019-00020-5

Ayoubi, S., Adman, V., Yousefifard, M., 2019. Use of magnetic susceptibility to assess metals concentration in soils developed on a range of parent materials. Ecotoxicol. Environ. Saf. 168, 138–145. https://doi.org/10.1016/j.ecoenv.2018.10.024

Ayoubi, S., Mirsaidi, A., 2019. Magnetic susceptibility of Entisols and Aridisols great groups in southeastern Iran. Geoderma Reg. 16, e00202. https://doi.org/10.1016/j.geodrs.2018.e00202

Barlow, J., Lennox, G.D., Ferreira, J., Berenguer, E., Lees, A.C., Nally, R. Mac, Thomson, J.R., Ferraz, S.F.D.B., Louzada, J., Oliveira, V.H.F., Parry, L., Ribeiro De Castro Solar, R., Vieira, I.C.G., Aragaõ, L.E.O.C., Begotti, R.A., Braga, R.F., Cardoso, T.M., Jr, R.C.D.O., Souza, C.M., Moura, N.G., Nunes, S.S., Siqueira, J.V., Pardini, R., Silveira, J.M., Vaz-De-Mello, F.Z., Veiga, R.C.S., Venturieri, A., Gardner, T.A., 2016. Anthropogenic disturbance in tropical forests can double biodiversity loss from deforestation. Nature 535, 144–147. https://doi.org/10.1038/nature18326

Baumann, M., Gasparri, I., Piquer-Rodríguez, M., Gavier Pizarro, G., Griffiths, P., Hostert, P., Kuemmerle, T., 2017. Carbon emissions from agricultural expansion and intensification in the Chaco. Glob. Chang. Biol. 23, 1902–1916. https://doi.org/10.1111/gcb.13521

Bazaglia Filho, O., Rizzo, R., Lepsch, I.F., Prado, H. do, Gomes, F.H., Mazza, J.A., Demattê, J.A.M., 2013. Comparison between detailed digital and conventional soil maps of an area with complex geology. Rev. Bras. Ciência do Solo 37, 1136–1148. https://doi.org/10.1590/s0100-06832013000500003

Beamish, D., 2015. Relationships between gamma-ray attenuation and soils in SW England. Geoderma 259–260, 174–186. https://doi.org/10.1016/j.geoderma.2015.05.018

Beamish, D., 2013. Gamma ray attenuation in the soils of Northern Ireland, with special reference to peat. J. Environ. Radioact. 115, 13–27. https://doi.org/10.1016/j.jenvrad.2012.05.031

Becegato, V.A., Becegato, V.R., Baum, C.A., Lavnitcki, L., Paulino, A.T., 2019. Multivariate statistical analysis correlating 238 U, 232 Th, and 40 K equivalent activities in soil to geochemical data from an agricultural area. J. Soils Sediments 19, 1901–1910. https://doi.org/10.1007/s11368-018-2161-6

Berkowitz, B., Dror, I., Yaron, B., 2008. Contaminant Geochemistry, Contaminant Geochemistry. https://doi.org/10.1007/978-3-540-74382-8

Binley, A., Hubbard, S.S., Huisman, J.A., Revil, A., Robinson, D.A., Singha, K., Slater, L.D., 2015. The emergence of hydrogeophysics for improved understanding of subsurface processes over multiple scales. Water Resour. Res. 1–30. https://doi.org/10.1002/2015WR017016.Received

Blundell, A., Dearing, J.A., Boyle, J.F., Hannam, J.A., 2009. Controlling factors for the spatial variability of soil magnetic susceptibility across England and Wales. Earth-Science Rev. 95, 158–188. https://doi.org/10.1016/j.earscirev.2009.05.001

Brevik, E.C., Calzolari, C., Miller, B.A., Pereira, P., Kabala, C., Baumgarten, A., Jordán, A., 2016. Soil mapping, classification, and pedologic modeling: History and future directions. Geoderma 264, 256–274. https://doi.org/10.1016/j.geoderma.2015.05.017

Broschat, T.K., 1995. Nitrate, phosphate, and potassium leaching from container-grown plants fertilized by several methods. HortScience 30, 74–77.

Camargo, O.A.; Moniz, A.C.; Jorge, J.A. & Valadares, J.M.A.S., 1986. Métodos de análise química, mineralógica e física de solos do Instituto Agronômico do estado de São Paulo. Bol. técnico 106, 94.

Camargo, L.A., Marques Júnior, J., Pereira, G.T., Bahia, A.S.R. de S., 2014. Clay mineralogy and magnetic susceptibility of Oxisols in geomorphic surfaces. Sci. Agric. 71, 244–256. https://doi.org/10.1590/S0103-90162014000300010

Cervi, E.C., Maher, B., Poliseli, P.C., de Souza Junior, I.G., da Costa, A.C.S., 2019. Magnetic susceptibility as a pedogenic proxy for grouping of geochemical transects in landscapes. J. Appl. Geophys. 169, 109–117. https://doi.org/10.1016/j.jappgeo.2019.06.017

Coey, J.M.D., 1987. Magnetic order in trioctahedral sheet silicates: A review, in: Proceedings of the International Clay Conference, Denver, 1985, The Clay Minerals Society, Bloomington,. pp. 261–266.

Cook, S.E., Corner, R.J., Groves, P.R., Grealish, G.J., 1996. Use of airborne gamma radiometric data for soil mapping. Aust. J. Soil Res. 34, 183–194. https://doi.org/10.1071/SR9960183

Cooper, M., Vidal-Torrado, P., Grimaldi, M., 2010. Soil structure transformations from ferralic to nitic horizons on a toposequence in southeastern Brazil. Rev. Bras. Ciência do Solo 34, 1685–1699. https://doi.org/10.1590/s0100-06832010000500021

Coulouma, G., Caner, L., Loonstra, E.H., Lagacherie, P., 2016. Analysing the proximal gamma radiometry in contrasting Mediterranean landscapes: Towards a regional prediction of clay content. Geoderma 266, 127–135. https://doi.org/10.1016/j.geoderma.2015.12.006

Curi, N., Franzmeier, D.P., 1984. Toposequence of Oxisols from the Central Plateau of Brazil. Soil Sci. Soc. Am. J. 48, 341–346. https://doi.org/10.2136/sssaj1984.03615995004800020024x

D. A. Clarck & D. W. Emerson, 1991. Notes on rock magnetization characteristics in applied geophysical studies. Explor. Geophys. 22, 547–555.

Da Costa, A.C.S., Bigham, J.M., Rhoton, F.E., Traina, S.J., 1999. Quantification and characterization of maghemite in soils derived from volcanic rocks in southern Brazil. Clays Clay Miner. 47, 466–473. https://doi.org/10.1346/CCMN.1999.0470408

Dahlkamp, F.J., 1993. Uranium Ore Deposits. Springer.

Damaceno, J.G., de Castro, D.L., Valcácio, S.N., Souza, Z.S., 2017. Magnetic and gravity modeling of a Paleogene diabase plug in Northeast Brazil. J. Appl. Geophys. 136, 219–230. https://doi.org/10.1016/j.jappgeo.2016.11.006

De Jong, E., Pennock, D.J., Nestor, P.A., 2000. Magnetic susceptibility of soils in different slope positions in Saskatchewan, Canada. Catena 40, 291–305. https://doi.org/10.1016/S0341-8162(00)00080-1

De Wispelaere, L., Marcelino, V., Regassa, A., De Grave, E., Dumon, M., Mees, F., Van Ranst, E., 2015. Revisiting nitic horizon properties of Nitisols in SW Ethiopia. Geoderma 243–244, 69–79. https://doi.org/10.1016/j.geoderma.2014.12.021

Dearing, J.A., 1999. Environmental Magnetic Susceptibility., 2 nd. ed, Using the Bartington MS2 system. Chi Publishing, Kenilworth, UK.

Dearing, J.A., 1994. Environmental magnetic susceptibility, using the Bartington MS2 system.

Dearing, J.A., Hay, K.L., Baban, S.M.J., Huddleston, A.S., Wellington, E.M.H., Loveland, P.J., 1996. Magnetic susceptibility of soil: An evaluation of conflicting theories using a national data set. Geophys. J. Int. 127, 728–734. https://doi.org/10.1111/j.1365-246X.1996.tb04051.x

Demattê, J.A.M., Araújo, S.R., Fiorio, P.R., Fongaro, C.T., Nanni, M.R., 2015. Espectroscopia VIS-NIR-SWIR na avaliação de solos ao longo de uma topossequência em Piracicaba (SP). Rev. Cienc. Agron. 46, 679–688. https://doi.org/10.5935/1806-6690.20150054

Deng, D.N., 2015. A comparative study of hand-held magnetic susceptibility instruments. M.Sc. Thesis 207.

Dennerley, C., Huang, J., Nielson, R., Sefton, M., Triantafilis, J., 2018. Identifying soil management zones in a sugarcane field using proximal sensed electromagnetic induction and gamma-ray spectrometry data. Soil Use Manag. 34, 219–235. https://doi.org/10.1111/sum.12410

Dickson, B.L.; Scott, K.M., 1997. Interpretation of aerial gamma-ray surveys – adding the geochemical factors. J. Aust. Geolology Geophys. 17, 187–200.

Dierke, C., Werban, U., 2013. Relationships between gamma-ray data and soil properties at an agricultural test site. Geoderma 199, 90–98. https://doi.org/10.1016/j.geoderma.2012.10.017

Domra Kana, J., Djongyang, N., Raïdandi, D., Njandjock Nouck, P., Dadjé, A., 2015. A review of geophysical methods for geothermal exploration. Renew. Sustain. Energy Rev. 44, 87–95. https://doi.org/10.1016/j.rser.2014.12.026

Egmond, F.M. Van, Veeke, S. Van Der, Knotters, M., Koomans, R.L., Limburg, J., 2018. Mapping soil texture with a gamma-ray spectrometer : comparison between UAV and proximal measurements and traditional sampling. WOt-technical Rep. 137, 58p.

EMBRAPA, 2017. Manual de metodos de analises, Manual de métodos de análise de solo.

EMBRAPA, 2011. Documentos 132 Manual de Métodos de. Embrapa 230.

Fabris, J.D., De Jesus Filho, M.F., Coey, J.M.D., Mussel, W.D.N., Goulart, A.T., 1997. Iron-rich spinels from Brazilian soils. Hyperfine Interact. 110, 23–32. https://doi.org/10.1023/A:1012619331408

Falco, N., Wainwright, H., Dafflon, B., Léger, E., Peterson, J., Steltzer, H., Wilmer, C., Rowland, J.C., Williams, K.H., Hubbard, S.S., 2019. Investigating Microtopographic and Soil Controls on a Mountainous Meadow Plant Community Using High-Resolution Remote Sensing and Surface Geophysical Data. J. Geophys. Res. Biogeosciences 124, 1618–1636. https://doi.org/10.1029/2018JG004394

FAOSTAT, 2003. Food and Agriculture Organization of the United Nations, Statistical Databases.

Ferreira, A., Daraktchieva, Z., Beamish, D., Kirkwood, C., Lister, T.R., Cave, M., Wragg, J., Lee, K., 2018. Indoor radon measurements in south west England explained by topsoil and stream sediment geochemistry, airborne gamma-ray spectroscopy and geology. J. Environ. Radioact. 181, 152–171. https://doi.org/10.1016/j.jenvrad.2016.05.007

Filho, B., 2012. Universidade de São Paulo Escola Superior de Agricultura " Luiz de Queiroz " Comparação entre mapas de solos obtidos pelos métodos convencional e digital numa área complexa Osmar Bazaglia Filho Piracicaba. Master Diss. Soils Plant Nutr. 190 p.

Filistovič, V., Maceika, E., Tarasiuk, N., Lukšiene, B., Konstantinova, M., Buivydas, Š., Koviazina, E., Puzas, A., 2015. Model of Non-equilibrium Multiphase Contaminant Transport in Lake Water-Sediment System. Water. Air. Soil Pollut. 226. https://doi.org/10.1007/s11270-015-2455-x

Fine, P., Singer, M.J., Verosub, K.L., 1992. Use of magnetic-susceptibility measurements in assessing soil uniformity in chronosequence studies. Soil Sci. Soc. Am. J. 56, 1195–1199. https://doi.org/10.2136/sssaj1992.03615995005600040032x

Foley, 2011. Sustain the Planet ? Sci. Am. 305, 60–65.

Fontes, M.P.F., De Oliveira, T.S., Da Costa, L.M., Campos, A.A.G., 2000. Magnetic separation and evaluation of magnetization of Brazilian soils from different parent materials. Geoderma 96, 81–99. https://doi.org/10.1016/S0016-7061(00)00005-7

Ghilardi, M., Kunesch, S., Styllas, M., Fouache, E., 2008. Reconstruction of Mid-Holocene sedimentary environments in the central part of the Thessaloniki Plain (Greece), based on microfaunal identification, magnetic susceptibility and grain-size analyses. Geomorphology 97, 617–630. https://doi.org/10.1016/j.geomorph.2007.09.007

Gholamzadeh, M., Ayoubi, S., Shahrivar, F.S., 2019. Using magnetic susceptibility measurements to differentiate soil drainage classes in central Iran. Stud. Geophys. Geod. 63, 465–484. https://doi.org/10.1007/s11200-018-0679-0

Gillot, P.Y., Hildenbrand, A., Lefèvre, J.C., Albore Livadie, C., 2006. The K/Ar dating method: principle, analytical techniques, and application to holocene volcanic eruptions in Southern Italy. Acta Vulcanol. 18, 55–66.

Godfray, H.C.J., Beddington, J.R., Crute, I.R., Haddad, L., Lawrence, D., Muir, J.F., Pretty, J., Robinson, S., Thomas, S.M., Toulmin, C., 2010. Food Security: The Challenge of Feeding 9 Billion People. Science (80-.). 327, 812 LP – 818. https://doi.org/10.1126/science.1185383

Govedarica, D.D., Gavrilov, M.B., Zeremski, T.M., Govedarica, O.M., Hambach, U., Tomić, N.A., Sentić, I., Marković, S.B., 2019. Relationships between heavy metal content and magnetic susceptibility in road side loess profiles: A possible way to detect pollution. Quat. Int. 502, 148–159. https://doi.org/10.1016/j.quaint.2018.01.020

GRANT, U.S., 1900. Contact metamorphism of a basic igneous rock. Geol. Soc. Am. Bull. 11, 503–510. https://doi.org/10.1130/gsab-11-503

Grimley, D.A., Arruda, N.K., Bramstedt, M.W., 2004. Using magnetic susceptibility to facilitate more rapid, reproducible and precise delineation of hydric soils in the midwestern USA. Catena 58, 183–213. https://doi.org/10.1016/j.catena.2004.03.001

Grimley, D.A., Vepraskas, M.J., 2000. Magnetic susceptibility for use in delineating hydric soils. Soil Sci. Soc. Am. J. 64, 2174–2180. https://doi.org/10.2136/sssaj2000.6462174x

Grison, H., Petrovsky, E., Kapicka, A., Stejskalova, S., 2016. Magnetic and chemical parameters of andic soils and their relation to selected pedogenesis factors. Catena 139, 179–190. https://doi.org/10.1016/j.catena.2015.12.005

Guagliardi, I., Buttafuoco, G., Apollaro, C., Bloise, A., De Rosa, R., Cicchella, D., 2013. Using gamma-ray spectrometry and Geostatistics for assessing geochemical behaviour of radioactive elements in the lese catchment (southern Italy). Int. J. Environ. Res. 7, 645–658.

Hanesch, M., Rantitsch, G., Hemetsberger, S., Scholger, R., 2007. Lithological and pedological influences on the magnetic susceptibility of soil: Their consideration in magnetic pollution mapping. Sci. Total Environ. 382, 351–363. https://doi.org/10.1016/j.scitotenv.2007.04.007

Hartemink, A.E., Krasilnikov, P., Bockheim, J.G., 2013. Soil maps of the world. Geoderma 207–208, 256–267. https://doi.org/10.1016/j.geoderma.2013.05.003

Heggemann, T., Welp, G., Amelung, W., Angst, G., Franz, S.O., Koszinski, S., Schmidt, K., Pätzold, S., 2017. Proximal gamma-ray spectrometry for site-independent in situ prediction of soil texture on ten heterogeneous fields in Germany using support vector machines. Soil Tillage Res. 168, 99–109. https://doi.org/10.1016/j.still.2016.10.008

Herrmann, L., Schuler, U., Rangubpit, W., Erbe, P., Surinkum, A., Zarei, M., Stahr, K., 2010. The potential of gamma-ray spectrometry for soil mapping. 19th World Congr. Soil Sci. 117–120.

Hooper, R.L., 1987. Factors affecting the magnetic susceptibility of baked rocks above a burned coal seam. Int. J. Coal Geol. 9, 157–169.

IUSS Working Group WRB, 2015. World reference base for soil resources 2014. International soil classification system for naming soils and creating legends for soil maps, World Soil Resources Reports No. 106. https://doi.org/10.1017/S0014479706394902

Ivanovich, M., Harmon, R.S., 1982. Uranium series disequilibrium: applications to environmental problems. Oxford University Press, USA.

J. A. Quaggio, Raij, B., 2001. Determination of pH in calcium chloride and total acidity. Chem. Anal. Fertil. Eval. Trop. Soils. Inst. Agronômico Campinas, Campinas 181–188.

Jiménez, C., Benavides, J., Ospina-Salazar, D.I., Zúñiga, O., Ochoa, O., Mosquera, C., 2017. Relationship between physical properties and the magnetic susceptibility in two soils of Valle del Cauca Relación entre propiedades físicas y la susceptibilidad magnética en dos suelos del Valle del Cauca. Cauca. Rev. Cienc. Agri 34, 33–45. https://doi.org/10.22267/rcia.173402.70

Johansson, M., Åkerman, H.J., 2008. Thawing Permafrost and Thicker Active Layers in Sub-arctic Sweden. Permafr. Periglac. Process. 19, 279–292. https://doi.org/10.1002/ppp

Jordanova, N., Jordanova, D., Mokreva, A., Ishlyamski, D., Georgieva, B., 2019. Temporal changes in magnetic signal of burnt soils – A compelling three years pilot study. Sci. Total Environ. 669, 729–738. https://doi.org/10.1016/j.scitotenv.2019.03.173

Jordanova, N., Jordanova, D., Petrov, P., 2016. Soil magnetic properties in Bulgaria at a national scale-Challenges and benefits. Glob. Planet. Change 137, 107–122. https://doi.org/10.1016/j.gloplacha.2015.12.015

Kelly, J.M., Resources, N., Lafayette, W., 1977. Acid precipitation effects on soil pH and base saturation of exchangeable sites 1, 401–408.

Kempen, B., Brus, D.J., Stoorvogel, J.J., Heuvelink, G.B.M., de Vries, F., 2012. Efficiency Comparison of Conventional and Digital Soil Mapping for Updating Soil Maps. Soil Sci. Soc. Am. J. 76, 2097. https://doi.org/10.2136/sssaj2011.0424

Khan, F.A., Fenton, T.E., 2010. Factors Affecting Potassium Status of Alluvial-Derived Soils of Western Iowa. Soil Sci. Soc. Am. J. 60, 836. https://doi.org/10.2136/sssaj1996.03615995006000030023x

Koch-Steindl, H., Pröhl, G., 2001. Considerations on the behaviour of long-lived radionuclides in the soil. Radiat. Environ. Biophys. 40, 93–104. https://doi.org/10.1007/s004110100098

Koons, R.D., Helmke, P.A., Jackson, M.L., 1980. Association of Trace Elements with Iron Oxides During Rock Weathering1. Soil Sci. Soc. Am. J. 44, 155. https://doi.org/10.2136/sssaj1980.03615995004400010032x

Lancmuir, D., Herman, J.S., 2002. 1-S2.0-0016703780902264-Main 44, 1–14.

Laubenstein, M., Plastino, W., Povinec, P.P., Fabbri, V., Aprili, P., Balata, M., Bella, F., Cardarelli, A., De Deo, M., Gallese, B., Ioannucci, L., Nisi, S., Antonecchia, D., Del Pinto, C., Giarrusso, G., 2013. Radionuclide mapping of the Molise region (Central Italy) via gamma-ray spectrometry of soil samples: Relationship with geological and pedological parameters. J. Radioanal. Nucl. Chem. 298, 317–323. https://doi.org/10.1007/s10967-012-2353-2

Li, J., Heap, A.D., 2008. A Review of Spatial Interpolation Methods for Environmental Scientists. Aust. Geol. Surv. Organ. GeoCat# 68, 154. https://doi.org/http://www.ga.gov.au/image_cache/GA12526.pdf

Lim, C.H., Jackson, M.L., 1986. Dissolution for total elemental analysis, in: Madison (Ed.), Methods of Soil Analysis. Part 2: Chemical and Microbiological Properties. American Society of Agronomy, pp. 1–12.

Lindon, J.C.G.E.T.D.W.K., 2016. Encyclopedia of Spectroscopy and Spectrometry, 3 edition. ed. Elsevir.

Lourenço, A.M., Sequeira, E., Sant'Ovaia, H., Gomes, C.R., 2014. Magnetic, geochemical and pedological characterisation of soil profiles from different environments and geological backgrounds near Coimbra, Portugal. Geoderma 213, 408–418. https://doi.org/10.1016/j.geoderma.2013.07.035

Lu, S., Wang, H., Bai, S., 2009. Heavy metal contents and magnetic susceptibility of soils along an urban - Rural gradient in rapidly growing city of eastern China. Environ. Monit. Assess. 155, 91–101. https://doi.org/10.1007/s10661-008-0420-5

Luque, E.C.L., 2008. Propiedades magnéticas de los óxidos de hierro en suelos mediterráneos. Universidad de Córdoba, Córdoba.

Maher, B.A., 1998. Magnetic properties of modern soils and quaternary loessic paleosols: Paleoclimatic implications. Palaeogeogr. Palaeoclimatol. Palaeoecol. 137, 25–54. https://doi.org/10.1016/S0031-0182(97)00103-X

Maher, B.A., Taylor, R.M., 1988. Formation of ultrafine-grained magnetite in soils. Nature 336, 368–370. https://doi.org/10.1038/336368a0

Marques, J., Siqueira, D.S., Camargo, L.A., Teixeira, D.D.B., Barrón, V., Torrent, J., 2014. Magnetic susceptibility and diffuse reflectance spectroscopy to characterize the spatial variability of soil properties in a brazilian haplustalf. Geoderma 219–220, 63–71. https://doi.org/10.1016/j.geoderma.2013.12.007

Mathé, V., Lévêque, F., 2003. High resolution magnetic survey for soil monitoring: Detection of drainage and soil tillage effects. Earth Planet. Sci. Lett. 212, 241–251. https://doi.org/10.1016/S0012-821X(03)00241-3

Maxbauer, D.P., Feinberg, J.M., Fox, D.L., 2016. Magnetic mineral assemblages in soils and paleosols as the basis for paleoprecipitation proxies: A review of magnetic methods and challenges. Earth-Science Rev. 155, 28–48. https://doi.org/10.1016/j.earscirev.2016.01.014

McBratney, A.B., Mendonça Santos, M.L., Minasny, B., 2003. On digital soil mapping, Geoderma. https://doi.org/10.1016/S0016-7061(03)00223-4

McFadden, M., Scott, W.R., 2013. Broadband soil susceptibility measurements for EMI applications. J. Appl. Geophys. 90, 119–125. https://doi.org/10.1016/j.jappgeo.2013.01.009

Mernagh, T.P., Miezitis, Y., 2008. A Review of the Geochemical Processes Controlling the Distribution of Thorium in the Earth ' s Crust and Australia ' s Thorium Resources 48.

Meyer, S. et al, 2019. Creating soil texture maps for precision liming using electrical resistivity and gamma ray mapping, 19th ed.

Michel, F.M., Barrón, V., Torrent, J., Morales, M.P., Serna, C.J., Boily, J.F., Liu, Q., Ambrosini, A., Cismasu, A.C., Brown, G.E., 2010. Ordered ferrimagnetic form of ferrihydrite reveals links among structure, composition, and magnetism. Proc. Natl. Acad. Sci. U. S. A. 107, 2787–2792. https://doi.org/10.1073/pnas.0910170107

Minty, B.R.S., 1997. GA1687.pdf.

Minty, B.R.S., 1988. A Review of Airborne Gamma-Ray Spectrometric Data-Processing Techniques. Aust. Gov. Publ. Serv.

Mokhtari Karchegani, P., Ayoubi, S., Lu, S.G., Honarju, N., 2011. Use of magnetic measures to assess soil redistribution following deforestation in hilly region. J. Appl. Geophys. 75, 227–236. https://doi.org/10.1016/j.jappgeo.2011.07.017

Moonjun, R., Shrestha, D.P., Jetten, V.G., van Ruitenbeek, F.J.A., 2017. Application of airborne gamma-ray imagery to assist soil survey: A case study from Thailand. Geoderma 289, 196–212. https://doi.org/10.1016/j.geoderma.2016.10.035

Morais, P.A. de O., Souza, D.M. de, Carvalho, M.T. de M., Madari, B.E., de Oliveira, A.E., 2019. Predicting soil texture using image analysis. Microchem. J. 146, 455–463. https://doi.org/10.1016/j.microc.2019.01.009

Muhammad Aqeel Ashraf;Mohd Jamil MaahMohd Jamil Maah; Ismail Bin YusoffIsmail Bin Yusoff, 2011. Introduction to Remote Sensing of Biomass. https://doi.org/10.5772/16462

Mullins, C.E., 1977. Magnetic Susceptibility of the Soil and Its Significance in Soil Science – a Review. J. Soil Sci. 28, 223–246. https://doi.org/10.1111/j.1365-2389.1977.tb02232.x

Nanni, M.R., Demattê, J.A.M., 2006. Spectral Reflectance Methodology in Comparison to Traditional Soil Analysis. Soil Sci. Soc. Am. J. 70, 393. https://doi.org/10.2136/sssaj2003.0285

Nico Van Breemen and Peter Buurman, 2003. Soil Formation, 2 nd. ed, KLUWER ACADEMIC PUBLISHERS. Laboratory of Soil Science and Geology, NEW YORK, BOSTON, DORDRECHT, LONDON, MOSCOW. https://doi.org/10.1017/CBO9781107415324.004

Oliveira, D. De, Santos, A.H.B. dos, 2008. Trajetórias do rio Capivari : implicações de um impacto meteorítico na drenagem no reverso. Geografias 04, 69–76.

P. Driessen, J. Deckers, O. Spaargaren, F.N., 2001. Lecture notes on the major soils of the world.

Paisani, J.C., Pontelli, M.E., de Barros Corrêa, A.Ô.C., Rech Rodrigues, R.A., 2013. Pedogeochemistry and micromorphology of oxisols - A basis for understanding etchplanation in the Araucárias Plateau (Southern Brazil) in the Late Quaternary. J. South Am. Earth Sci. 48, 1–12. https://doi.org/10.1016/j.jsames.2013.07.011

Pansu, M., Gautheyrou, J., 2006. Handbook of Soil Analysis – Mineralogical, Organic and Inorganic Methods. Springer, Netherlands.

Parasnis, D.S., 1986. Principles of Applied Geophysics, 4[a]. ed.

Parker, R., Ruffell, A., Hughes, D., Pringle, J., 2010. Geophysics and the search of freshwater bodies: A review. Sci. Justice 50, 141–149. https://doi.org/10.1016/j.scijus.2009.09.001

Phil Bierwirth,Paul Gessler, McKane, and D., 1996. Proceedings of the 8th Australasian Remote Sensing Conference. Proc. 8th Australas. Remote Sens. Conf. 1–3.

Pinheiro, E.A.R., de Jong van Lier, Q., Inforsato, L., Šimůnek, J., 2019. Measuring full-range soil hydraulic properties for the prediction of crop water availability using gamma-ray attenuation and inverse modeling. Agric. Water Manag. 216, 294–305. https://doi.org/10.1016/j.agwat.2019.01.029

Priori, S., Bianconi, N., Costantini, E.A.C., 2014. Can γ-radiometrics predict soil textural data and stoniness in different parent materials? A comparison of two machine-learning methods. Geoderma 226–227, 354–364. https://doi.org/10.1016/j.geoderma.2014.03.012

R W Boyle, 1982. Geochemical prospecting for thorium and uranium deposits. Elsevier Scientific Publishing Company, Amsterdan.

Rahimi, M.R., Ayoubi, S., Abdi, M.R., 2013. Magnetic susceptibility and Cs-137 inventory variability as influenced by land use change and slope positions in a hilly, semiarid region of west-central Iran. J. Appl. Geophys. 89, 68–75. https://doi.org/10.1016/j.jappgeo.2012.11.009

Randall Schaetzel and Sharon Anderson, 2005. Soil Genesis and Geomorphology.

Rawlins, B.G., Lark, R.M., Webster, R., 2007. Understanding airborne radiometric survey signals across part of eastern England. Earth Surf. Process. Landforms 32, 1503–1515. https://doi.org/10.1002/esp.1468

Read, C.F., Duncan, D.H., Ho, C.Y.C., White, M., Vesk, P.A., 2018. Useful surrogates of soil texture for plant ecologists from airborne gamma-ray detection. Ecol. Evol. 8, 1974–1983. https://doi.org/10.1002/ece3.3417

Reinhardt, N., Herrmann, L., 2019. Gamma-ray spectrometry as versatile tool in soil science: A critical review. J. Plant Nutr. Soil Sci. 182, 9–27. https://doi.org/10.1002/jpln.201700447

Ribeiro, F.C.A., Silva, J.I.R., Lima, E.S.A., do Amaral Sobrinho, N.M.B., Perez, D. V., Lauria, D.C., 2018. Natural radioactivity in soils of the state of Rio de Janeiro (Brazil): Radiological characterization and relationships to geological formation, soil types and soil properties. J. Environ. Radioact. 182, 34–43. https://doi.org/10.1016/j.jenvrad.2017.11.017

Robinson, D.A., Panagos, P., Borrelli, P., Jones, A., Montanarella, L., Tye, A., Obst, C.G., 2017. Soil natural capital in Europe; A framework for state and change assessment. Sci. Rep. 7, 1–14. https://doi.org/10.1038/s41598-017-06819-3

Rochette, P., Jackson, M., Aubourg, C., 1992. Rock magnetism andn the interpretation of magnetic susceptibility. Rev. Geophys. 30, 209–226.

Rodríguez Martín, J.A., Arias, M.L., Grau Corbí, J.M., 2006. Heavy metals contents in agricultural topsoils in the Ebro basin (Spain). Application of the multivariate geoestatistical methods to study spatial variations. Environ. Pollut. 144, 1001–1012. https://doi.org/10.1016/j.envpol.2006.01.045

Roman, S.A., Johnson, W.C., Geiss, C.E., 2013. Grass fires-an unlikely process to explain the magnetic properties of prairie soils. Geophys. J. Int. 195, 1566–1575. https://doi.org/10.1093/gji/ggt349

Romero-Ruiz, A., Linde, N., Keller, T., Or, D., 2018. A Review of Geophysical Methods for Soil Structure Characterization. Rev. Geophys. 56, 672–697. https://doi.org/10.1029/2018RG000611

Rossel, R.A.V., Taylor, H.J., McBratney, A.B., 2007. Multivariate calibration of hyperspectral γ-ray energy spectra for proximal soil sensing. Eur. J. Soil Sci. 58, 343–353. https://doi.org/10.1111/j.1365-2389.2006.00859.x

Rutherford and Soddy, 1902. The cause and nature of radioactivity - Part I, Journal of African Earth Sciences. https://doi.org/10.1016/j.jafrearsci.2017.04.031

Rutherford, E., Soddy, F., 1902. XLI. The cause and nature of radioactivity .—Part I . London, Edinburgh, Dublin Philos. Mag. J. Sci. 4, 370–396. https://doi.org/10.1080/14786440209462856

S. R. Cattle, S. N. Meakin, P.R. and R.G.C., 2003. Using radiometric data to identify æolian dust additions to topsoil of the Hillston district, western NSW. Aust. J. Soil Res.

Santos-Francés, F., Gil Pacheco, E., Martínez-Graña, A., Alonso Rojo, P., Ávila Zarza, C., García Sánchez, A., 2018. Concentration of uranium in the soils of the west of Spain. Environ. Pollut. 236, 1–11. https://doi.org/10.1016/j.envpol.2018.01.038

Santos, H.L., Júnior, J.M., Matias, S.S.R., Siqueira, D.S., Pereira, G.T., 2011. Suscetibilidade magnética na identificação de compartimentos da paisagem em uma vertente. Rev. Bras. Ciencias Agrar. 6, 710–716. https://doi.org/10.5039/agraria.v6i4a1347

Sarmast, M., Farpoor, M.H., Esfandiarpour Boroujeni, I., 2017. Magnetic susceptibility of soils along a lithotoposequence in southeast Iran. Catena 156, 252–262. https://doi.org/10.1016/j.catena.2017.04.019

Sawyer, E.W., 1986. The influence of source rock type, chemical weathering and sorting on the geochemistry of clastic sediments from the Quetico Metasedimentary Belt, Superior Province, Canada. Chem. Geol. 55, 77–95. https://doi.org/10.1016/0009-2541(86)90129-4

Schuler, U., Erbe, P., Zarei, M., Rangubpit, W., Surinkum, A., Stahr, K., Herrmann, L., 2011. A gamma-ray spectrometry approach to field separation of illuviation-type WRB reference soil groups in northern Thailand. J. Plant Nutr. Soil Sci. 174, 536–544. https://doi.org/10.1002/jpln.200800323

Schwertmann, U., 1988. Occurrence and formation of iron oxides in various pedoenvironments. Iron soils clay Miner. 267–308. https://doi.org/10.1007/978-94-009-4007-9_11

Shenggao, L., 2000. Lithological factors affecting magnetic susceptibility of subtropical soils, Zhejiang Province, China. Catena 40, 359–373. https://doi.org/10.1016/S0341-8162(00)00092-8

Shenggao, L., 1998. Magnetic properties and iron oxide mineralogy of subtropical soils and environmental implications. Zhejiang University, China.

Silva, S.M.P. da, Crósta, A.P., Ferreira, F.J.F., Beurlen, H., Silva, A.M., Santos, L.F. dos, 2010. Espectrometria de raios gama de granitos pegmatíticos da Província Pegmatítica da Borborema (PPB), nordeste do Brasil. Rev. Bras. Geofísica 28, 673–690. https://doi.org/10.1590/s0102-261x2010000400011

Silvério, D. V., Bustamante, M., Brando, P.M., Macedo, M.N., Coe, M.T., Beck, P.S.A., 2015. Agricultural expansion dominates climate changes in southeastern Amazonia: The overlooked non-GHG forcing. Environ. Res. Lett. 10. https://doi.org/10.1088/1748-9326/10/10/104015

Singer, M.J., Fine, P., 1989. Pedogenic factors affecting magnetic susceptibility of northern California soils. Soil Sci. Soc. Am. J. 53, 1119–1127. https://doi.org/10.2136/sssaj1989.03615995005300040023x

Singer, M.J., Verosub, K.L., Fine, P., TenPas, J., 1996. A conceptual model for the enhancement of magnetic susceptibility in soils. Quat. Int. 34–36, 243–248. https://doi.org/10.1016/1040-6182(95)00089-5

Siqueira, D.S., Marques, J., Matias, S.S.R., Barrón, V., Torrent, J., Baffa, O., Oliveira, L.C., 2010. Correlation of properties of Brazilian Haplustalfs with magnetic susceptibility measurements. Soil Use Manag. 26, 425–431. https://doi.org/10.1111/j.1475-2743.2010.00294.x

Smith, R.C., Rose, A.W., 1975. Geology and Geochemistry of Triassic Diabase in Pennsylvania. Bull. Geol. Soc. Am. 86, 943–955. https://doi.org/10.1130/0016-7606(1975)86<943:GAGOTD>2.0.CO;2

Snnecker, J.P., 2000. Materiais Magnéticos Doces e Materiais Ferromagnéticos Amorfos. Rev. Bras. Ensino Física 22, 396–405.

Solutions, R., 2009. Spectrum stabilization and calibration for the RSI RS-125 and RS-230 handheld spectrometers.

Souza Junior, I.G. de, Costa, A.C.S. da, Vilar, C.C., Hoepers, A., 2010. Mineralogia e susceptibilidade magnética dos óxidos de ferro do horizonte B de solos do Estado do Paraná. Ciência Rural 40, 513–519. https://doi.org/10.1590/s0103-84782010000300003

Spassov, S., Egli, R., Heller, F., Nourgaliev, D.K., Hannam, J., 2004. Magnetic quantification of urban pollution sources in atmospheric particulate matter. Geophys. J. Int. 159, 555–564. https://doi.org/10.1111/j.1365-246X.2004.02438.x

Staff, S.S., 2017. Soil Survey Manual - Soil Taxonomy, Soil Survey Manual.

Sturchio, N.C., 2003. Uranium-series disequilibrium: Applications to Earth, Marine, and environmental sciences. Geochim. Cosmochim. Acta 57, 4327–4328. https://doi.org/10.1016/0016-7037(93)90331-p

Taylor, M J, Smettem, K., Pracilio, G., Verboom, W., 2002. Relationships between soil properties and high-resolution radiometrics, central eastern Wheatbelt, Western Australia. Explor. Geophys. 33, 95–102.

Taylor, Miranda J, Smettem, K., Smettem, K., Pracilio, G., Verboom, W., 2002. Relationships between soil properties and high-resolution radiometrics , central eastern Relationships between soil properties and high-resolution radiometrics , central eastern Wheatbelt , Western Australia 33, 95–102. https://doi.org/10.1071/EG02095

Thompson, R., Oldfield, F., 1986. Environmental Magnetism. Allen and, 227.

Triantafilis, J., Gibbs, I., Earl, N., 2013. Digital soil pattern recognition in the lower Namoi valley using numerical clustering of gamma-ray spectrometry data. Geoderma 192, 407–421. https://doi.org/10.1016/j.geoderma.2012.08.021

U. C. Sharma, 1998. Influence of soil texture and rainfall on leaching of potassium and its recovery by potato (Solonum tuberosum). Indian J. Agric. Sci. 59, 713–717.

Ulbrich, H.H.G.J., Ulbrich, M.N.C., Ferreira, F.J.F., Alves, L.S., Guimaraes, G.B., Fruchting, A., 2009. Gamma-spectrometric surveys in differentiated granites. I: A review of the method, and of the geochemical behavior of K, Th and U\rLevantamentos gamaespectrometricos em granitos diferenciados. I: Revisao da metodologia e do comportamento geoquimico dos el. Geol. USP - Ser. Cient. 9, 33–53.

Valaee, M., Ayoubi, S., Khormali, F., Lu, S.G., Karimzadeh, H.R., 2016. Using magnetic susceptibility to discriminate between soil moisture regimes in selected loess and loess-like soils in northern Iran. J. Appl. Geophys. 127, 23–30. https://doi.org/10.1016/j.jappgeo.2016.02.006

van Dam, R.L., Hendrickx, J.M., Harrison, B., Borchers, B., Norman, D.I., Ndur, S., Jasper, C., Niemeyer, P., Nartey, R., Vega, D.N., Calvo, L., Simms, J.E., 2004. Spatial variability of magnetic soil properties. Detect. Remediat. Technol. Mines Minelike Targets IX 5415, 665. https://doi.org/10.1117/12.540693

Vandenhove, H., Van Hees, M., Wouters, K., Wannijn, J., 2007. Can we predict uranium bioavailability based on soil parameters? Part 1: Effect of soil parameters on soil solution uranium concentration. Environ. Pollut. 145, 587–595. https://doi.org/10.1016/j.envpol.2006.04.011

Viscarra Rossel, R.A., Webster, R., Kidd, D., 2014. Mapping gamma radiation and its uncertainty from weathering products in a Tasmanian landscape with a proximal sensor and random forest kriging. Earth Surf. Process. Landforms 39, 735–748. https://doi.org/10.1002/esp.3476

W.K. Jung, N.R. Kitchen, S.H. Anderson, E.J.S., 2007. Crop management effects on water infiltration for claypan soils. J. Soil Water Conserv. 62, 55–63.

Wang, X., Li, Z., Cai, C., Shi, Z., Xu, Q., Fu, Z., Guo, Z., 2012. Effects of rock fragment cover on hydrological response and soil loss from Regosols in a semi-humid environment in South-West China. Geomorphology 151–152, 234–242. https://doi.org/10.1016/j.geomorph.2012.02.008

Wilford, J., 2012. A weathering intensity index for the Australian continent using airborne gamma-ray spectrometry and digital terrain analysis. Geoderma 183–184, 124–142. https://doi.org/10.1016/j.geoderma.2010.12.022

Wilford, P.N., Bierwirth, J.R., Craig, M.A., 1997. Application of airborne gamma-ray spectrometry in soiVregolith mapping and Applied Geomorphology 17.

Yates, F., 1934. The Analysis of Multiple Classifications with Unequal Numbers in the Different Classes. J. Am. Stat. Assoc. 29, 51–66. https://doi.org/10.1080/01621459.1934.10502686

Zhou, L.P., Oldfield, F., Wintle, A.G., Robinson, S.G., Wang, J.T., 1990. Partly pedogenic origin of magnetic variations in Chinese loess. Nature 346, 737–739. https://doi.org/10.1038/346737a0

Zolfaghari, Z., Mosaddeghi, M.R., Ayoubi, S., 2015. ANN-based pedotransfer and soil spatial prediction functions for predicting Atterberg consistency limits and indices from easily available properties at the watershed scale in western Iran. Soil Use Manag. 31, 142–154. https://doi.org/10.1111/sum.12167

APPENDICES

Article under review - ***Soils natural radiological characterization and its relation with pedogenesis, pedogeomorphological and pedogeochemical processes in the tropical environment***

12/11/2019 My Co-authored Submission

ELSEVIER

Danilo Mello Sign out Help

My Co-authored Submissions

Geoderma

< Overview

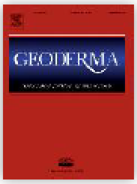

Research Paper | GEODER_2019_2597

Soils natural radiological characterization and its relation with pedogenesis, pedogeomorphological and pedogeochemical processes in the tropical environment

Jose Alexandre Dematte, Danilo Mello, Fellipe Alcantara de Oliveira Mello, Raúl Roberto Poppiel, Nélida Elizabet Silvero, José Lucas Safanelli, ARNALDO BARROS E SOUZA, Luis Di Raimo, Rodnei Rizzo, Maria E. B. Rezende

Submitted 25 Nov 2019

Under Review 09 Dec 2019 View PDF >

☐ Alert: keep me informed about the submission status for this manuscript

Abstract +

Decision Letter - RESUBMISSION: 25 November 2019 −

Ref: GEODER_2019_2597
Title: Soils natural radiological characterization and its relation with pedogenesis, pedogeomorphological and pedogeochemical processes in the tropical environment
Journal: Geoderma

https://www.evise.com/co-author/?dgcid=invite_email_coauthoroutreach00167061#/GEODER/submission/GEODER_2019_2597 1/3

Article submission for chapter 2 - Geoderma - Journal Elsevier

Article under review - ***Soil magnetism and its relationship with pedosphere naturally occurring processes, soil attributes and survey, in heterogeneous tropical environment***

12/16/2019 My Co-authored Submission

ELSEVIER

Danilo Mello   Sign out   Help

My Co-authored Submissions

Geoderma

< Overview

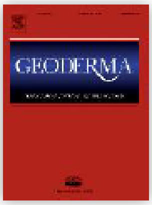

Research Paper | GEODER_2019_2762

Soil magnetism and its relationship with pedosphere naturally occurring processes, soil attributes and survey, in heterogeneous tropical environment

Jose Alexandre Dematte, Danilo Mello, Nélida Elizabet Silvero, Luis Di Raimo, Raúl Roberto Poppiel, Fellipe Alcantara de Oliveira Mello, ARNALDO BARROS E SOUZA, José Lucas Safanelli, Maria Rezende, Rodnei Rizzo

Submitted 12 Dec 2019

Under Review 16 Dec 2019   View PDF >

☐ Alert: keep me informed about the submission status for this manuscript

Abstract +

https://www.evise.com/co-author/?dgcid=invite_email_coauthoroutreach00167061#/GEODER/submission/GEODER_2019_2762   1/2

Article submission for chapter 3 - Geoderma - Journal Elsevier